Understanding the Impact of Social Factors on the Transmission Dynamics of Infectious Diseases Across Highly Heterogeneous Risk Environments.

by

Víctor Manuel Moreno Martínez

A Dissertation Presented in Partial Fulfillment
of the Requirements for the Degree
Doctor of Philosophy

Approved March 2018 by the
Graduate Supervisory Committee:

Carlos Castillo-Chávez, Chair
Yun Kang
Anuj Mubayi

ARIZONA STATE UNIVERSITY

May 2018

ABSTRACT

This dissertation explores the impact of environmental dependent risk on disease dynamics within a Lagrangian modeling perspective; where the identity (defined by place of residency) of individuals is preserved throughout the epidemic process. In Chapter Three, the impact of individuals who refuse to be vaccinated is explored. MMR vaccination and birth rate data from the State of California are used to determine the impact of the anti-vaccine movement on the dynamics of growth of the anti-vaccine sub-population. Dissertation results suggest that under realistic California social dynamics scenarios, it is not possible to revert the influence of anti-vaccine contagion. In Chapter Four, the dynamics of Zika virus are explored in two highly distinct idealized environments defined by a parameter that models highly distinctive levels of risk, the result of vector and host density and vector control measures. The underlying assumption is that these two communities are intimately connected due to economics with the impact of various patterns of mobility being incorporated via the use of residency times. In short, a highly heterogeneous community is defined by its risk of acquiring a Zika infection within one of two "spaces," one lacking access to health services or effective vector control policies (lack of resources or ignored due to high levels of crime, or poverty, or both). Low risk regions are defined as those with access to solid health facilities and where vector control measures are implemented routinely. It was found that the better connected these communities are, the existence of communities where mobility between risk regions is not hampered, lower the overall, two patch Zika prevalence. Chapter Five focuses on the dynamics of tuberculosis (TB), a communicable disease, also on an idealized high-low risk set up. The impact of mobility within these two highly distinct TB-risk environments on the dynamics and control of this disease is systematically explored. It is found that collaboration and mobility, under some circumstances, can reduce the overall TB burden.

DEDICATION

Para mis padres José y Catalina que han sido y seguirán siendo mi mayor fuente de admiración e inspiración. Para mis hermanos Josesito, Lupillo, Nena y Anita que con su arduo trabajo y sacrificios me brindaron la oportunidad de cumplir mis metas, siempre me enseñaron a nunca perder el piso.

"Los quiero mucho."

ACKNOWLEDGMENTS

I was aware, even before I began the pursuit of a doctoral degree, that the journey was going to be long, difficult, and challenging. Nonetheless, throughout this long journey, I have counted on the support and contributions of many friends that have helped me learn to persevere despite hardship. For that, I will always be grateful.

First and foremost, I would like to express my sincerest appreciation to my advisor Professor Carlos Castillo-Chávez, a true inspiration and an example to follow, whose thoughtful consideration and guidance have been invaluable. Without his guidance, support, and inspiration during my doctoral studies, I would not have been able to accomplish this dream. My sincere thanks also go to Professor Cynthia J. Wyels for her guidance and for always taking time out of her busy schedule to provide valuable feedback and direction. My appreciation also goes to Professor Jorge García, for his professional advice and for not letting me quit when I was most vulnerable. Without their support, none of this would have been possible. To them, I wish to say "Thank you for believing in me."

Second of all, I would also like to thank my committee members Professors Yun Kang and Anuj Mubayi, for their continuous support and guidance during my doctoral studies. They are truly wonderful teachers, researchers, and passionate individuals who have inspired me and taught me critical skills essential for a successful career. I am especially thankful to Professor Fred Brauer for his academic guidance and insightful discussions. I will always be in debt to Professor Sherry Towers for her ability to explain complex topics in a simple and straightforward way. I am also grateful for her painless introduction to the R language, for her collaboration, and most importantly, for sharing her expertise with me.

I am grateful to my colleagues in the Simon A Levin Mathematical, Computational and Modeling Sciences Center, for all their support, encouragement, and for putting

up with me throughout the doctoral program. Special thanks to Baltazar, Ana, and Juan for making these past four years a memorable journey. I will always be indebted to you for the invaluable support, motivation, discussions, advise, and for treating me like family. I would like to thank all my friends, Jose Juan, Juanito, and my brothers from the Fillmore Celtic Football Club, there would be no "safety net" without any of you.

I want to thank Sherry, Margaret, Dawn, Rebecca, Ciera, Cindy, Shelly, and all the staff at the SAL MCMSC that have made this possible, they are true enablers, dedicated people, and most importantly, friends. Your support has made me a stronger person and I will forever be grateful. Lastly, I wanted to reiterate my thanks to Professor Carlos Castillo-Chávez, who I met unexpectedly. During the past 4 years, he has been instrumental to my growth as a scholar and as a person. The countless hours spent inside and outside the office, along with his dedication and patience have been crucial in reaching the dream of finally putting the "Ph.D" after my name. Thank you!

This material is based upon work supported by the Extreme Science and Engineering Discovery Environment (XSEDE), which is supported by National Science Foundation grant number ACI-1548562, the National Science Foundation under Grants No. DMS-1263374 and DUE-1101782, the National Security Agency under Grant No. H98230-14-1-0157, the Office of the President of ASU, and the Office of the Provost of ASU . Any opinions, findings and conclusions or recommendation expressed in this material are those of the author(s) and do not necessarily reflect the views of the funding agencies.

TABLE OF CONTENTS

Page

LIST OF TABLES viii

LIST OF FIGURES ix

CHAPTER

1 COMPLEXITY OF INFECTIOUS DISEASES 1

1.1 The Possible Role of Abiotic, Biotic, and Social Factors in the Spread of Disease Epidemics. 4

1.2 The Emergence and Reemergence of Arboviral Diseases 10

2 MATHEMATICAL MODELS IN EPIDEMIOLOGY 17

2.1 Metapopulation Models 18

2.2 Lagrangian Models: A New Approach 20

2.2.1 Residence Times 20

3 ANTI-VACCINE MOVEMENT: A SOCIAL CONTAGION 24

3.1 Introduction 24

3.2 Methodology 27

3.2.1 Data 27

3.2.2 Model 29

3.2.3 Estimation of Model Parameters 32

3.3 Results 33

3.4 Discussion 33

3.5 Conclusion 36

4 THE ROLE OF SHORT-TERM DISPERSAL AND SOCIAL INSECURITY ON THE TRANSMISSION DYNAMICS OF ZIKA VIRUS IN AN EXTREME IDEALIZED ENVIRONMENT: THE CASE OF ZIKA VIRUS IN EL SALVADOR. 37

CHAPTER Page

4.1 Introduction 38
4.2 Single Patch Model 42
4.2.1 The *Aedes Aegypti* Mosquito Feeding Habits 44
4.2.2 Force of Infection and Model 45
4.3 Basic Reproductive Number Sensitivity Analysis 50
4.4 Residence Times and Two-Patch Models 54
4.4.1 Two Patch Model 55
4.5 Results 58
4.5.1 Risk Defined by Poor Bite Prevention. 60
4.5.2 Risk Defined by Poor Vector Control. 68
4.5.3 Risk Defined by Poor Bite Prevention and Poor Vector Control. 76
4.6 Conclusions and Discussion. 87
5 THE ROLE OF MOBILITY AND HEALTH DISPARITIES ON THE TRANSMISSION DYNAMICS OF TUBERCULOSIS. 92
5.1 Background 93
5.2 Methods: TB Dynamic Modeling Framework 96
5.2.1 A Simple Single Patch TB Model with Homogenous Mixing . 96
5.2.2 A Two-patch TB Model with Heterogeneity in Population Through Residence Times 99
5.3 Results 102
5.3.1 Model Analysis 102
5.3.2 The Role of Risk and Mobility on TB Prevalence. 107
5.4 Discussion 112

CHAPTER Page

5.5 Conclusions 115
6 DISCUSSION 117
7 CONCLUSION 122
REFERENCES 124

LIST OF TABLES

Table Page

3.1 KSI Model Best Fit Parameters. 34

4.1 Force of Infection Parameters 46

4.2 Description of the Parameters Used in System (4.1). 48

4.3 Parameters Used for the Sensitivity Analysis of Formula (4.2). 51

4.4 Definitions and Scenarios for ZIKV 59

4.5 Scenario One: Final Size (Patch 1, Patch 2), $\mathcal{R}_{01} = 2$, $\mathcal{R}_{02} = 0.9$ and $p_{21} = 0.10$. 66

4.6 Scenario One: Final Size (Patch 1, Patch 2), $\mathcal{R}_{01} = 1.52$, $\mathcal{R}_{02} = 0.9$ and $p_{21} = 0.10$. 67

4.7 Scenario Two: Final Size (Patch 1, Patch 2), $\mathcal{R}_{01} = 2$, $\mathcal{R}_{02} = 0.9$ and $p_{21} = 0.10$. 75

4.8 Scenario Two: Final Size (Patch 1, Patch 2), $\mathcal{R}_{01} = 1.52$, $\mathcal{R}_{02} = 0.9$ and $p_{21} = 0.10$. 75

4.9 Scenario Three: Final Size (Patch 1, Patch 2), $\mathcal{R}_{01} = 2$, $\mathcal{R}_{02} = 0.9$ and $p_{21} = 0.10$. 86

4.10 Scenario Three: Final Size (Patch 1, Patch 2), $\mathcal{R}_{01} = 1.52$, $\mathcal{R}_{02} = 0.9$ and $p_{21} = 0.10$. 86

5.1 Definitions and Scenarios for TB 96

5.2 Description of the Parameters Used in System (5.5) 101

LIST OF FIGURES

Figure Page

2.1 Dispersal of Individuals via a Lagrangian Approach. 22

3.1 Time Series of the Population Data Including Children and Adult Populations in a given Year. 30

3.2 Time Series of the Data Including Population of Vaccinated and Unvaccinated Children in a given Year. 31

3.3 KSI Model where the Flow γ from A_i to A_s is Zero. 33

3.4 Population Parameters and Overlay of Best Fit Model (Log Scale) on the Data. 34

3.5 Anti-vaccine Parameters and Overlay of Best Fit Model (Log Scale) on the Data. 35

4.1 Flow Diagram of Model (4.1) 49

4.2 Basic Reproductive Number as a Function of the Vector-Host Ratio; Biting Rate. 50

4.3 Partial Rank Correlation Coefficients For The Basic Reproductive Number and Each Input Parameter Variables. 52

4.4 Partial Rank Correlation Coefficients For The Basic Reproductive Number and Each Input Parameter Variables When $\Lambda = \frac{N_v}{N_h}$. 53

4.5 Scenario One: Patch Incidence and Final Size Proportions for $p_{21} = 0.10$, $p_{12} = 0, 0.2, 0.4$ and 0.6 for Best Case. 60

4.6 Scenario One: Patch Incidence and Final Size Proportions for $p_{21} = 0.10$, $p_{12} = 0, 0.2, 0.4$ and 0.6 for Worst Case. 61

4.7 Scenario One: Final Sizes for Worst Case (Top) and Best Case (Bottom). 62

Figure Page

4.8 Scenario One: Total Final Size and Global Basic Reproductive Number Through Mobility Values When $p_{21} = 0.10$, $\mathcal{R}_{02}$ Varies and $\mathcal{R}_{01} = 1.52$ (Top); 2 (Bottom). 64

4.9 Scenario One: Total Final Size and Global Basic Reproductive Number Through Mobility Values When $p_{21} = 0.10$ Population Size Varies, $\mathcal{R}_{02} = 0.9$, and $\mathcal{R}_{01} = 1.52$ (Top); 2 (Bottom). 65

4.10 Scenario One: Effect of Mobility and Population Size Proportions on the Global Basic Reproductive Number $\mathcal{R}_0$ When $\mathcal{R}_{02} = 0.9$, and $\mathcal{R}_{01} = 1.52$. 67

4.11 Scenario Two: Patch Incidence and Final Size Proportions for $p_{21} = 0.10$, $p_{12} = 0, 0.2, 0.4$ and 0.6 for Best Case. 69

4.12 Scenario Two: Patch Incidence and Final Size Proportions for $p_{21} = 0.10$, $p_{12} = 0, 0.2, 0.4$ and 0.6 for Worst Case. 70

4.13 Scenario Two Final Sizes for Worst (Top) and Best (Bottom) Cases. . . . 71

4.14 Scenario Two: Total Final Size and Global Basic Reproductive Number Through Mobility Values When $p_{21} = 0.10$, $\mathcal{R}_{02}$ Varies and $\mathcal{R}_{01} = 1.52$ (Top); 2 (Bottom). 72

4.15 Scenario Two: Total Final Size and Global Basic Reproductive Number Through Mobility Values When $p_{21} = 0.10$, Population Size Varies, $\mathcal{R}_{02} = 0.9$, and $\mathcal{R}_{01} = 1.52$ (Top); 2 (Bottom). 74

4.16 Scenario Two: Effect of Mobility and Population Size Proportions on the Global Basic Reproductive Number $\mathcal{R}_0$ When $\mathcal{R}_{02} = 0.9$, and $\mathcal{R}_{01} = 1.52$. 76

Figure Page

4.17 Scenario Three: Patch Incidence and Final Size Proportions for $p_{21} = 0.10$, $p_{12} = 0, 0.2, 0.4$ and 0.6 for Worst Case. 77

4.18 Scenario Three: Patch Incidence and Final Size Proportions for $p_{21} = 0.10$, $p_{12} = 0, 0.2, 0.4$ and 0.6 for Best Case. 79

4.19 Scenario Three Final Sizes for Worst (Top) and Best (Bottom) Cases. . 81

4.20 Scenario Three: Total Final Size and Global Basic Reproductive Number Through Mobility Values When $p_{21} = 0.10$, $\mathcal{R}_{02}$ Varies and $\mathcal{R}_{01} = 1.52$ (Top); 2 (Bottom). 83

4.21 Scenario Three: Total Final Size and Global Basic Reproductive Number Through Mobility Values When $p_{21} = 0.10$, Population Size Varies, $\mathcal{R}_{02} = 0.9$, and $\mathcal{R}_{01} = 1.52$ (Top); 2 (Bottom). 85

4.22 Scenario Three: Effect of Mobility and Population Size Proportions on the Global Basic Reproductive Number $\mathcal{R}_0$ When $\mathcal{R}_{02} = 0.9$, and $\mathcal{R}_{01} = 1.52$. 87

5.1 Flow Diagram for the Single Patch Three Compartment TB Model: Susceptible (S), Infected Latent (L) and Infectious (I). 98

5.2 Schematic Description of the Lagrangian Approach Between Two Patches. 100

5.3 Dynamics of Infectious and Latent When the Two Patches Are Strongly Connected and $\mathcal{R}_0 > 1$. 104

5.4 The Infectious and Latent Populations in the Two Patches Converge to Zero for Four Different Initial Conditions When $\mathcal{R}_0 \leq 1$. 105

5.5 Dynamics of Two Weakly Connected Patches When $\mathcal{R}_0 > 1$ Reach an Endemic Level but Patch 2 Approaches a Lower Level of Endemicity ($\mathcal{R}_{01} = 1.4150$ and $\mathcal{R}_{02} = 0.1417$) If Completely Isolated. 105

Figure Page

5.6 Effects of the Residence Time Matrix on the Basic Reproduction Number and the Disease Dynamics of the Latent Class. 106

5.7 Effects of the Residence Time Matrix on the Basic Reproduction Number and the Disease Dynamics of the Infected Class. 106

5.8 Effect of Mobility for $p_{12} = 0\%$, 3%, 6% and 9%, When Risk is Defined by Direct First Time Transmission Rates $0.13 = \beta_1 > \beta_2 = 0.07$ ($\mathcal{R}_{01} = 1.5$, $\mathcal{R}_{02} = 0.8$) and $\delta_1 = \delta_2 = 0.0026$. 108

5.9 Effect of Mobility When Risk Is Defined by Direct First Time Transmission Rates $0.13 = \beta_1 > \beta_2 = 0.07$ ($\mathcal{R}_{01} = 1.5$, $\mathcal{R}_{02} = 0.8$) and $\delta_1 = \delta_2 = 0.0026$. 109

5.10 Effect of Mobility for $p_{12} = 0\%$, 20%, 40% and 60%, When Risk Is Defined by the Exogenous Reinfection Rates $0.0053 = \delta_1 > \delta_2 = 0.0026$ and $\beta_1 = \beta_2 = 0.1$ ($\mathcal{R}_{01} = \mathcal{R}_{02} = 1.155$). 110

5.11 Effect of Mobility When Risk Is Defined by the Exogenous Reinfection Rates $0.0053 = \delta_1 > \delta_2 = 0.0026$ and $\beta_1 = \beta_2 = 0.1$ ($\mathcal{R}_{01} = \mathcal{R}_{02} = 1.155$). 111

5.12 Effect of Mobility and Population Size Proportions on the Global Basic Reproductive Number $\mathcal{R}_0$ When $0.13 = \beta_1 > \beta_2 = 0.07$ and $\delta_1 = \delta_2 = 0.0026$. 112

Chapter 1

COMPLEXITY OF INFECTIOUS DISEASES

The use of mathematical models in the study of disease dynamics have been useful in estimating the course of recent epidemics. In essence, the usefulness of the models is based on whether the models are able to incorporate key factors that ultimately decided the course of the epidemic even when these are incorporated as mere assumptions. For this, one can conclude that the ultimate goal of a mathematical model should be to develop hypotheses about the communities affected rather than to predict the outcome of an epidemic. The case of the 2009 N1H1 epidemic solely depended in the realization that the contacts between individuals could be described by a periodic function (Towers and Feng, 2009). In this case, hypothesizing a secondary wave of infection was invaluable, but a social or abiotic interpretation as the cause of the second wave would have had a bigger impact for global public health. Similarly, in the case of Ebola in West Africa, the early stages of the epidemic were analyzed and resulted in a close estimate in the final epidemic size (Towers *et al.*, 2014). While this result was useful, their biggest contribution was their observations in regards to the epidemic growth, it grew exponentially. This observation led to a possible connection between the implementation of *cordon sanitaire* (a medieval control strategy) and the explosion of the epidemic in August 2014; corroborated by the work in (Espinoza *et al.*, 2016). These are only two recent examples in which models served as a tool to identify the existence of ignored factors driving these outbreaks of disease, but there are many more.

The complexity of infectious diseases combined with limited information about their dynamics create a tremendous challenge on the effective use of mathematical

models. In general, this complexity often arises from the impact of social and abiotic factors. It is expected that social heterogeneity could have a direct impact in the risk of infection, but since little is known, it is often ignored in mathematical models. In the case of new diseases, in which little to none is known about their dynamics or their long lasting consequences, it is paramount to determine important transmission factors in order to create adequate time frames for the implementation of control measures. In addition, exogenous factors like current conditions as well as social behavior of the affected communities need to be taken in to account since they have the potential to magnify the final size of the outbreak. Furthermore, an understanding of the composition of the at-risk population should be the first priority since controlling a disease outbreak depends mainly on their cooperation and secondly on the availability of resources and infrastructure.

The aforementioned characteristics require a mathematical model where the incorporation of risk of infection heterogeneity is one of the main drivers of the dynamical system. This heterogeneity can be expressed in many forms ranging from age structure to differences in vector-host ratios to more individualized forms, like for instance, population adaptive behavior. All of which translate into a higher or lower expected number of contacts per individual and are usually directly reflected in the basic reproductive number; which gives us an early idea about the course of the outbreak. In consequence, individuals might experience different levels of the risk of infection based on factors predetermined by their community. In short, in order to identify the main factors driving disease dynamics, the ideal approach is to have a clear understanding of key aspects of the at-risk population and the specific process of disease transmission, that is, a clear understanding of biotic, abiotic and social factors. In some cases, it is crucial to understand the ecosystem in which this population lives, particularly when the disease studied involves zoonoses or vectors. A community

with an abundance of reservoirs and vectors increases the exposure probability of humans to reservoirs or vectors, and we can reasonably assume that individuals in the community are more likely to have a higher number of zoonotic contacts than average. Consequently, we expect such communities to have a higher risk of infection and therefore their existence are a cause for public health concern.

It is clear that while abiotic and biotic factors determine the basic dynamics of disease, social factors determine their spread. Most specifically, social factors influence the probability of contacts between susceptible and infectious individuals. In particular, membership in social and ethnic groups that allow participation in social activities and or associated ethnic customs used to be cultural barriers as a result of distance, nowadays, easily broken by affordable travel. These factors in the absence of travel create a nonrandom mixing within these membership clusters, which on their own, have many consequences on their epidemic spread ranging from time of introduction to the severity of an epidemic (Sattenspiel and Dietz, 1995). Incorporating constant travel by tourist visiting these areas only increases the probability of an effective contact and thus a greater and longer epidemic.

Today, it is difficult to find communities that are not interconnected, meaning completely isolated. Hence, models that do not account for social and abiotic factors specific to the at-risk population are not likely to be useful in designing policies that could help eradicate disease and most importantly prevent transmission. Likewise, policies that ignore these social and abiotic factors, or attributes of the at-risk population, are unlikely to be effective. It should be clear that without a complete description of the attributes of the community in question, it is almost impossible to implement successful intervention programs that are capable of reducing transmission rates. Furthermore, failure to understand the attributes of the at-risk population jeopardizes the success of intervention programs due to the fact that intervention pro-

grams must educate both the at-risk population as well as their government officials on the benefits, factors, and costs associated with population-based disease prevention and control. Lastly, intervention programs must account for the risks that are inherent with high levels of migration as well as with local and regional mobility patterns between areas defined by risk heterogeneity.

Our ability to accurately interpret the social and abiotic factors, directly effect the response time in the critically early stages of an epidemic. Consequently, the development and implementation of interventions can greatly benefit in the form of training and educational programs for governmental personnel in order to avoid stigmatization and further marginalization of groups. A lack of an accurate analysis is known to promote isolation, prevent integration, and reduce compliance (Gushulak and MacPherson, 2000a), and as a result many experience some kind of discrimination. A situation that is not uncommon in today's world where the role of dramatic changes in initial conditions could easily be described by the displacement of large groups of individuals, which cause catastrophes, conflicts, and generate new migration patterns in the process. Failure to adequately incorporate and address these challenges may result in considerable delays and increase epidemic impact.

1.1 The Possible Role of Abiotic, Biotic, and Social Factors in the Spread of Disease Epidemics.

Currently, disease outbreak analysis depends mainly on the dynamics of how a pathogen affects humans directly. In particular, the main emphasis focuses on the different kinds of transmission for such pathogen; it often relies on the interaction among humans and in some cases between humans and animals (vectors). Nonetheless, many important factors are ignored and many of these factors have the potential of magnifying disease proliferation and can lead to the regional endemicity of new

diseases. According to the Centers for Disease Control and Prevention (CDC), it is estimated that at least 6 out of every 10 infectious diseases in humans are zoonotic (Centers for Disease Control and Prevention (b), 2016). Human interaction with animals may consist of farming for food, interactions at zoos or fairs, family pets, or in extreme cases, wild encounters; the latter usually as a result of deforestation for construction purposes. Commonly, people acquire zoonotic diseases when coming in contact with body fluids, get bitten, or by eating unsafe products from infected animals.

Zoonotic infections are the origin of most established pathogens in humans, usually transmitting rapidly in immunologically naive communities. Zoonotic infections are a cause for concern due to their potential for devastating consequences, take for instance the SARS epidemic in Canada, the 2009 N1H1 global epidemic and more recently, the West Africa Ebola outbreak. Furthermore, spillover events could lead to the adaptation of pathogens in humans and often making horizontal transmission possible without the need for a reservoir. This shows the importance of monitoring spillover diseases since repeated events could help the pathogen evolve from stage 1 (animal-animal) to stage 5 (human-human without the need of a reservoir), based on the scale presented in (Wolfe *et al.*, 2007). This is exactly what has been happening with Ebola, human to human transmission has been growing and while it is considered stage 4 since the epidemic still requires a reservoir, but Ebola was considered stage 3 in 2007 when (Wolfe *et al.*, 2007) was published.

Zoonotic spillovers and their spread are a serious threat to global public health since they are no longer confined to remote regions (Iacono *et al.*, 2016). Again, the case of Ebola in West Africa exemplifies this to perfection. During the last forty years, there has been multiple outbreaks with none of them reaching 1000 cases until the 2014 West Africa outbreak, in which over 28,000 people were infected and over

11,000 died. Comparing the previous outbreaks with the latter, points to population size and density as a potential factor for large outbreaks. In the past, Ebola was confined only to humans, the population size was small, and the epidemic was terminated locally; likely due to the high disease induced mortality rates as well as a very limited pool of susceptible individuals. In a large and dense population, disease can persist, travel to adjacent regions and eventually return once the susceptible population gets replenished. Nonetheless, small populations also have the potential to host persisting diseases as well. Small population with transmission between reservoirs and humans, short immunity periods, and long infectious periods are among some of the characteristics that will ensure a long disease outbreak (Wolfe *et al.*, 2007).

Since most major epidemics involve abiotic, biotic, and social factors, it is important to have a rich understanding of the different biological, environmental, and socio-economic factors responsible for spillovers and thus epidemic spread (Iacono *et al.*, 2016). Recent studies have been trying to explain the impact of these factors on disease spread but unfortunately, most of them are arbitrary or specific to only a single factor. Environmentally speaking, most studies focus on the impact that could come as a consequence of climate change. In particular, for any zoonotic disease, the growth rate of reservoirs is of great importance. A possible consequence of climate change is the acceleration of biomass growth when temperatures rises; this could be an explanation of why there are so many species living in the tropics. In particular, in the case of vectors, which might be a factor that amplifies disease proliferation, their natural life cycle is accelerated at the earlier stages, and their survival probability is negatively affected. It would seem like climate change favors the shift rather than the spread of epidemics. While the spread of the distribution of epidemics can be attributed to social factors that increase disease sustainability, the abiotic factors like climate change have the ability to increase the severity of diseases like malaria by

increasing the length of the transmission season (Lafferty, 2009). When the accelerated growth coincides with an epidemic, then the consequences could be catastrophic. Keep in mind that seasonality could also be a factor, because, it doesn't always depend only on climate. Sometimes abundance doesn't affect or amplify an epizootic, particularly if there is none in the beginning; its magnitude will depend on how late in the season it starts. Events like El Niño might have similar effects, since it promotes growth in the mosquito population. In addition, the disease season might have an earlier start reaching catastrophic proportions (Lafferty, 2009).

Furthermore, extinction or predator depletion promotes vector population growth. In the case of mosquitoes, common ways of reaching predator depletion levels are through drought or ecosystem degradation, often caused by humans. Once an ecosystem has been damaged and mosquito predator numbers have been depleted, minimal water accumulations are enough for mosquito eggs to hatch and larvae is free to grow at a logistic rate without experiencing any harvesting and thus able to reach a maximum population size. If abundance of mosquitoes and a mosquito-borne disease endemic to the region, and the lag is not long enough, then it will result in a huge outbreak. This scenario could be the case of Malaria in Africa or Dengue fever (DENV) in many places. At the same time, habitat destruction might be the main factor responsible for the shifts in distribution of species (Lafferty, 2009). In the case of vector borne diseases, it is capable of increasing the epidemic toll since this exposes new populations with little resistance to these diseases and thus higher mortality rates.

In the case of malaria, the latest increase on disease burden has been attributed to new population mobility patterns, changes in agricultural practices, irrigation schemes, dam construction, deforestation, weakening of public health systems, and climate change (Sachs and Malaney, 2002). A small amount of empirical evidence

suggests that nature is capable of delivering public health benefits. Bauch *et. al* using a combination of of municipal-level data set on diseases that includes public health services, conservation policies, climate factors, demographics and other drivers of land use, were able to show a negative correlation in the frequencies between malaria and other diseases with an area that is under strict environmental protection in the Brazilian Amazon. Moreover, their results also suggest that malaria occurrences would be reduced by expanding these strict environmental protected areas and incidence levels could be reduced even further if the construction of roads and mining practices are restricted (Bauch *et al.*, 2015). This suggests that the implementation of ecological conservation practices aimed at preserving the natural capital of these at-risk regions can deliver co-benefits by increasing human health and therefore increasing human capital (Bauch *et al.*, 2015).

In many cases, it is known that diseases are able to create both a social and an economic burden for the affected communities. Diseases like tuberculosis, HIV and malaria are thought to have a direct impact on the economies of those countries with heavy disease burden. Due to the high number of casualties they cause, it is believed that the impact it creates in human capital is great enough to prevent economic growth in the affected region. Furthermore, the effects of these diseases are suspected to affect these countries by preventing population growth, work productivity and savings or investments as a result of medical costs. In many cases, child nutrition plays a major role, as well as deaths caused by disease outbreaks since both usually prevent labor productivity. While these direct consequences are important, it is also imperative to think and explore the direct consequences that arise from overcrowding in the context of disease incidence, prevalence and amplification. These kind of conditions preventing economic growth are believed to create poverty traps. Using deterministic models, it is believed to be impossible to escape poverty traps

without substantial external changes impacting the existing conditions (Bonds *et al.*, 2010). On the other hand, the work of Plucinski *et. al* suggests that the efficient implementation of control measures could create small changes in the probability of leaving or escaping the poverty trap. These changes via externally enforced levels of improved health or economic conditions will ultimately guarantee an escape from poverty traps even when the control measure or safety net is within the basin of attraction of the poverty trap (Pluciński *et al.*, 2011). This reinforces the importance of understanding the attributes of the community in an attempt to analyze which control measure, whether economic or medical, will have the most favorable impact on a community.

Recently, control policies have been focusing on motivating people to take preventive measures. For instance, during the 2009 N1H1 epidemic, Mexican authorities recommended people to stay in their homes for an entire week since it is known that person to person contacts are the ones that drive human disease (Althaus and Schiller, 2009). Similarly, during the recent Zika virus (ZIKV) outbreak, people were recommended to practice safe sex in order to prevent an elevated number of mycrocephaly cases in the Americas. Lastly, in the southern United States, local governments were authorized to pay residents $20 for testing themselves for TB, another $20 for returning two days after for the test check up, $20 for keeping an appointment for a chest X-ray if tested positive, and finally $100 for completing the treatment if they had active TB (Blinder, 2016). It is believed that if people takes into account the trade-offs that drive person to person contact, they will ultimately make good decisions or adaptive decisions during active disease outbreaks. It is suggested that human adaptive behavior could significantly change the course of ongoing epidemics (Fenichel *et al.*, 2011). This suggest that prevention measures could be paramount in disease control as long as you have a well educated population in which the majority

of the individuals are able to assess contact trade-offs whether they are based on a profit or a health perception, particularly during active disease outbreaks in or close to endemic areas.

Generally, having a complete understanding about the emergence and re-emergence of infectious disease should be a public health priority. Current, efforts to control and eradicate disease need to focus on determining factors specific to the at-risk communities and policies in place; if any,are they increasing the spread of disease? The existence of these factors (social, abiotic, and biotic) and their impact on disease dynamics needs to be addressed in the study of infectious diseases. Ignoring these factors might be detrimental in the implementation of control measures because social and abiotic factors could become catalysts for biotic factors that ultimately may magnify the proliferation of a disease. Ecological degradation could be an example that is capable of directly promoting the spread of vector borne diseases like DENV and Malaria. The combination of social, abiotic, and biotic knowledge helps determine the risk of infection as well as the risk of a spillover event. Unfortunately, due to the complexity of these rare events it is hard to measure and forecast spillover events. The need of a framework that incorporates abiotic, biotic, and social factors with mathematical models would be of tremendous help in explaining the constant emergence and reemergence of epizootics.

1.2 The Emergence and Reemergence of Arboviral Diseases

Arboviral diseases are those viruses that need a blood sucking arthropod (vector) to complete their life cycle. Typically, arboviruses are zoonoses that depend on a host (vertebrate) for replication and to reach ecosystem endemicity. The most important hosts or reservoirs are birds and rodents while the most important vectors are mosquitoes and ticks. According to the International Catalog of Arboviruses, there

are 537 registered viruses, of which about 214 are recognized as known or probable arboviruses and about 134 have caused illness in humans (Gubler, 2002).

Between 1970 and 2000, we have witnessed the emergence of over 100 new viruses. The majority of them are zoonoses that as a result of social and abiotic factors have been able to jump species and infect humans. While few of these new pathogens are arboviruses and all are considered unimportant for humans from a public health point of view, the recent Zika virus (ZIKV) outbreak made us reconsider their importance. Importance is determined by the level of viremia the pathogen is able to produce in humans. Most arboviruses of importance belong to three families: *Flaviviridae, Togaviridae* and *Bunyaviridae* (Gubler, 2002). During thesame period, the world has witnessed the resurgence of arboviral diseases that were thought to be well under control like Dengue fever (DENV), Chikungunya (CHIKV), West Nile Fever and Yellow Fever. DENV and CHIKV produce high levels of viremia and in fact, DENV is one of the few arboviruses that has completely adapted to humans and established itself in those large tropical urban communities and no longer requires a sylvatic reservoir (Gubler, 2002).

Global dispersal of arboviruses could be attributed to the evolution of factors that support their expansion: anthropological behavior, commercial transportation, and land-remediation (Liang *et al.*, 2015). In addition, the huge variety of available arthropods helps arboviruses thrive in tropical environments. Furthermore, the adaptability of arthropods to change their meal preferences when host populations decrease is a cause for concern and something that needs to be incorporated into the development of control strategies, otherwise vector expansion will remain a challenge for future generations. This ability to modify meal preferences promotes the accelerated expansion and colonization of new ecosystems rich in biomass diversity, like the tropics. Incidentally, arthropod and migratory reservoir abundance facili-

tates arbovirus dispersion through large regions. Finally, this abundance of possible vectors and reservoirs allows arboviruses to survive in the sylvatic environment even when it seems to have run its epidemic course. Alternatively, some arboviruses can also survive in unhatched eggs for months or even years. For these reasons, arbovirus reemergence is very possible and at the same time these survival strategies and others not mentioned here make arbovirus eradication practically impossible.

Hence, control measures that only focus on humans and domestic reservoirs are not likely to completely eradicate arboviruses since they could stay in their sylvatic environment and eventually reemerge once the human population is replenished. This will happen when reservoir surveillance is low or lacking. In addition, implementing vector control in sylvatic environments has to be environment friendly since vector control could destroy the ecosystem and bring catastrophic reactions. Nonetheless, in the case of DENV it helps to have control measures that control the population of *aedes aegypti* in urban and semi-urban areas. Currently, the best strategy is to reduce exposure to vectors but the development of vaccines, treatment, and education campaigns are among the top suggestions for addressing the main objectives for arboviruses control (see (Liang *et al.*, 2015) for a list of strategies).

While there are many diseases that have reemerged during the last couple of years, Dengue fever (DENV) exemplifies a case that requires a new modeling approach and hence customized control strategies. Even though DENV is an old disease initially spreading globally as a result of commercial shipping during the eighteenth and nineteenth centuries, and first became a major public health problem in most tropical countries by the beginning of the 20th century, nowadays, it is still considered an emergent disease. There are 4 different DENV serotypes (DEN-1, DEN-2, DEN-3, and DEN-4) that have the same epidemiology. The dengue viruses are *Flaviviruses* (family: *Flaviviridae*). During the 1950s and 1960s, DENV was controlled in most

tropical countries (except in Southeast Asia) as a result of the efficient implementation of control measures for malaria and yellow fever.

DENV or Dengue Hemorrhagic Fever (DHF) has once again become a major public health problem. During the last part of the twentieth century, the American tropics experienced a dramatic resurgence of DENV and the emergence of DHF. DENV is one of the few arboviruses that has fully adapted to the human host and their environment and no longer needs to maintain a sylvatic cycle, making DENV the most important arboviral disease of humans. DENV maintains an endemic cycle (one to four serotypes in the same human population) in large urban and suburban centers throughout tropical and subtropical regions across Asia, Africa, Central America, South America, and the Pacific where its principal vector, *Aedes aegypti*, thrives. Due to its worldwide widespread, there are about 3 billion people at risk of a DENV infection. It is estimated that each year there are at least 100 million DENV infections, more than 250,000 cases of DHF and thousands of deaths. This goes without saying, in many countries DHF is one of the leading causes of death in children.

Generally, DENV symptoms are mild and include fever, headache, eye pain, myalgia, arthralgia and rash and epidemics, while more severe diseases tend to cycle every 3 to 5 years. Nonetheless, during the 1950's DENV began to show severe symptoms characterized by defects in hemostasis and plasma leakage, which could lead to death if not treated early. This new manifestation is known as the Dengue Hemorrhagic Fever (DHF) and is one of the main reasons why DENV is a public health problem. While current practices of dealing with DHF are to hospitalize individuals with early signs, the lack of understanding about early determinants of DENV severity prevents the implementation of an optimal cost-effective strategy. Hyperendemicity, the co-circulation of various DENV serotypes, is the most common risk factor associated with DHF in an area. While the factors responsible for hyperendemicity are not well

understood, it is suspected that they are associated with the increased movement of people between communities, existing levels of immunity to specific virus serotypes in a given community, and genetic changes in circulating or introducing viruses.

Secondary DENV infections are more likely to produce DHF as a result of immune enhancement. The binding of non-neutralizing antibodies from a previous DENV infection with new infecting serotype facilitates the entry of virus to bearing cells. This tends to increase the amounts of cells with antigen that could activate preexisting DENV *T lymphocytes* from the primary DENV infection and ultimately lead to the release of cytokines and other chemical mediators that could cause plasma leakage. In addition, it is believed that certain pathological factors could play an important role in the development of DHF, such factors include: risk factors (age, sex and nutrition), population-specific genetic predisposition and increased immune response due to a highly virulent genotype.

While there are no specific factors that could explain the sudden reemergence of DENV during the waning years of the 20th century, there are certain trends that could help us understand how particular factors could have contributed to its world-wide proliferation. In particular, it is known that demographic and societal changes in urban areas of the tropical developing world along with population movement within these areas and the lack of mosquito control, tend to increase DENV disease incidence. This change in epidemiology and reemergence of epidemic DENV are associated with demographic and societal changes that occurred as a result of conflicts during the last 70 years. Without a doubt, World War II has been the most significant event that has promoted the biggest population growth in this period. Consequently, this unprecedented growth has also driven urbanization factors that promoted mosquito growth near human centers and hence DENV proliferation. Furthermore, transportation systems have also improved as a result of population growth directly impacting DENV

distribution and transmission. Due to poor surveillance measures in place, modern transportation facilitates the undetected introduction of new vectors and pathogens into new geographic areas. The recent introductions of West Nile Virus in 1999 and Zika Virus in 2014 to the western hemisphere corroborates the impact of transportation and the poor communication between public and animal health officials, which leads to new pathogen discovery once a disease has been already established, making it almost impossible to eliminate in some cases.

The complex dynamics of emergent and re-emergent diseases like DENV within heterogeneous environments directly impacted by the effects of evolution, adaptive human behaviors, and public health policies, highlight the need of mathematical models to gain a better understanding of the transmission dynamics of arboviruses, including the possible challenges that emerge in the context of sustainability and human cooperation. Although there is a DENV vaccine which is currently being used in many countries, DENV control still depends on prevention and vector control. Unfortunately, there seems to be a complacency towards vector borne diseases to the point that very few improvements or effective control measures have been developed in the last couple of years. In addition, most countries have poor public health infrastructure and disease surveillance needs to improve. Furthermore, if developing countries have poor public infrastructure in regards to their dams, irrigation, sewer and waste management systems, or if they have poor housing, and unreliable water storage systems, it will be impossible to prevent the introduction and treatment of new arboviral diseases.

It is crucial to know how these demographic and societal changes impact the use of new control measures like vaccines and vector control. As a result, we will be using mathematical models to explore how factors like mobility, population size and risk of infection, which might be impacted by social factors, might impact the course of an

outbreak.

Chapter 2

MATHEMATICAL MODELS IN EPIDEMIOLOGY

The use of mathematical epidemiological models to study the evolution, dynamics, and control of diseases has increased in the last century since the development of the most celebrated epidemic model (SIR model) by Kermack and McKendrick in 1927. While the iconic SIR model is useful, it also relies on many assumptions that are questioned from time to time; take for instance population homogeneity. In addition, transmission depends completely on the intensity and frequency of encounters (effective contacts) between susceptible and infected individuals. Nonetheless, its applicability to everyday problems along with the easy calculation of a reproduction threshold ($\mathcal{R}_0$), makes it a powerful mechanism to create hypothesis that ultimately could even change policies. $\mathcal{R}_0$ is the basic reproductive number or the average number of new infections an infectious individual causes during the average infectious period in a completely susceptible population. Thus, an outbreak is possible when $\mathcal{R}_0 > 1$ and the disease eventually collapses when $\mathcal{R}_0 < 1$. Due to its simplicity, modifications of the SIR model has been used widely to explain social and natural phenomena. Some examples include the study of the dynamics of antibiotic resistance at the population level. In particular, persistence, evolution, and the expansion of resistance to antibiotics are of great importance due to the limited number of antibiotic drugs available. On the other hand, Michael Gladwell used the insights he had gained from understanding the SIR model and applied them to explain crime epidemics in a city. He saw crime as a contagion process and recognized the existence of a threshold and significance of crossing this tipping point. The wide adaptability of the SIR model along with the complexity of the problems at hand require a holistic approach

and thus the collaboration of a multidisciplinary team is paramount in order to fully address the problem in question.

2.1 Metapopulation Models

During the middle of the twentieth century, improvements in transportation, for both leisure and commerce, made it possible for diseases to move from their endemic regions and colonize new and completely susceptible regions in a rapid manner. As a result, it is important to somehow incorporate travel when modeling epidemics; depending on time scales and transmission dynamics of the disease. In particular, it is essential to start modeling populations of populations (metapopulations) or patchy environments with mobile individuals. These models are called metapopulation models which usually consist of a large system of nonlinear ordinary differential equations with coupling interactions between patches (communities). The ideal scenario to model the spread of a communicable disease would include all interacting patches that could cause an infection. Many scenarios that incorporate the travel of individuals between communities could be found in (Arino *et al.*, 2007; Arino and Van Den Driessche, 2003; Arino and Van den Driessche, 2003; Arino and van den Driessche, 2006; Arino, 2009; Sattenspiel and Dietz, 1995; Allen *et al.*, 2008; Hanski and Gilpin, 1991).

Nonetheless, spatial heterogeneity along with different time scales require a model approach in which infectious individuals are able to successfully infect susceptible individuals from multiple patches, including their own. In (Sattenspiel and Dietz, 1995), an epidemic metapopulation model was used in which place of residence and current location was tracked at any given time. It was assumed that, in a two patch setting, $N_{ij}(t)$ represented the number of i-residents currently in j at time t in which residents would travel at a per capita rate $g_i \geq 0$ and would return at the per capita

rate $r_{ij} \geq 0$ with $r_{11} = r_{22} = 0$. In essence, this scenario would be easily represented in a directed graph and assumed to be strongly connected (significant travel rates). Moreover, an infection process was added on top of the demography and a two patch SIR model with constant population was formulated. In this case, it is assumed that individuals on patch i on average have $\kappa_i > 0$ contacts and the proportion of effective contacts is $\beta_{ikj} > 0$ in patch j for individuals from i being infected by infectious individuals from k. In a strongly connected system at an equilibrium implies that when one patch is at the disease free equilibrium (DFE), all patches are also at DFE. Similarly, when one is at the endemic equilibrium (EE), all other patches are also at EE. When not all patches are strongly connected, then only those that are strongly connected would be at the same equilibrium. Interestingly, changes in the traveling rates can reverse the stability of the DFE and EE (Arino and Van den Driessche, 2003, see Figure 3a). Meaning that traveling rates could have a big impact in the course of a disease outbreak since they have the ability to stabilize and destabilize the DFE.

While the model used in (Sattenspiel and Dietz, 1995) is a good way to model some epidemics it is clear that for highly complex diseases like measles, simulations would be challenging due to the amounts of required data, particularly, the way in which the population gets structured. In addition, modeling diseases like SARS in which infectious individuals also travel could be a great application but again a great deal of data would be required, not to mention the difference of time scales between disease dynamics and travel rates. However, insights from simple metapopulation models could be of great benefit in the understanding of global disease spread. Nonetheless spatial heterogeneity along with different time scales require a metapopulation model approach in which infectious individuals are able to successfully infect susceptibles from multiple patches without explicitly incorporating the movement of individuals

nor the concept of contacts.

2.2 Lagrangian Models: A New Approach

In this dissertation, a new approach for modeling disease dynamics is used, attempting to analyze the main factors driving disease spread. It is known that disease spread is facilitated by human (or in some cases reservoir) travel. The proposed approach tries to incorporate social factors, or their consequences, that modify the average pathogen transmission rates of communities. In addition, it uses a Lagrangian approach to keep track of individuals when they don't spend all their time in one particular community. Furthermore, population size heterogeneity is also considered since overcrowding, in some cases like vector borne diseases, could accelerate the spread of outbreaks.

This approach will ultimately require the use of social ecological tools, well known in resource allocation, in order to incorporate the direct impact of social factors into the transmission rates of individual communities. In particular, risk heterogeneity is studied here by assuming that social factors like violence, poverty, and lack of resources heavily burden a community, while good access to disease control measures, health care facilities, and availability of resources to minimize local crime and violence are the norm in one or more neighboring communities. Characteristics that are not foreign to conflict zones and neighboring communities in most developing countries heavily burdened by disease outbreaks.

2.2.1 Residence Times

In (Mossong *et al.*, 2008), the authors suggest the need of analyzing the clustering of individuals during the start of an epidemic. This is clearly what the new modeling approach (Lagrangian approach) in mathematical epidemiology is trying to

do. Nonetheless, even when more information about the different kinds of contacts is known, there are scenarios in which counter intuitive results are obtained. One would suggest that in a very congested area, TB would proliferate but this is not always the case. It also seems as most infections are generated at home. This could be because of our behavior towards strangers is more protective than towards our own family members. Perhaps, because in a congested public area, such as a train, we tend to modify our behavior to adhere to the norm or equilibrium established by the majority. Meaning that, depending on the place we find ourselves, we will have different behaviors and thus different risks of infections completely determined by the overall behavior of that place (cluster or patch).

Since the concept of contacts or effective contacts during an epidemic outbreak is somewhat ambiguous, in this section a different perspective will be used; one that indirectly keeps track of individuals. In particular, the proportion of time in a given unit (usually a day) an individual spends in a specific environment is explored. Due to the heterogeneity found in neighboring communities or even neighborhoods suggests the need to have a system that describes contagion depending on where an individual spends his/her time. In this case, heterogeneity is expressed as the level of risk of infection inherent to each environment or community. This method incorporates both the process of contagion while at the same time, it incorporates in an indirect way the spread of disease between interconnected environments via the visitation of individuals for leisure or work. At the same time it is assumed that the initial conditions of each individual environment promotes disease transmission heterogeneously. When considering epidemic models in a two environment (patches) setting, it is usually assumed that one has a significantly higher risk of infection and that individuals of both patches perform short term trips between the two patches without loosing their identity. By quantifying the average time an individual spends

in each patch (residence time) allows to indirectly track individuals, that is, following a Lagrangian perspective as shown in Figure 2.1 (Bichara *et al.*, 2015; Bichara and Castillo-Chavez, 2016). Notice that most models that incorporate mobility use an Eulerian perspective that describes migration between the patches.

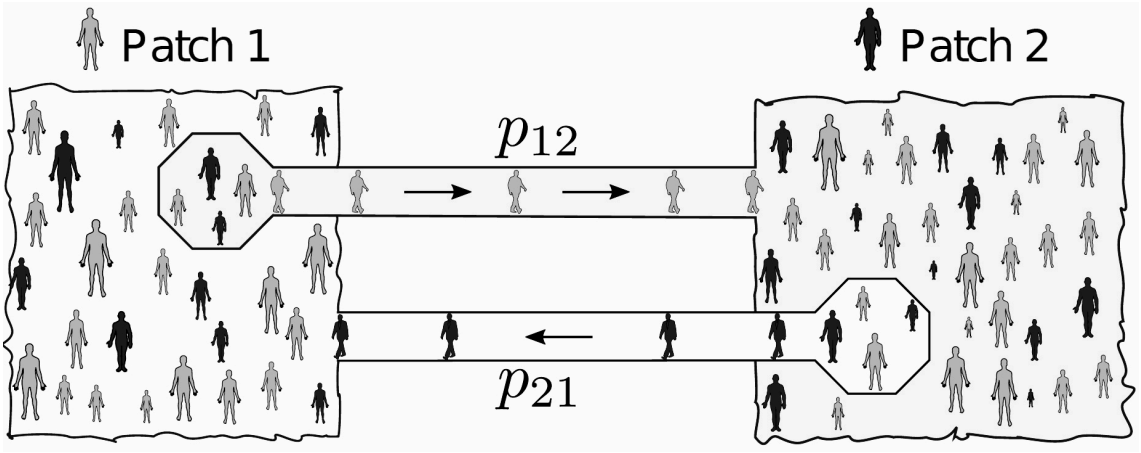

Figure 2.1: Dispersal of Individuals via a Lagrangian Approach.

Assuming that residents from Patch i spend a proportion of their time in Patch j (p_{ij}) and the rest of their time in their patch of origin, then for a two patch system

$$p_{11} + p_{12} = 1, \quad p_{21} + p_{22} = 1.$$

Similarly, the risk of infection in Patch i is β_i, and assuming that Patch 1 is the riskiest then $\beta_1 > \beta_2$ (for a two patch system). Notice that in this case susceptible individuals could get infected in either patch. In particular, susceptibles from Patch 1 present in Patch 1 ($p_{11}S_1$) could get infected from infectious individuals present in Patch 1 from any of the other patches. Similarly, susceptibles from Patch 1 present in Patch 2 ($p_{12}S_1$) could get infected from infectious individuals present in Patch 2 from any of the other patches. Following the same construction, the number of infectives in Patch 1 at a given time is determined by the sum of the infectives from both patches at that specific time, that is:

$$p_{11}I_1(t) + p_{21}I_2(t),$$

while the total number of individuals in Patch 1 is:

$$p_{11}N_1 + p_{21}N_2.$$

Thus the density of infected individuals in Patch 1 at time t, that is, the effective infectious proportion in Patch 1 is:

$$\frac{p_{11}I_1(t) + p_{21}I_2(t)}{p_{11}N_1 + p_{21}N_2}.$$

Hence, the rate of new infections of members of Patch 1 in Patch 1 is:

$$\beta_1 p_{11} S_1 \frac{p_{11}I_1(t) + p_{21}I_2(t)}{p_{12}N_1 + p_{22}N_2},$$

and the rate of new infections of members of Patch 1 in Patch 2 is:

$$\beta_2 p_{12} S_1 \frac{p_{12}I_1(t) + p_{22}I_2(t)}{p_{11}N_1 + p_{21}N_2}.$$

Similarly, the rate of new infections for individuals from Patch 2 can be found. Notice that the infectious in Patch i are only able to infect susceptible individuals present in Patch i.

As expected, the calculation of the basic reproduction number (using the next generation matrix approach as in (Van den Driessche and Watmough, 2002)) and the final epidemic size are quite complicated. Nonetheless, the special case:

$$p_{11} = p_{22} = 1, \quad p_{12} = p_{21} = 0,$$

in the absence of mobility is extremely useful, again for a two patch system. Modifying the residence times for both patches would allow to estimate the effect of certain mobility patterns or imposed travel restrictions, defined by all the residence times p_{ij} from the system (mobility matrix $\mathbb{P}$), on the final epidemic size.

While this approach helps incorporate some of the main types of heterogeneity influencing the spread of disease, a more advanced mathematical background or data availability is required in order to analyze more complex scenarios for instance, heterogeneity caused by the age of individuals.

Chapter 3

ANTI-VACCINE MOVEMENT: A SOCIAL CONTAGION

Vaccines and their impact on morbidity and mortality rates from infectious diseases are commonly considered one of the greatest public health success stories (Centers for Disease Control and Prevention (g), 2011). Nonetheless, there has been a growing anti-vaccine movement likely leading to a rise in incidence of highly preventable diseases such as measles. Anti-vaccine dialogue is prevalent both in celebrity culture and on the Internet. In this chapter, a compartmental model to study the anti-vaccine movement as a social contagion was developed. The model is then fit to population, birth rates, and vaccination rates data focusing on California, using time series data covering 19 years starting in 1995. The best fit model has good agreement with the data providing insight into the dynamics of the anti-vaccine movement.

3.1 Introduction

Infectious diseases have been a challenge for our society and a major factor shaping the history of man (Black *et al.*, 1977). According to the Centers for Disease Control (CDC), vaccines and their impact on infection and morbidity/mortality rates from infectious diseases can be considered one of the most significant public health success stories. As discussed in (Centers for Disease Control and Prevention (g), 2011) vaccination of each US birth cohort prevents "42,000 deaths and 20 million cases of disease".

Vaccination is one of the few cost-effective medical measures that result in population level broad benefit across the multiple dimensions of the population spectrum. Despite this, there is evidence in Western Europe, the United States, Japan, Aus-

tralia, and other countries of a growing anti-vaccine movement. The media plays a big role in the dissemination and sensationalization of vaccine objections, which is known as the "anti-vaccine movement" and has had a demonstrable impact on vaccination policies and individual and community health. In addition, our society is poorly educated on practical applications of risk and probability thus lacking the expertise and understanding that our individual choices can cause significant hardship to the broader public (Poland and Jacobson, 2001).

Since the publication in 1998, of the now retracted paper by (Wakefield *et al.*, 1998), that connected a number of disorders, including potential increased occurrence of autism, to Measles, Mumps, and Rubella (MMR) vaccine, there emerged an active anti-vaccine movement in the United States and the United Kingdom (Chen and DeStefano, 1998). At the current time, there are well over four hundred thousand anti-vaccine internet sites from a single simple Google search. A telephone survey was conducted in 2000 to a nationally representative sample of 1600 US parents of children < 6 years old (Gellin *et al.*, 2000). The results revealed that 1 in 4 parents believed that a child's immune system was 'weakened' by too many vaccines. Twenty-three percent believed that children got more immunizations than was good for their health, and fifteen percent did not want their next child to get at least one of the currently recommended vaccines.

Furthermore, internet usage statistics show approximately 84.9% of Americans are online. An estimated $75\% - 80\%$ of users search for health information online (Fox, 2008). Over half (52%) of users believe "almost all" or "most" information on health websites is credible (Fox and Rainie, 2000). In fact, many parents who exempt children from vaccination are more likely to have obtained information from the internet and more likely to have used certain anti-vaccination websites (Salmon *et al.*, 2005). Many would argue that we have become an information society where

information, accurate or inaccurate, is widely available, utilized, and promulgated across the world via the internet. This plays into widespread feelings on the part of many Americans who now view their government with various levels of mistrust (some legitimate, some not) further fueling concerns over 'governmental' recommendations regarding vaccine use, and governmental assurances regarding vaccine safety (Poland and Jacobson, 2001).

Unfortunately, parents who seek to delay or avoid routine vaccinations for their children put their own children at risk and their actions contribute to herd immunity failure even among highly vaccinated populations (Jacobson *et al.*, 2007). This movement has likely led to increase in cases of highly preventable diseases, including record cases of measles in 2014 as reported by the Center for Disease Control and Prevention. As of September 29, 2014, there have been 594 cases of measles, including 18 outbreaks accounting for 89% of reported cases that year (Centers for Disease Control and Prevention (f), 2014). Since 2001, this was the largest number of cases by almost a factor of 3 as compared to any other year. The majority of the cases have occurred in unvaccinated individuals.

The anti-vaccine movement has seen significant support from celebrities, who have a disproportionate access to a public platform (as compared to an average individual or parent). Recently, the news sources such as the New York Times have written extensively on the topic, predominantly critically. A few examples are included in (Shih, 2014; Norton, 2014; Chen, 2014).

While the anti-vaccine movement has been studied in the medical and social science community (Poland and Jacobson, 2001; Kata, 2010) and in context of the logical flaws in arguments against vaccines (Jacobson *et al.*, 2007), there has not been previous work done on the anti-vaccine movement as a social contagion. On the other hand, epidemiological models have been applied to spread of other ideas (Feynman

diagrams) as in (Bettencourt *et al.*, 2006) giving indication that the approach would be potentially applicable in this case.

Of particular interest in this context is that the spread of the social construct leads to literal epidemics, potentially elucidating the interactions between social and disease mechanisms. In this analysis, the anti-vaccine movement is treated as a contagious disease. Specifically, the interest lies in identifying recovery rates and transmission rates. This type of information could be beneficial to public health officials in understanding the nature of the anti-vaccine movement, potentially allowing for optimization and targeting of information campaigns.

Here, the analysis of vaccination trends in California, United States and the fit of a compartmental model to the vaccination data is presented. Leveraging birth rate information, the goal is to study whether spread of the anti-vaccine movement can be detected and modeled in vaccination rates for MMR: Measles, Mumps, and Rubella vaccine over the course of 19 years starting in 1995. The State of California was chosen as the focus of the analysis due to significant measles activity in the state as indicated in (California Department of Public Health, 2014). Preliminary analysis indicates that there doesn't appear to be an epidemic-like behavior in the data. One possibility to explain this outcome is that we are at the peak of the anti-vaccine "epidemic" and the current record number of cases of measles in 2014 will serve as a negative feedback mechanism for the trend.

3.2 Methodology

3.2.1 Data

As discussed above, while the model is for a social process, it will leverage measurable outcomes of the social process. Specifically, by using the data on vaccination

rates and birth rates. The incidence of new cases, will be estimated by multiplying the (1-vaccination rate) by the birth rate. For this analysis, it was also decided to focus specifically on the state of California, as the California data on birthrates is more extensive (covering more years) than national US birthrate data. Additionally, since there has been population growth but effectively constant number of births, population data was also included in the analysis in order to fit birth and death rates.

Specific data sources are described below.

Immunization Rates

www.cdc.gov/vaccines/imz-managers/coverage/imz-coverage.html: This website provides immunization rates for Children, Teens, and Adults for the United States as a whole and by state (and by vaccine type). This study will focus on the "Children Only" data. The data is available by year from 2013 back to 1995. An example data table from 2013 is found by navigating from the website above to "Children Only" to "Tables" on the 2013 line to the pdf of the table. In California, in 2013, the vaccination rate is 90.7 ± 5.3 (as can be read from the table). This study will focus its analysis on the vaccination rate. This will serve as the incidence data to fit the model (from this data, specifically, MMR vaccination rate, and the birth rate, will serve to estimate the number of unvaccinated children). As the data is provided by state, California data will be used.

Births Data

This website has California birth rates going back to 1960.
www.cdph.ca.gov/data/statistics/Pages/StatewideBirthStatisticalDataTables.aspx
This particular table:

www.cdph.ca.gov/data/statistics/Documents/VSC-2011-0201.pdf
provides birthrates from 2011 to 1960. For example, in 2011, there were 509,979 live births in CA.

The model will be set to 1994-2013 time interval, estimating births in 2012 and 2013 based on birthrate scaling from 1960-2011. The time interval of 1 year will be used with potential interpolation of 6 months to create more data points.

The time series of the vaccination data is presented in Figure 3.2. Birth rates for 2012 and 2013 were estimated by computing averages of previous years' birthrate data. The count data was derived by multiplying vaccination rates by the birthrate. In the model fitting methodology as described later, the S and I compartments are treated separately from the K_S and the K_I compartments.

Population Data

www.calrecycle.ca.gov/lgcentral/goalmeasure/disposalrate/Graphs/PopEmploy.html
This website provides California time series data. In addition to the population data, to fit fractions of the population that are children the time series data in the following link that provides information on number of children under the age of 18 was used:
www.kidsdata.org/topic/32/childpopulation/table#fmt=139&tf=79&sort
ColumnId=0&sortType=asc.

3.2.2 Model

Population model

To model the vital dynamics of the population a compartmental population model with two age groups, kids (K) and adults (A), and birth rate μ, where kids are defined to be 18 years and younger was used. As shown in Figure 3.1, the number of births in California has remained approximately constant for several years, but the population

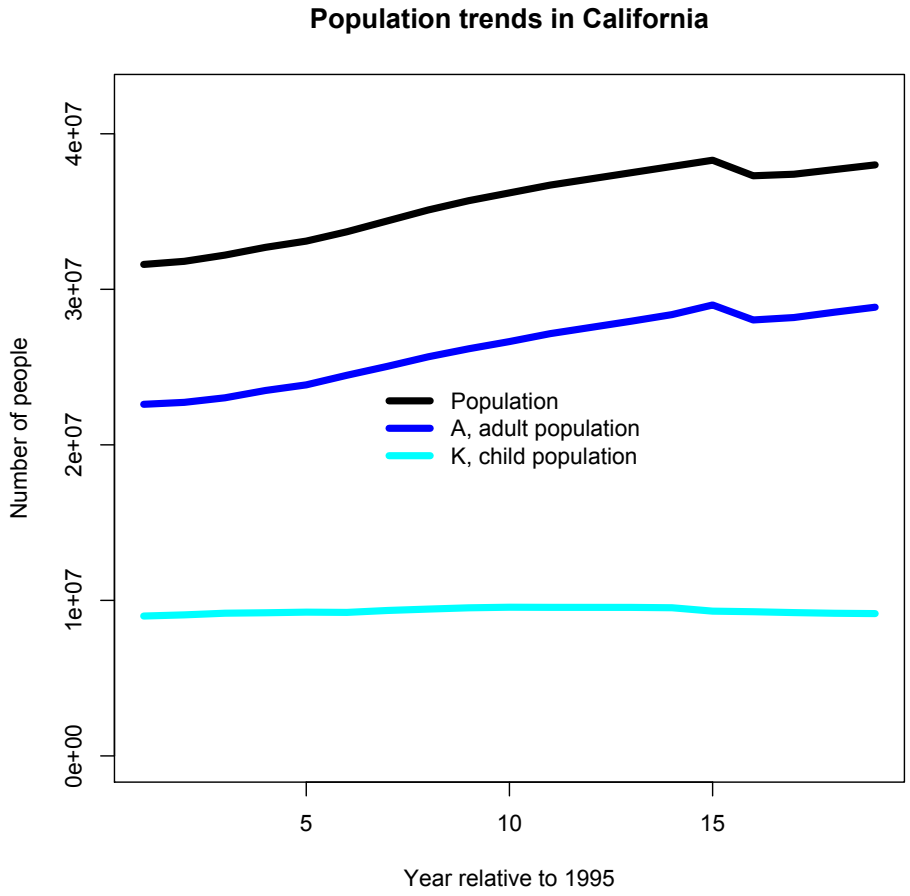

Figure 3.1: Time Series of the Population Data Including Children and Adult Populations in a given Year.

size is growing. This indicates that the birth rate of the adults must be falling in time. This effect was then approximated using a linear formulation of the birth rate, $\mu = \mu_0 + \mu_1 t$, where t is the time, in years, relative to January 1, 1995.

The equations for the model are:

$$dK/dt = (\mu_0 + \mu_1 t)A - \omega K$$
$$dA/dt = \omega K - \delta A, \tag{3.1}$$

where ω is the rate at which children mature to the adult compartment, and δ is the net rate at which individuals leave the adult compartment, through the processes of

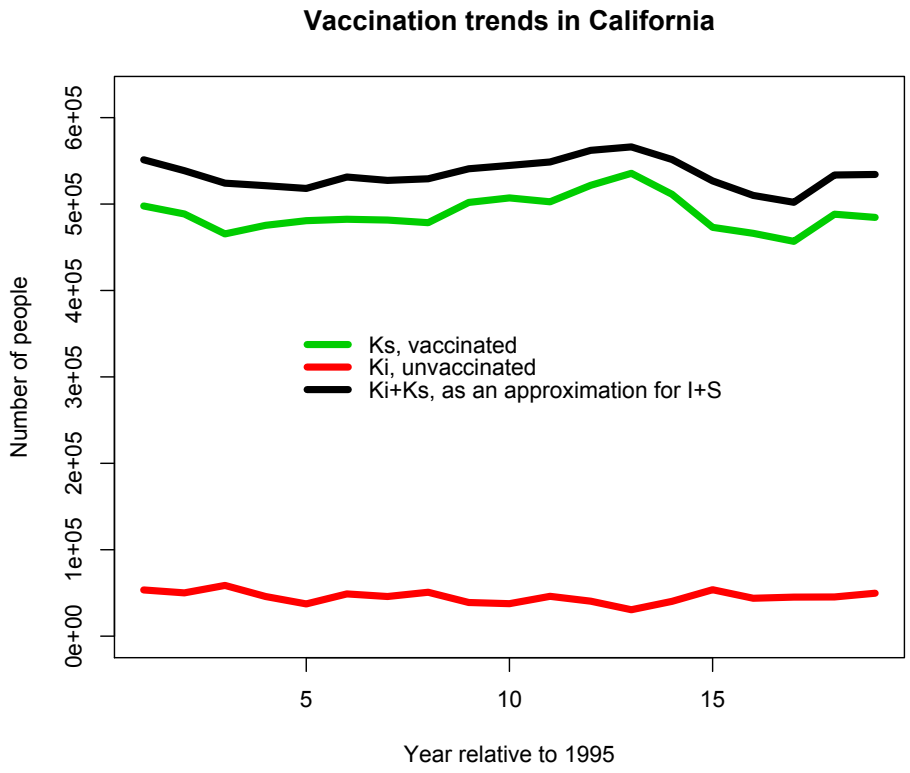

Figure 3.2: Time Series of the Data Including Population of Vaccinated and Unvaccinated Children in a given Year.

emigration/immigration or death. The death rate of children was ignored. The total population size is $N = K + A$.

The parameters of this model (μ_0, μ_1, ω, and δ) are fit to the time series of California population data for kids and adults.

Anti-vaccine contagion model

To model the social contagion of anti-vaccination ideology, a four compartment contagion model was employed, with adults divided into vaccinators and anti-vaccinators. Vaccinators were considered to be susceptible to be infected with the ideology of the anti-vaccination movement. These two types of adults will be refere as A_S and A_I,

for the vaccinators and anti-vaccinators, respectively. Children of these two groups are K_S and K_I, respectively.

The model equations are:

$$\begin{aligned}
\frac{dK_S}{dt} &= (\mu_0 + \mu_1 t)A_S - \omega K_S \\
\frac{dK_I}{dt} &= (\mu_0 + \mu_1 t)A_I - \omega K_I \\
\frac{dA_S}{dt} &= \omega K_S - \beta A_S A_I/(A_S + A_I) - \delta A_S + \gamma A_I \\
\frac{dA_I}{dt} &= \omega K_I + \beta A_S A_I/(A_S + A_I) - \delta A_I - \gamma A_I,
\end{aligned} \tag{3.2}$$

where β is the transmission rate of anti-vaccination ideology from the A_I class to the A_S class, and γ is the rate at which anti-vaccinators "recover" from their ideology and become vaccinators. All other parameters related to the population dynamics are as described in the previous section.

The model parameters β and γ are fit to the time series of data on the number of vaccinated and unvaccinated children in California. The initial fractions of vaccinated kids, f_{K_S}, and adults who vaccinate, f_{A_S}, at time $t = 0$ is also estimated.

3.2.3 Estimation of Model Parameters

To estimate the parameters of the population and contagion model that optimally describe the associated data samples, the parameters of the models were randomly sampled from broad uniform distributions, and calculate the Pearson χ^2 goodness-of-fit statistic comparing the model to the data sample. The uniform distribution sampling range is chosen to be large enough to ultimately include the parameter optimal value and at least a ± 5 standard deviation range about that value. This procedure is repeated one million times for each sample with the use of NSF XSEDE high-throughput computing resources in order to determine the parameter hypotheses

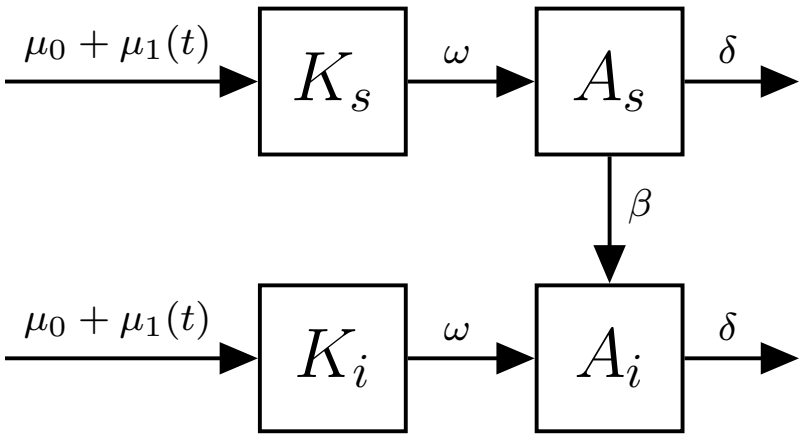

Figure 3.3: *KSI* Model where the Flow γ from A_i to A_s is Zero.

that minimize the Pearson χ^2 goodness-of-fit statistic. To determine the parameter 95% confidence intervals, the Pearson χ^2 statistic is corrected for over-dispersion using (McCullagh *et al.*, 1973).

3.3 Results

The parameter fitting procedure was performed in two tiers. The parameter hypotheses for the population parameters (μ_0, μ_1, ω, δ) in the 95% confidence interval are presented in Figure 3.4. The parameter hypotheses for the anti-vaccine and initial condition parameters (β, f_{Ks}, f_S) in the 95% confidence interval are presented in Figure 3.5. The best fit parameters values along with the 95% confidence interval for each fitted parameter are in Table 3.1

3.4 Discussion

In this analysis, a compartmental model of the anti-vaccine movement was developed. To account for the variability in birth rates over the temporal window under consideration, 7 parameters were fitted. The recovery parameter (γ) was identified

Table 3.1: KSI Model Best Fit Parameters.

Parameter	Value	95% Confidence Interval
μ_0	0.0235	[0.0216, 0.0250]
μ_1	-0.0003	[-0.0005, -0.0002]
δ	0.0104	[0.0070, 0.0130]
ω	0.0821	[0.0668, 0.0964]
β	0.1295	[0.0404, 0.1609]
γ	0	not fitted
f_{Ks}	0.9958	[0.5599, 1]
f_S	0.9098	[0.8870, 0.9310]

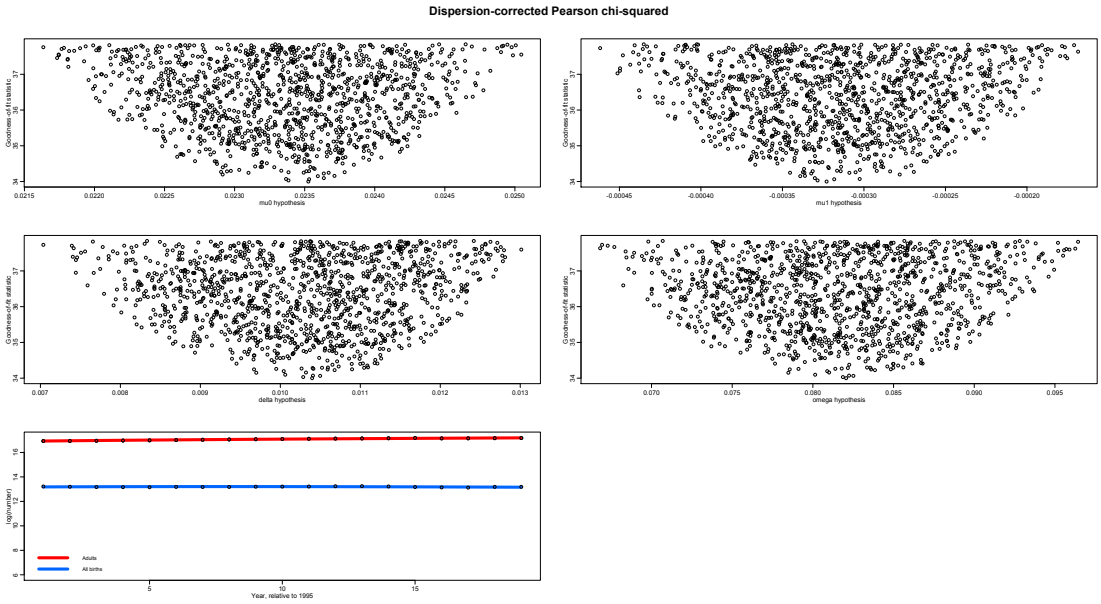

Figure 3.4: Population Parameters and Overlay of Best Fit Model (Log Scale) on the Data.

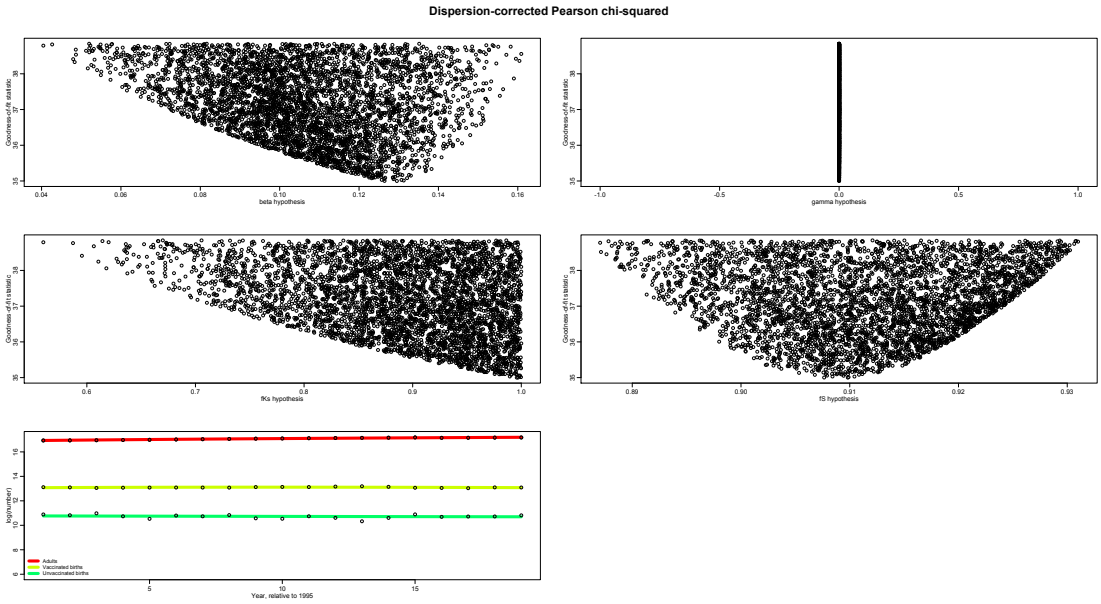

Figure 3.5: Anti-vaccine Parameters and Overlay of Best Fit Model (Log Scale) on the Data.

to be 0 in early experiments and as illustrated in Figure 3.5. This, in itself, is an interesting outcome of the analysis, as it appears that once an individual is infected with the anti-vaccine philosophy, there is no recovery. Therefore, it is likely valuable to focus the public health and vaccine information campaigns on susceptible populations (as opposed to infected) to minimize the number of individuals that move between those classes.

Almost all of the parameters fitted (μ_0, μ_1, δ, ω, β, f_S) had very narrow ranges in the 95% confidence interval, indicating a rather good fit to the existing data. Fitting of f_{Ks} (the initial fraction of children vaccinated), on the other hand, did not produce a close fit. The best fit model, however, is produced with the parameter hypothesis of almost 1 (100% of children are initially vaccinated). This is consistent with the fact that much of the anti-vaccination trend has been attributed to the retracted Wakefield paper which was published in 1998.

Generally, the data and the resulting model do not have the shape of an epidemic,

and yet, the occurrence of measles has been rising. This is potentially due to such phenomena as herd immunity, where just a small fraction of anti-vaccinators (which could remain constant) lead to outbreaks of the disease. One other hypothesis that may explain this data is that we have reached the peak of the anti-vaccine epidemic and the trend is now beginning to reverse. The reversal of the trend is not at the moment observed in the data, but may be apparent with analysis covering more recent years (once the data becomes available).

As potential future work, a vector model of infection where the vector could be the prevalence of celebrity advocacy for the anti-vaccine movement or anti-vaccine websites may be considered. At writing, it is not clear that data sets that would support such analysis exist.

3.5 Conclusion

In order to provide insight into the anti-vaccine social movement, parameters for a compartmentalized model were defined and fitted. In this research, the social contagion was modeled leveraging measurable outcomes (specifically, vaccination rates). This is the first analysis of its kind and the best fit model is indeed a good fit to the data. This analysis can be used to inform public health officials on the dynamics of the anti-vaccine movement and allow optimization of resources. In future work, it may be worthwhile to consider other factors - such as celebrity advocacy for the anti-vaccine movement and the fear inflicted by websites or social media using a vector-based approach.

Chapter 4

THE ROLE OF SHORT-TERM DISPERSAL AND SOCIAL INSECURITY ON THE TRANSMISSION DYNAMICS OF ZIKA VIRUS IN AN EXTREME IDEALIZED ENVIRONMENT: THE CASE OF ZIKA VIRUS IN EL SALVADOR.

Background During the last months of 2015, Zika virus (ZIKV) reached El Salvador. The first case of Zika virus infection was reported in November 2015, an event followed by an explosive outbreak that generated over 6000 suspected cases by January 2016. National agencies promptly began the implementation of known control measures like vector control and recommending the use of repellents. Further, in response to the alarming and growing number of microcephaly cases in Brazil, the importance of safe sex and avoiding pregnancies for a period of two years was stressed.

Methods The goal of this study is to explore the role of short-term mobility within communities characterized by extreme poverty, crime, and violence. Specifically, the role of short-term mobility between two idealized interconnected, highly distinct communities is explored in the context of ZIKV outbreaks, in which mobility patterns are affected by social factors inherent to each community. In order to highlight the possible effects that short-term mobility might have on the dynamics of a ZIKV outbreak, a Lagrangian modeling approach within a two-patch setting within highly distinct environments is used. Moreover, the overall goal is to understand how mobility might reduce the overall number of cases, not just in the most affluent areas but everywhere. Outcomes depend on existing mobility patterns, levels of disease risk, and the ability of federal or state public health services to invest and effectively implement in resource limited areas, particularly in those where violence is systemic.

Results The results, via simulations, of highly polarized and simplified scenarios

are used to assess the role of mobility. Observing the results, it was evident that matching observed patterns of ZIKV outbreaks could not be captured without incorporating increasing levels of heterogeneity, particularly those associated with the vector populations.

Conclusions As a result, short-term mobility along with elevated violence rates, that somehow have a negative impact on the ability for health crews to establish effective vector control measures (in certain communities), leads to the existence of disease sources (under certain mobility patterns) and to the literal waste of resources allocated to vector control efforts, if these are not implemented in the entire region in a reasonable way. Without loss of generality, similar results during a Dengue fever and Chikungunya outbreak are expected. Moreover, the number of highly heterogeneous environments (patches), as well as, the variations on patch connectivity structure required to match ZIKV patterns could not be met within the highly aggregated two-patch model used in the simulations.

4.1 Introduction

Zika virus (ZIKV), an emerging vector-borne disease closely related to yellow fever, dengue and West Nile (Hayes *et al.*, 2009), has taken the Americas by storm. ZIKV is a flavivirus, transmitted primarily by female *Aedes aegypti* mosquitoes, which is also a competent vector in the transmission of dengue and chikungunya. According to the (Centers for Disease Control and Prevention (n), 2016), as of February 9, 2016, ZIKV cases had been reported throughout the Caribbean, Mexico and South America with the exception of Chile, Uruguay, Argentina, Paraguay and Peru. As of September 23, 2016, only Canada, Chile and Uruguay haven't confirmed autochthonous, vector-borne transmission of Zika virus disease (Centers for Disease Control and Prevention (i), 2016; Pan American Health Organization, 2017). In fact, several states within

the United States had also reported ZIKV cases(Petersen, 2016) and while ZIKV was expected to be managed effectively within the USA, the possibility of localized ZIKV outbreaks couldn't be ruled out since there were many areas in which capable vectors were endemic.

While phylogenetic analyses have revealed the existence of two main virus lineages (African and Asian) (Faye *et al.*, 2014; Haddow *et al.*, 2012), no concise clinical differences have been identified between infections with different strains. Nonetheless, it is important to note that most African samples come from a rhesus sentinel in Uganda during primate and mosquito surveillance efforts aimed at assessing Yellow Fever trends in 1947, when ZIKV was first discovered (Dick *et al.*, 1952). It is believed that the African lineage has circulated primarily in wild primates and arboreal mosquitoes, such as *Aedes africanus*, within a narrow equatorial belt running across Africa and into Asia. Spillover events to humans have rarely occurred, or not recorded, even in areas found to be highly enzootic (Fauci and Morens, 2016; Musso *et al.*, 2015). The Asian lineage, seems to have originated from the adaptation of the virus as it successfully invaded a different vector, *Aedes aegypti*, a vector capable of infecting human populations rather effectively due to its adaptability to urban and semi-urban environments, (Fauci and Morens, 2016; Haddow *et al.*, 2012).

While ZIKV was first found in 1947, the first human infection was reported in Nigeria in 1954 (Macnamara, 1954). It is believed that the first time ZIKV moved out of Africa and Asia was during the 2007 outbreak in Yap Island in the Federated States of Micronesia (Duffy *et al.*, 2009); followed by an even larger outbreak in French Polynesia in 2013-2014 (Cao-Lormeau and Musso, 2014); then reaching New Caledonia, the Cook Islands and Eastern Islands (Musso *et al.*, 2014). Decades old data, from African researchers, support the possibility that ZIKV spread might have been facilitated by prior chikungunya outbreaks (Fauci and Morens, 2016). A pattern

seen once again in 2013 when chikungunya spread from west to east and then followed by ZIKV outbreaks (Fauci and Morens, 2016).

In early 2015, ZIKV was detected in Brazil and phylogenetic analyses placed the Brazilian strains within the Asian lineage (Zanluca *et al.*, 2015); the same strain detected during the 2013-2014 French Polynesian outbreak (Cao-Lormeau *et al.*, 2014). Since the first detection of ZIKV in Brazil, we have seen an explosive outbreak quickly reached Bolivia, Brazil, Colombia, Ecuador, French Guyana, Guyana, Paraguay, Suriname, and Venezuela (Centers for Disease Control and Prevention (l), 2016). Furthermore, within few months from the first case in Brazil, several Central America countries have been invaded by ZIKV, including Costa Rica, El Salvador, Guatemala, Honduras, Nicaragua, and Panama (Centers for Disease Control and Prevention (m), 2016). As of September 23, 2016, all of the nations in the Americas have experience active ZIKV outbreaks with the exception of Canada, Chile, and Uruguay(Centers for Disease Control and Prevention (i), 2016; Pan American Health Organization, 2017). This rapid geographic expansion of ZIKV led the World Health Organization (WHO) to declare it an international public health emergency (World Health Organization (b), 2016).

It has been estimated that about 4 out of 5 ZIKV infections are asymptomatic (Centers for Disease Control and Prevention (i), 2016; Duffy *et al.*, 2009), something common among vector born diseases spread by *Aedes aegypti* mosquitoes. ZIKV clinical manifestations include, arthralgia, particularly swelling, mild fever, lymphadenopathy, skin rash, headaches, retro orbital pain, and conjunctivitis, which normally last for 2-7 days (Centers for Disease Control and Prevention (i), 2016; World Health Organization (b), 2016; Zanluca *et al.*, 2015). It is important to note that many of these symptoms are also associated with Dengue infections. These similarities, could cause high levels of uncertainty in the efforts to asses the total number

of patients infected with ZIKV. As a result of these sources of mis-identification, it is believed that the total ZIKV burden may be higher than what it has been reported (Fauci and Morens, 2016; Salvador and Fujita, 2015). Moreover, co-infection with other diseases like dengue are not uncommon and as a result ZIKV diagnosis is difficult (Dupont-Rouzeyrol *et al.*, 2015). Nonetheless, scientists from Arizona State University and Harvard University have created a diagnostic tool, similar to a pregnancy test, capable of given a quick, effective, simple and inexpensive way of diagnosing ZIKV infections (Harvard Gazette, 2016; The Biodesign Institute, 2016), and a powerful tool that could be used to prevent the uncontrolled spread of ZIKV countries with limited resources.

Since, ZIKV infections have been linked with neurological (microcephaly) and auto-immune (Guillain-Barré syndrome) complications, the lack of an approved vaccine is a concern. In addition, evidence supports sexual transmission, a new transmission pathway for a vector born disease (Centers for Disease Control and Prevention (k), 2016; World Health Organization (b), 2016). Preventive education on ZIKV transmission modes are essential in order to halt its spread at the regional, national and global levels. Basic control measures are limited to vector control, including the use of insect repellents, the use of protection while engaged in sexual activity and sex abstinence (Centers for Disease Control and Prevention (k), 2016).

Furthermore, resource limited and poor nations face additional challenges that make the use of standard efforts and approaches aimed at controlling vector borne diseases ineffective. These challenges are often driven by social factors that cause extreme variations in the levels of public safety, gang violence and conflict. Ignoring these factors affecting the weakest communities, promotes the global spread of diseases and poses a serious threat to global health [see (Patterson-Lomba *et al.*, 2016; Espinoza *et al.*, 2016; Perrings *et al.*, 2014; Castillo-Chavez *et al.*, 2015; Patterson-

Lomba *et al.*, 2015; Zhao *et al.*, 2014; Chowell *et al.*, 2015)]. The importance of focusing on the weakest links of global transmission networks becomes obvious when analyzing the levels of violence in Latin America and the Caribbean, housing 9% of the global population but accounting for 33% of the world's homicides (Jaitman, 2015). In this study, the impact associated with restrictions to public safety, which affect mobility and subsequently the local risk of infection, might have on the dynamics of ZIKV transmission and control are analyzed. The long-term goal is to limit the role violence and conflict play on the overall health patterns of individuals living in the Caribbean, particularly in El Salvador.

4.2 Single Patch Model

A simplified vector-borne transmission model is used as a building block for the derivation of highly simplified two-patch scenarios. A two-patch models is then used to explore the role of residence times and risk of infection (possibly defined by underlying levels of violence or a lack of a health-medical infrastructure or a combination of both) on the dynamics of ZIKV. The general version of an n-patch framework and its analysis can be found in (Bichara and Castillo-Chavez, 2016) and similar studies can be found in (Espinoza *et al.*, 2016; Moreno *et al.*, 2017a).

Patch heterogeneity is incorporated by the assumption that, while the first patch experiences low levels of security, making it difficult to carry out sustainable vector control efforts, the second patch is considered to be safe with access to reasonable health services on demand. In other words, a highly bi-modal situation, an idealized situation, that does not capture the levels of complexity and heterogeneity experienced in conflict or crime ridden communities.

Hence, the simulations are based on highly idealized exploratory settings that might lead to realistic conclusions when these models are parameterized using "re-

alistic" parameter estimates. While highly detailed models require huge amounts of data including information that needs to be collected or measured within accepted protocols, the proper parametrization of these detailed models may require detailed accounts of the individuals involved. An example is the work done by the EpiSims project (Stroud *et al.*, 2007) that used individuals' daily mobility activities to model spread of disease in the city of Seattle. The kind of worthwhile and far reaching project this paper aims to motivate in the context of the interconnection of communities where violence and health disparities are the norm.

In this study, it is assumed that there are two patches with contrasting risks of infection (high and low risk). Each patch is made up of individuals experiencing the same degree of risk of infection throughout the patch, risk is an inherent function of the patch. Consequently, all individuals while in Patch 1 will be experiencing high risk of infection, while those in Patch 2 will be experiencing low risk. In short, the movement of individuals as a consequence of daily activities could alter the proportion of the time each individual spends on a given patch. The longer an individual stays in Patch 1, the more likely it is to become infected. The level of patch-specific risk to infection in this study is captured by the parameter $\hat{\beta}_i$, $i = 1, 2$. More specifically, $\hat{\beta}_1 \gg \hat{\beta}_2$. This assumption models, in a rather simplistic way, the health disparities that could be addressed within highly polarized settings. In short, this is a first effort aimed at exploring the role of risk and mobility on the dynamics of ZIKV in a world where two highly-distinct mobile communities co-exist. The case of Johannesburg and Soweto in South Africa, or North and South Bogota in Colombia, or Rio de Janeiro and adjacent favelas in Brazil, or gang-controlled and gang-free areas within San Salvador, are but some of the unfortunately large number of pockets dominated by conflict or high crime within urban centers around world. The short time scale dynamics of individuals (daily mobility as they go to work or carry out on other

activities including attendance to schools and universities) in both patches are incorporated within this model with the analysis (numerical simulations) carried out over the duration of a single outbreak.

4.2.1 The Aedes Aegypti Mosquito Feeding Habits

ZIKV transmission is the result of a bite from an infected female mosquito of the genus *Aedes* (subgenus *Stegomyia*) (Engelthaler *et al.*, 1997; WHO (a), 2017). The most predominant and at the same time the most effective ZIKV vector is *Aedes aegypti*. However, the Asian tiger mosquito, *Aedes albopictus*, is also able to transmit ZIKV (WHO (a), 2017). In addition, their ability to breed in small amounts of still water, as small as a bottle cap, and egg resistance to long periods of drought (as long as one year) makes them ideal for an environment with excess trash and decaying infrastructure, usually found around large urban centers. Consequently, unplanned rapid urbanization or poorly planned urbanization has the potential to provide abundant nesting grounds for mosquitoes and when combined with rapid human population growth, it increases the average number of encounters between humans and mosquitoes. Not to mention that in some regions, abiotic factors support the *Aedes aegypti* breeding cycle throughout the entire year.

While female *Aedes aegypti* mosquitoes consume plant carbohydrates for energy and maintenance reserves, blood meals are required in order to provide enough nutrients to complete the vitellogenesis process during each gonotrophic cycle (Scott and Takken, 2012). Female *Aedes aegypti* mosquitoes are diurnal and usually prefer to have multiple blood meals during every gonotrophic cycle. In addition, *Aedes aegypti* exhibits a preference for human blood and will not feed on sugar when human blood meals are available. Studies show that in some cases over 90% of the blood meals come from humans (Scott and Takken, 2012). A behavior that seems to improve the

nutritional aspects of survival and it is even suggested as an adaptation to optimize fitness (Scott and Takken, 2012). Furthermore, *Aedes aegypti* are considered efficient vectors since they are easily disturbed while feeding leading to multiple bites from multiple hosts to complete one blood meal (Jansen and Beebe, 2010). Meaning that entire families could get infected by a single mosquito in a period of 2 days. Moreover, their preference for human hosts has led DENV (another disease transmitted by this mosquito) to no longer require a sylvatic cycle and easily achieve endemicity in these environments. Mosquitoes are capable of transmitting the virus from one person to the next if it bites a susceptible individual immediately after biting and acquiring the virus from an infected individual (or within one day before the onset of symptoms). Otherwise, it takes between 4 to 15 days for the virus to replicate in the mosquito's salivary glands and become infectious for the rest of its life (Towers *et al.*, 2016). ZIKV infection doesn't have an adverse impact on mosquitoes. On average, *Aedes aegypti* mosquitoes live for 21 days but their life span ranges from two to three weeks in the wild and up to 65 days in a laboratory setting. In addition, while it is known that ZIKV could be transmitted vertically in mosquitoes (Ciota *et al.*, 2017) and humans, in this study the focus will be on direct transmission. Finally, since mosquitoes are restricted to a short range of travel, ZIKV spread depends mostly on human mobility patterns. Meaning that, highly mobile populations living in regions undergoing active ZIKV outbreaks are highly likely to be the main drivers of ZIKV spread.

4.2.2 Force of Infection and Model

One of the most important factors of the vector borne model is to determine an appropriate force of infection for both hosts and vectors. In particular, it is important to have a sense of the process and how both host and vectors get infected. It is

clear that female vectors require of a blood meal in order to lay eggs and reproduce. Then, the force of infection is determined by the product of: average number of meals a mosquito has during a day; the average proportion of meals that comes from a human host; the average number of bites it requires to complete a meal; the proportion of female mosquitoes to hosts; the probability of infection per bite; the number of susceptibles; and the proportion of infected mosquitoes (see Table 4.1 for parameter values).

Table 4.1: Force of Infection Parameters

Symbol	Description	Value	Units	Reference
m	Blood meals	0.76	$\frac{meal}{day*mosquito}$	(Scott and Takken, 2012)
ρ	Prop. human meals	0.9	$human$	(Scott and Takken, 2012)
α	Bites	$1-5$	$\frac{bites}{meal}$	(Scott and Takken, 2012)
f_v	Prop. Female vectors	0.5	–	–
β_{hv}	Prob. of Infection	$[0,1]$	$\frac{1}{bite}$	–

Notice that in this model $b = m\rho\alpha f_v$ ranging from 0.34 to 1.71, similar to the range used in (Maxian *et al.*, 2017). It is worth to mention that a study conducted on the susceptibility of Italian *Aedes aegypti* suggests that the probability of infection from an infected meal to mosquitoes is $\beta_{hv} = 26\%$ (Di Luca *et al.*, 2016).

As a result, the ZIKV dynamics single patch model involves hosts and vectors populations of size N_h and N_v, respectively. Both populations are then subdivided into sub-populations defined by ZIKV epidemiological states. The transmission process is then modeled as the result of the interactions of these sub-populations. On that account, the host population is subdivided into susceptible S_h, latent E_h, infectious asymptomatic $I_{h,a}$, infectious symptomatic $I_{h,s}$ and recovered R_h individuals. Similarly, S_v, E_v and I_v denote the susceptible, latent and infectious mosquito sub-

populations, respectively. Since the focus is on the study of disease dynamics over a single outbreak, hosts' demographics are neglected, while it is assumed that the vector's demographics do not change, meaning that, the per capita birth and death mosquito rates are the same. Since recent reports (Centers for Disease Control and Prevention (i), 2016; Duffy *et al.*, 2009) suggest the presence of large numbers of asymptomatic ZIKV infectious individuals, two classes of infectious $I_{h,a}$ and $I_{h,s}$, that is, asymptomatic and symptomatic infectious individuals will be considered. Moreover, due to the lack of knowledge regarding the dynamics of ZIKV transmission, it is assumed that $I_{h,a}$ and $I_{h,s}$ individuals are equally infectious. These assumptions support the reduction of the model to a single infectious class $I_h = I_{h,a} + I_{h,s}$, nonetheless, both infectious classes will be used as it may be desirable to keep track of both types and the overall burden of ZIKV. These assumptions might not be too bad given the current knowledge of ZIKV epidemiology and the fact that ZIKV infections, in general, are not severe. Meaning, that voluntary self-reporting are expected to be low. Furthermore, given that the infectious process of ZIKV is somewhat similar to that of dengue, parameters estimated in dengue transmission studies within El Salvador were used through out this study. In addition, ZIKV basic reproduction number estimates are taken from outbreak data collected in Barranquilla Colombia (Towers *et al.*, 2016). Furthermore, selected parameters ranges used in this study benefited from prior estimates using data from the 2013-2014 French Polynesia outbreak (Kucharski *et al.*, 2016), some of the best available at the time. The dynamics of the prototypic single patch system, single outbreak, can be modeled using the following standard nonlinear system of eight differential equations representing each of the epidemiological stages of ZIKV (Brauer *et al.*, 2012):

$$
\begin{cases}
\dot{S}_h = -b\beta_{vh} S_h \frac{I_v}{N_h} \\
\dot{E}_h = b\beta_{vh} S_h \frac{I_v}{N_h} - \nu_h E_h \\
\dot{I}_{h,s} = (1-q)\nu_h E_h - \gamma_h I_{h,s} \\
\dot{I}_{h,a} = q\nu_h E_h - \gamma_h I_{h,a} \\
\dot{R}_h = \gamma_h (I_{h,s} + I_{h,a}) \\
\dot{S}_v = \mu_v N_v - b\beta_{hv} S_v \frac{I_{h,s}+I_{h,a}}{N_h} - \mu_v S_v \\
\dot{E}_v = b\beta_{hv} S_v \frac{I_{h,s}+I_{h,a}}{N_h} - (\mu_v + \nu_v) E_v \\
\dot{I}_v = \nu_v E_v - \mu_v I_v
\end{cases}
\tag{4.1}
$$

The parameters of Model 4.1 are collected and described in Table 4.2, while the model flow diagram is presented in Fig 4.1.

Table 4.2: Description of the Parameters Used in System (4.1).

Parameter	Description	Value
β_{vh}	Infectiousness of human to mosquitoes	0.26
β_{hv}	Infectiousness of mosquitoes to humans	0.5
b_i	Biting rate in Patch i	0.8
ν_h	Humans' incubation rate	$\frac{1}{7}$
q	Fraction of latent becoming asymptomatic and infectious	0.1218
γ_i	Recovery rate in Patch i	$\frac{1}{5}$
p_{ij}	Proportion of time residents of Patch i spend in Patch j	$[0, 1]$
μ_v	Vectors' natural mortality rate	$\frac{1}{13}$
ν_v	Vectors' incubation rate	$\frac{1}{9.5}$

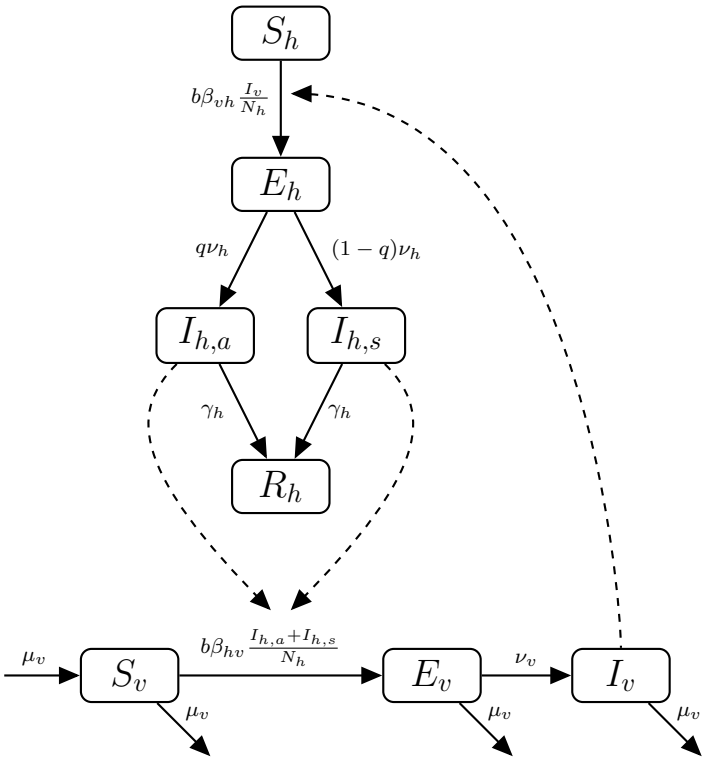

Figure 4.1: Flow Diagram of Model (4.1)

The basic reproduction number for this prototypic model, that is, the average number of secondary infections generated by a typical infectious individual in a completely susceptible population or where nobody has experienced a ZIKV-infection is computed by taking $S(0) = N_h$ in Model (4.1). The basic reproduction number is given by

$$\begin{aligned} \mathcal{R}_0^2 &= \frac{b^2 N_v \beta_{vh} \beta_{hv} \nu_v [(1-q)\gamma_h + q\gamma_h]}{N_h \gamma_h^2 \mu_v (\mu_v + \nu_v)} \\ &:= \mathcal{R}_{0,s}^2 + \mathcal{R}_{0,a}^2. \qquad (4.2) \\ \mathcal{R}_0 &= \sqrt{\frac{N_v b^2 \beta_{vh} \beta_{hv} \nu_v}{N_h \gamma_h \mu_v (\nu_v + \mu_v).}} \end{aligned}$$

Notice that the reduced form corresponds to the basic reproduction number when the two classes of infective are combined, that is, $I_h = I_{h,a} + I_{h,s}$.

The dynamics of the single patch model are well known. In short, an $\mathcal{R}_0 < 1$ indicates that an epidemic is unable to develop and the proportion of introduced infected individuals decrease, while an $\mathcal{R}_0 > 1$ indicates that the infected host population grows, and an outbreak takes place since the number of cases from the second generation exceeds the initial size of the introduced infected population at time $t = 0$. Finally, when $\mathcal{R}_0 > 1$, the population of infected individuals eventually decreases and the disease dies out since it is only modeling a single outbreak.

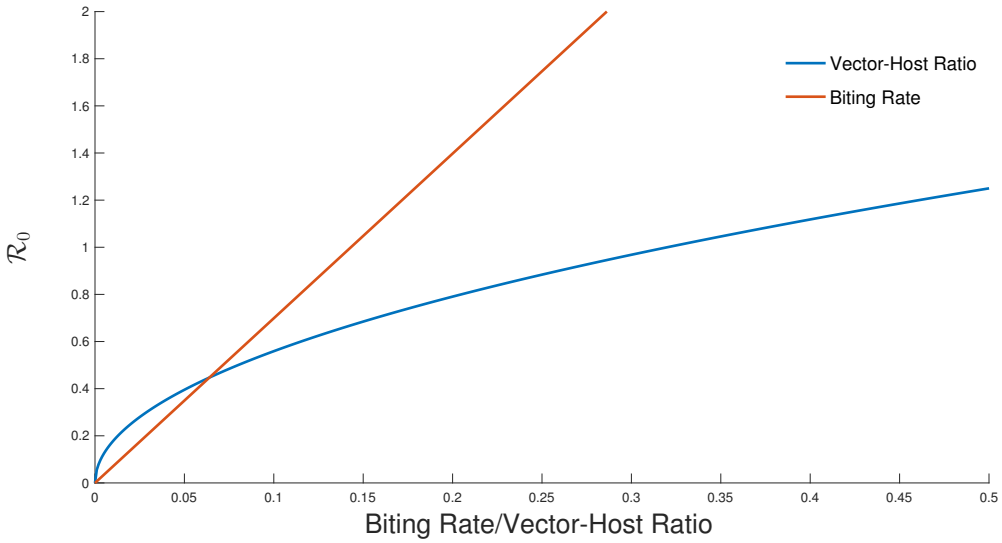

Figure 4.2: Basic Reproductive Number as a Function of the Vector-Host Ratio; Biting Rate.

4.3 Basic Reproductive Number Sensitivity Analysis

Partial rank correlation coefficients (PRCCs) for the aggregate $\mathcal{R}_0$ and each of the input parameters were produced from a single replication with 1,000,000 runs to graphically evaluate the monotonicity between a given input parameter and the aggregate $\mathcal{R}_0$ using the distributions from Table 4.3 (see figures 4.3 and 4.4). The corresponding value of these PRCCs corresponds to the level of statistical influence

the associated input parameter has on the variability of the aggregate $\mathcal{R}_0$ due to its own estimation uncertainty. PRCCs are statistically significant when $|PRCC| > 0.5$. The larger the magnitude of the PRCC, the more significant the parameter is in generating uncertainty or variability in $\mathcal{R}_0$. The sign of the PRCC indicates whether an increase in a parameter will lead to a higher $\mathcal{R}_0$ or lower $\mathcal{R}_0$.

Table 4.3: Parameters Used for the Sensitivity Analysis of Formula (4.2).

Parameter	Description	Distribution
β_{vh}	Infectiousness of human to vectors	$\mathcal{U}(0, 1)$
β_{hv}	Infectiousness of vector to humans	$\mathcal{U}(0, 1)$
b_i	Biting rate in Patch i	$\mathcal{U}(0, 2.5)$
γ_i	Recovery rate in Patch i	$\mathcal{U}(3, 7)$
N_{hi}	Humans in Patch i	$\mathcal{U}(10^3, 10^4)$
N_{vi}	Vectors in Patch i	$\mathcal{U}(10^4, 10^5)$
μ_v	Vectors' natural mortality rate	$\mathcal{U}(6, 21)$
ν_v	Vectors' incubation rate	$\mathcal{U}(4, 15)$

Clearly, uncertainty or variability in b; β_{vh}; β_{hv}; and N_v positively influence the magnitude of the $\mathcal{R}_0$ and consequently the infectious class, while N_h influences the magnitude of the $\mathcal{R}_0$ negatively (see Figure 4.3). As expected, variability in the biting rate has the highest impact on the $\mathcal{R}_0$ (see Figure 4.2).

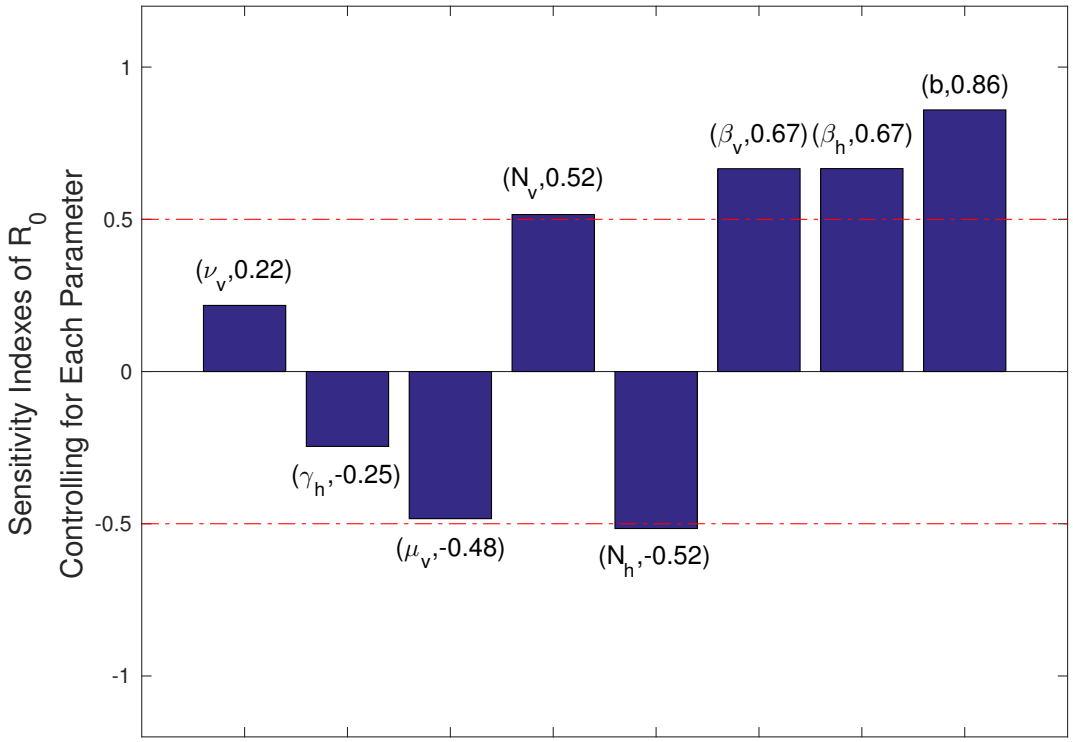

Figure 4.3: Partial Rank Correlation Coefficients For The Basic Reproductive Number and Each Input Parameter Variables.

Similarly, uncertainty or variability in b; β_{vh}; β_{hv}; and Λ positively influence the magnitude of the $\mathcal{R}_0$ and consequently the infectious class when $\Lambda = \frac{N_v}{N_h}$. Once again, variability in the biting rate has the highest impact on the $\mathcal{R}_0$, but notice that in this case there are no parameters that would influence the magnitude of the $\mathcal{R}_0$ negatively (see Figure 4.4).

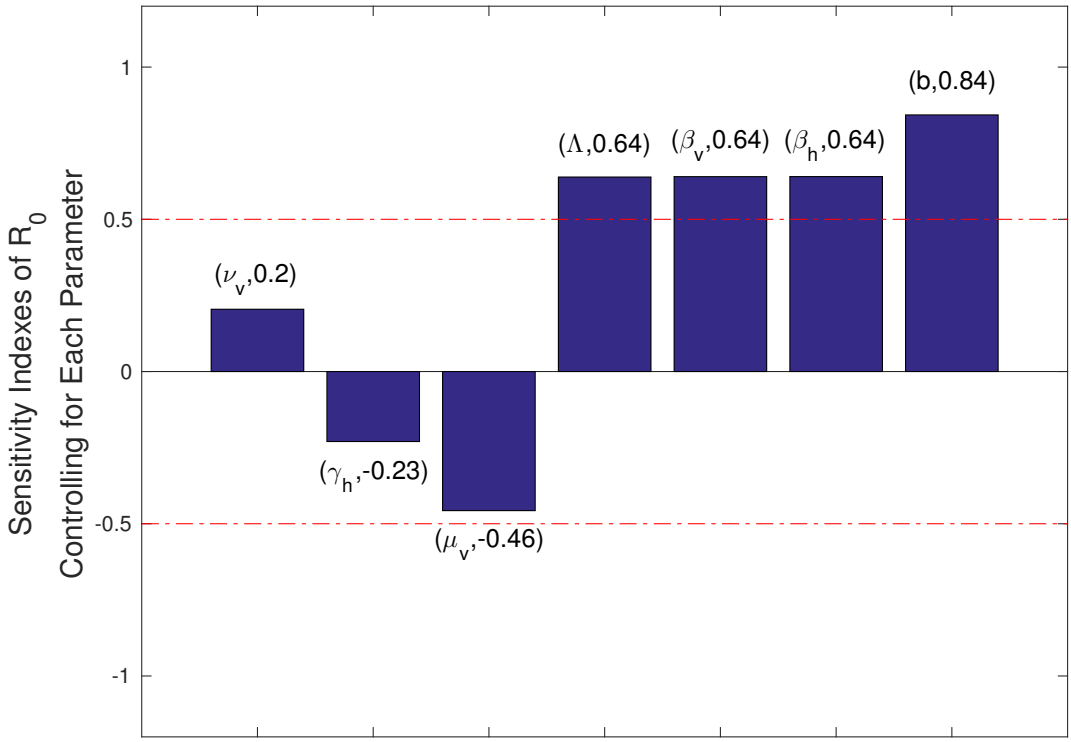

Figure 4.4: Partial Rank Correlation Coefficients For The Basic Reproductive Number and Each Input Parameter Variables When $\Lambda = \frac{N_v}{N_h}$.

Consequently, using a Latin Hypercube sampling design and applying sensitivity analysis techniques, the variability of $\mathcal{R}_0$ and thus the transmission dynamics of ZIKV depicted in Model (4.1) were explored. Applying these techniques made it possible to evaluate the sensitivity of the $\mathcal{R}_0$ estimate with respect to each of the parameter values from Table 4.3 and to determine which parameters have the greatest influence on the variability of $\mathcal{R}_0$. In particular, those that would create the worst case scenarios during a ZIKV outbreak.

In the next section, a two patch model using the Lagrangian approach specified in (Bichara and Castillo-Chavez, 2016; Bichara *et al.*, 2015) is introduced with individuals from Patch i $(i = 1, 2)$ maintaining their residency status regardless of the

proportion of time they spend in other patches as a result of their daily mobility patterns across distinct interconnected patches; an assumption captured with the use of a residence time matrix ($\mathbb{P}$). A matrix, where each entry p_{ij} models the average (in this study, fixed) proportion of time, a typical resident spends on his/her own patch or as a visitor to another patch per unit of time ($p_{i1} + p_{i2} = 1$). Hence, at any given time t, the effective population size in each patch accounts for both; patch residents and patch visitors. Moreover, the effective population size does not necessarily matches that given by the total number of patch residents. Simulations are then conducted using parameters specific to El Salvador, as well as the most recent estimates of $\mathcal{R}_0$ for ZIKV in an attempt to explore the consequences of mobility (described by the matrix $\mathbb{P}$) and the impact that the differences in risk (captured on the assumption $\hat{\beta}_1 \gg \hat{\beta}_2$) have on the transmission dynamics of ZIKV.

4.4 Residence Times and Two-Patch Models

The role of mobility between two communities, within the same city, living under dramatically distinct health, economic, social, and security settings is explored using a model as simple as possible, that is, a model that only considers two patches [prior modeling efforts that didn't account for the effective population size but that incorporated specific controls include, Lee and Castillo-Chavez (2015)]. It is assumed that Patch 2 has access to working health facilities, crime rate is low, adequate human and financial resources and adequate public health policies in place. On the other hand, Patch 1 lacks nearly everything and crime is high. Within this highly simplified settings, the differences in risk naturally need to be incorporated. In the case of ZIKV, risk of infection depends on host vector ratios, biting rates, the level of access and ability to buy repellents and nets, the regularity of visits by vector control crews, and more. These differences are captured by just postulating highly distinct transmission

rates; that is, to study the dynamics of host mobility in highly distinct environments, with risk being captured by one single parameter, the transmission rate, $\hat{\beta}$. As a result of the previously stated assumptions, $\hat{\beta}_1 \gg \hat{\beta}_2$ where $\hat{\beta}_i$ now defines the risk of infection in Patch i, $i = 1, 2$ [Patch 1 (high risk) and Patch 2 (low risk)].

As discussed in the previous sections, the host populations are stratified by epidemiological classes and now indexed by the patch of residency. More specifically, $S_{h,i}$, $E_{h,i}$, $I_{h,a,i}$, $I_{h,s,i}$ and $R_{h,i}$ denote the susceptible, latent, infectious asymptomatic, infectious symptomatic and recovered host populations in patch i, $i = 1, 2$. Similarly, $S_{v,i}$, $E_{v,i}$ and $I_{v,i}$ denote the susceptible, latent and infectious mosquito populations in patch i; $i = 1, 2$. As before, $N_{h,i}$ and $N_{v,i}$ denote the host population size and total vector population, respectively (in patch i; $i = 1, 2$). In this study, the vector is assumed to be incapable of moving between patches; a reasonable assumption in the case of *Aedes aegypti*, under the appropriate spatial scale. The two-patch model-parameters are also collected in Table 4.2 with the flow diagram (Fig 4.1), single-patch dynamics model, capturing the situation when residents and visitors do not move; that is, when the 2×2 residence times matrix $\mathbb{P}$ entries correspond to the case in which $p_{11} = p_{22} = 1$.

4.4.1 Two Patch Model

The Lagrangian framework, in the context of vector born and communicable diseases, is described in (Bichara and Castillo-Chavez, 2016; Bichara *et al.*, 2016, 2015). The application of this framework within a two patch model setting, where vectors are incapable of moving across patches, leads to the following set of nonlinear differential equations:

$$
\begin{cases}
\dot{S}_{h,i} = -\beta_{vh} S_{h,i} \sum_{j=1}^{2} b_j p_{ij} \frac{I_{v,j}}{p_{1j}N_{h,1}+p_{2j}N_{h,2}} \\
\dot{E}_{h,i} = \beta_{vh} S_{h,i} \sum_{j=1}^{2} b_j p_{ij} \frac{I_{v,j}}{p_{1j}N_{h,1}+p_{2j}N_{h,2}} - \nu_{h,i} E_{h,i} \\
\dot{I}_{h,s,i} = (1-q)\nu_{h,i} E_{h,i} - \gamma_{h,s} I_{h,s,i} \\
\dot{I}_{h,a,i} = q\nu_{h,i} E_{h,i} - \gamma_{h,a} I_{h,a,i} \\
\dot{R}_{h,i} = \gamma_{h,s} I_{h,s,i} + \gamma_{h,a} I_{h,a,i} \\
\dot{S}_{v,i} = \mu_v N_{v,i} - b_i \beta_{hv} S_{v,i} \frac{\sum_{j=1}^{2} p_{ji}(I_{h,s,j}+I_{h,a,j})}{\sum_{k=1}^{2} p_{ki} N_{h,k}} - \mu_v S_{v,i} \\
\dot{E}_{v,i} = b_i \beta_{hv} S_{v,i} \frac{\sum_{j=1}^{2} p_{ji}(I_{h,s,j}+I_{h,a,j})}{\sum_{k=1}^{2} p_{ki} N_{h,k}} - (\mu_v + \nu_v) E_{v,i} \\
\dot{I}_{v,i} = \nu_v E_{v,i} - \mu_v I_{v,i}
\end{cases}
\tag{4.3}
$$

where $\mathbb{P} = (p_{ij})$ and $p_{i,j}$ represent the residence time that an individual from Patch i spends in Patch j; $i, j = 1, 2$.

The basic reproduction number of this model is the largest eigenvalue of the matrix,

$$
M_1 = \begin{pmatrix} m_{11} & m_{12} \\ m_{21} & m_{22} \end{pmatrix}
$$

where

$$
\begin{aligned}
m_{11} &= \frac{p_{11}^2 N_{v,1} N_{h,1} b_1^2 \beta_{vh} \beta_{hv} \nu_v + p_{21}^2 N_{v,1} N_{h,2} b_1^2 \beta_{vh} \beta_{hv} \nu_v}{(p_{11}N_{h,1} + p_{21}N_{h,2})^2 \gamma_h \mu_v (\nu_v + \mu_v)} \\
&= \left(\frac{p_{11}^2 N_{h,1} + p_{21}^2 N_{h,2}}{(p_{11}N_{h,1} + p_{21}N_{h,2})^2} \right) \left(\frac{N_{v,1} b_1^2 \beta_{vh} \beta_{hv} \nu_v}{\gamma_h \mu_v (\nu_v + \mu_v)} \right),
\end{aligned}
$$

$$
\begin{aligned}
m_{12} &= \frac{p_{11}p_{12} N_{v,1} N_{h,1} b_1 b_2 \beta_{vh} \beta_{hv} \nu_v + p_{21}p_{22} N_{v,1} N_{h,2} b_1 b_2 \beta_{vh} \beta_{hv} \nu_v}{(p_{11}N_{h,1} + p_{21}N_{h,2})(p_{12}N_{h,1} + p_{22}N_{h,2}) \gamma_h \mu_v (\nu_v + \mu_v)} \\
&= \left(\frac{p_{11}p_{12} N_{h,1} + p_{21}p_{22} N_{h,2}}{(p_{11}N_{h,1} + p_{21}N_{h,2})(p_{12}N_{h,1} + p_{22}N_{h,2})} \right) \left(\frac{N_{v,1} b_1 b_2 \beta_{vh} \beta_{hv} \nu_v}{\gamma_h \mu_v (\nu_v + \mu_v)} \right),
\end{aligned}
$$

$$
\begin{aligned}
m_{21} &= \frac{p_{11}p_{12} N_{v,2} N_{h,1} b_1 b_2 \beta_{vh} \beta_{hv} \nu_v + p_{21}p_{22} N_{v,2} N_{h,2} b_1 b_2 \beta_{vh} \beta_{hv} \nu_v}{(p_{11}N_{h,1} + p_{21}N_{h,2})(p_{12}N_{h,1} + p_{22}N_{h,2}) \gamma_h \mu_v (\nu_v + \mu_v)} \\
&= \left(\frac{p_{11}p_{12} N_{h,1} + p_{21}p_{22} N_{h,2}}{(p_{11}N_{h,1} + p_{21}N_{h,2})(p_{12}N_{h,1} + p_{22}N_{h,2})} \right) \left(\frac{N_{v,2} b_1 b_2 \beta_{vh} \beta_{hv} \nu_v}{\gamma_h \mu_v (\nu_v + \mu_v)} \right).
\end{aligned}
$$

$$
\begin{aligned}
m_{22} &= \frac{p_{12}^2 N_{v,2} N_{h,1} b_2^2 \beta_{vh} \beta_{hv} \nu_v + p_{22}^2 N_{v,2} N_{h,2} b_2^2 \beta_{vh} \beta_{hv} \nu_v}{(p_{12} N_{h,1} + p_{22} N_{h,2})^2 \gamma_h \mu_v (\nu_v + \mu_v)} \\
&= \left(\frac{p_{12}^2 N_{h,1} + p_{22}^2 N_{h,2}}{(p_{12} N_{h,1} + p_{22} N_{h,2})^2} \right) \left(\frac{N_{v,2} b_2^2 \beta_{vh} \beta_{hv} \nu_v}{\gamma_h \mu_v (\nu_v + \mu_v)} \right).
\end{aligned}
$$

Specifically,

$$
\mathcal{R}_0^2 = \frac{1}{2} \left(m_{11} + m_{22} + \sqrt{(m_{11} - m_{22})^2 - 4 m_{12} m_{21}} \right).
$$

If the two patches are isolated, a case that allows us to estimate the impact ZIKV transmission has in each patch when each community deals with ZIKV independently, the local basic reproduction number is $\mathcal{R}_0 = \max\{\mathcal{R}_{0i}\}$, $i = 1, 2$, where,

$$
\mathcal{R}_{0i} = \sqrt{\frac{N_{v,i} b_i^2 \beta_{vh} \beta_{hv} \nu_v}{N_{h,i} \gamma_h \mu_v (\nu_v + \mu_v)}}
$$

that is, the expression found in Formula (4.2), where risk disparity in a patch is represented by the inequality $\hat{\beta}_1 \gg \hat{\beta}_2$, which turns out to be directly proportional to the local basic reproduction numbers ($\mathcal{R}_{0i}$) in the absence of mobility (decoupled patches). Changes in the entries of the coupling matrix $\mathbb{P}$, would naturally have an impact in the overall (two-patch) ZIKV dynamics. Consequently, the global basic reproduction number, the final epidemic size, and the ZIKV levels of infection within each patch depend on $\mathbb{P}$. Results are then collected from a series of observations based on the simulation of extreme scenarios designed to explore the role that mobility ($\mathbb{P}$), variations in the patch inherent risk ($\mathcal{R}_{0i}$), and population density have on ZIKV dynamic in each patch. While one can argue that the use of an extreme and simplistic set up is unlikely to yield a broad characterization of the role of mobility, variations in risk and host density on ZIKV outbreaks within heterogeneous populations, simulation results highlight nevertheless, the impact that mobility patterns shaped by economic necessity for survival has on ZIKV outbreaks; or the impact of high levels of crime and the restrictions that it imposes on vector borne control interventions (San Salvador, Rio de Janeiro, and others) have on ZIKV outbreaks. Consequently,

it is expected that the collaboration and sharing of health and security resources between resource-rich and resource-limited adjacent communities can make a difference whenever there is an agreement on the trade-offs between public good and individual safety.

4.5 Results

The use of a restricted bi-modal set-up, described in the previous section, is used to highlight the impact of risk and mobility under a few selected, non exhaustive, scenarios. As specified, Patch 1 experiences high levels of crime, poverty, and lack of resources, while Patch 2 has access to vector control measures, health care facilities, and resources to minimize local crime and violence; scenarios motivated by the dynamics of disease in conflict zones and highly disadvantaged neighborhoods.

Since it is assumed that the risk of infection is associated with high levels of social inequalities that could include high violence levels, it makes sense to assume that since individuals experience a higher risk of ZIKV infection in Patch 1 then mobility from Patch 2 to Patch 1 is expected to be unappealing. It is expected that typical Patch 2 residents spend (on average) a reduced amount of time, per unit of time, in Patch 1. Consequently, Patch 2 parameters are selected in such a way that the dynamics of ZIKV within Patch 2 cannot be supported, in the absence of mobility between Patch 1 and Patch 2. Thus, the local basic reproductive number for Patch 2 is less than one, namely, $\mathcal{R}_{02} = 0.9$. In addition, mobility is modeled under the residence times matrix $\mathbb{P}$ with entries given initially by, $p_{21} = 0.10$ and $p_{12} = 0$. In particular, using the results from the sensitivity analysis the study will focus on the case scenarios described in Table 4.4.

Table 4.4: Definitions and Scenarios for ZIKV

Nomenclature		
Risk	Interpreted based on levels of prevention (biting rate) or mosquito abundance (vector-host ratio)	
High-risk patch	Defined either by low prevention that leads to high biting rate (i.e., high b which leads to high corresponding $\mathcal{R}_0$) and/or by high vector-host ratio (i.e., high $\Lambda = \frac{N_v}{N_h}$)	
Enhanced socio-economic conditions (reducing health disparity)	Defined by better health-care infrastructure which is incorporated by high prevalence of a disease (i.e., high $I(0)/N$)	
Mobility	Captured by average residence times of an individual in different patches (i.e., by using $\mathbb{P}$ matrix)	
Scenarios (assume high-risk and diminished socio-economic conditions in Patch 1 as compared to Patch 2)		
Scenario 1	$\underbrace{b_1 > b_2,\ \Lambda_1 = \Lambda_2}_{\text{high risk}}$;	$\underbrace{\frac{I_1(0)}{N_1} > \frac{I_2(0)}{N_2}}_{\text{socio-economic conditions}}$; $\underbrace{\text{vary } p_{12} \text{ when } p_{21} \approx 0.1}_{\text{mobility}}$
Scenario 2	$\underbrace{b_1 = b_2,\ \Lambda_1 > \Lambda_2}_{\text{high risk}}$;	$\underbrace{\frac{I_1(0)}{N_1} > \frac{I_2(0)}{N_2}}_{\text{socio-economic conditions}}$; $\underbrace{\text{vary } p_{12} \text{ when } p_{21} \approx 0.1}_{\text{mobility}}$
Scenario 3	$\underbrace{b_1 > b_2,\ \Lambda_1 > \Lambda_2}_{\text{high risk}}$;	$\underbrace{\frac{I_1(0)}{N_1} > \frac{I_2(0)}{N_2}}_{\text{socio-economic conditions}}$; $\underbrace{\text{vary } p_{12} \text{ when } p_{21} \approx 0.1}_{\text{mobility}}$

In particular, two cases are explored: (i) A "worst case" scenario where control measures are hardly implemented due to crime, conflict or other factors on Patch 1. As a consequence, Patch 1 is considered a place where the risk of acquiring a ZIKV infection is high and thus it is assumed that $\mathcal{R}_{01} = 2$. (ii) On the other hand, the "best case" scenario corresponds to the case when Patch 1 can implement some control measures with some degree of effectiveness and, consequently Patch 1 experiences a reduction in the risk of infection, namely, $\mathcal{R}_{01} = 1.52$. The patch specific basic reproductive number ($\mathcal{R}_{0i}$) values used are in range with those previously estimated for ZIKV outbreaks in French Polynesia (Kucharski *et al.*, 2016) and in Colombia (Towers *et al.*, 2016). Simulations are seeded by introducing an asymptomatic infected individual in Patch 1 under the assumption that both the host and vector populations are fully susceptible in both patches.

4.5.1 Risk Defined by Poor Bite Prevention.

Considering the "best case" scenario under the assumption that the population in both patches is the same. Figure 4.5 shows that while some mobility values can increase the final Patch 1 epidemic size, the maximum epidemic size only reaches around 80% of the population when mobility is close to $p_{12} = 0.20$. Finally, observations from the simulations suggest the existence of a mobility threshold from which the final epidemic sizes in Patch 1 benefits.

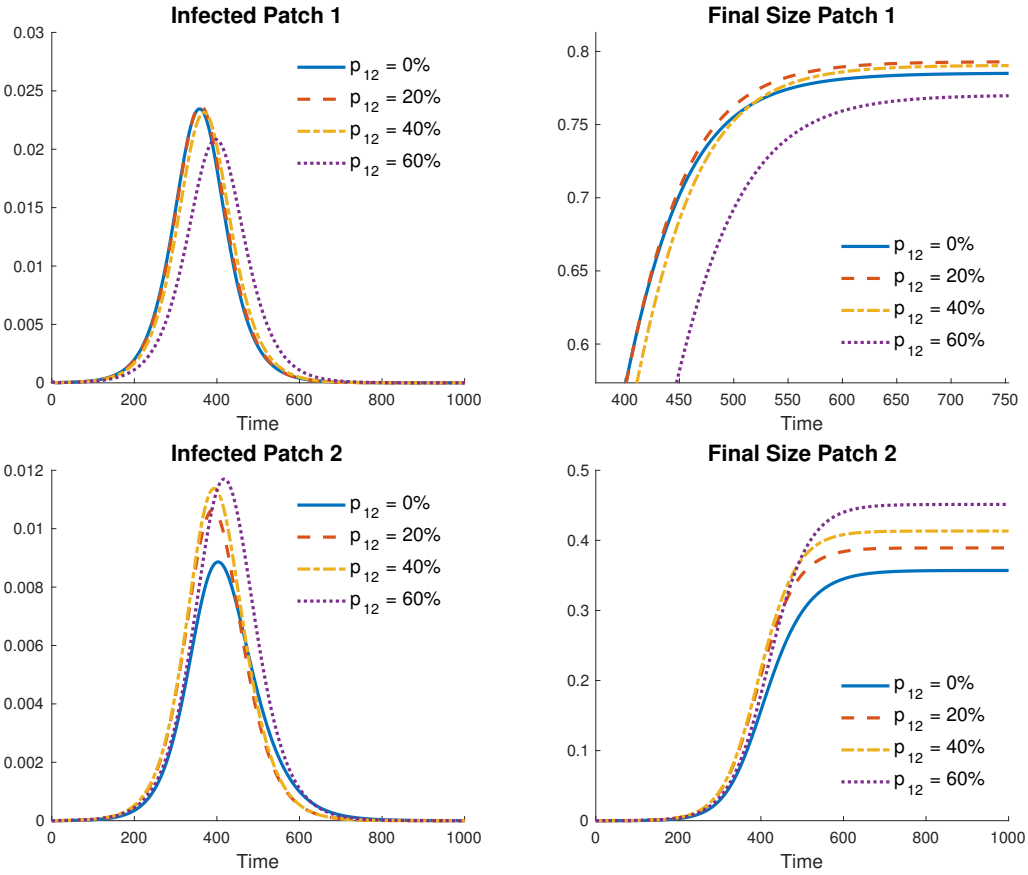

Figure 4.5: Scenario One: Patch Incidence and Final Size Proportions for $p_{21} = 0.10$, $p_{12} = 0, 0.2, 0.4$ and 0.6 for Best Case.

Figure 4.6 shows the incidence and final ZIKV epidemic size under the "worst case" scenario, defined by elevated risk and a basic reproduction number of $\mathcal{R}_{01} = 2$.

Figure 4.6 shows that around $p_{12} = 0.2$, the final number of infected residents in Patch 1 is larger to the number of infections caused by the baseline scenario when $p_{12} = 0$, but only for long outbreaks. As expected, the worst case scenario drives ZIKV infections in almost 96% of the population in Patch 1, an unrealistic value. Nonetheless, most p_{12} values show a beneficial reduction in the final Patch 1 epidemic size.

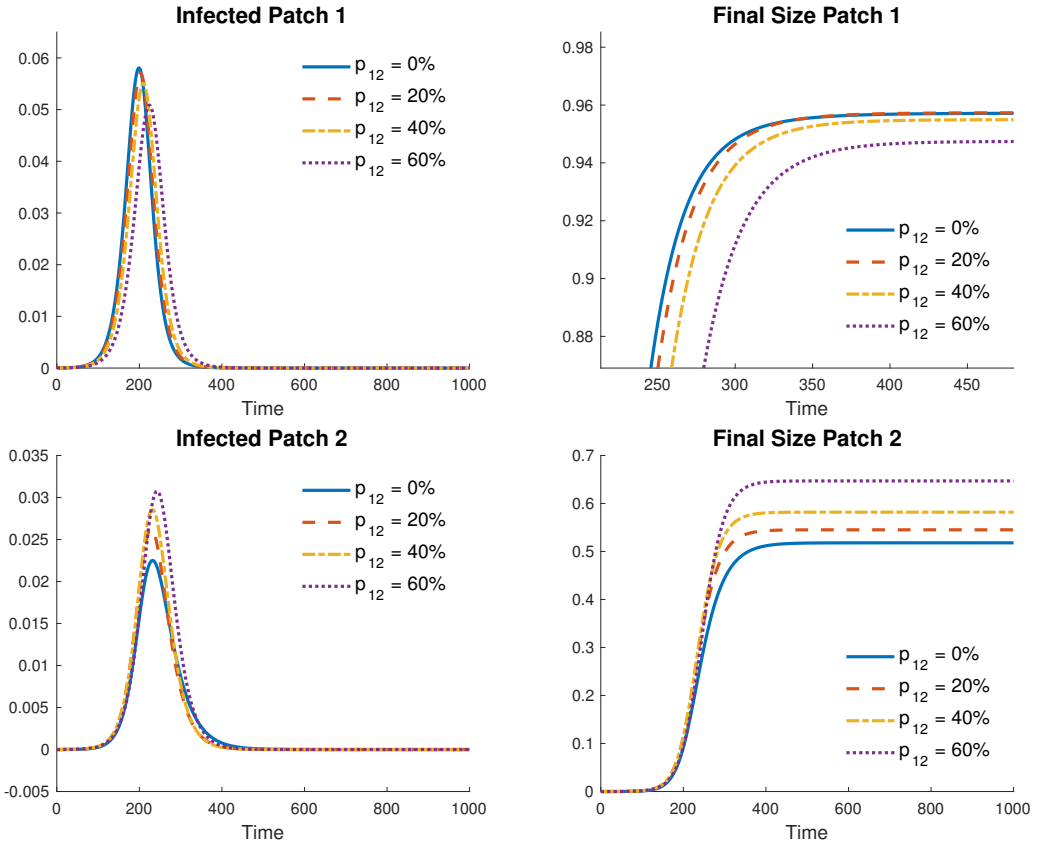

Figure 4.6: Scenario One: Patch Incidence and Final Size Proportions for $p_{21} = 0.10$, $p_{12} = 0, 0.2, 0.4$ and 0.6 for Worst Case.

Figure 4.6 highlights the case when the final Patch 2 epidemic size grows as mobility from Patch 1 increases, when compared with the baseline case (no mobility from Patch 1). In addition, reductions in the final Patch 1 epidemic size for some mobility values accompanied by increments in the final epidemic size in Patch 2 are observed.

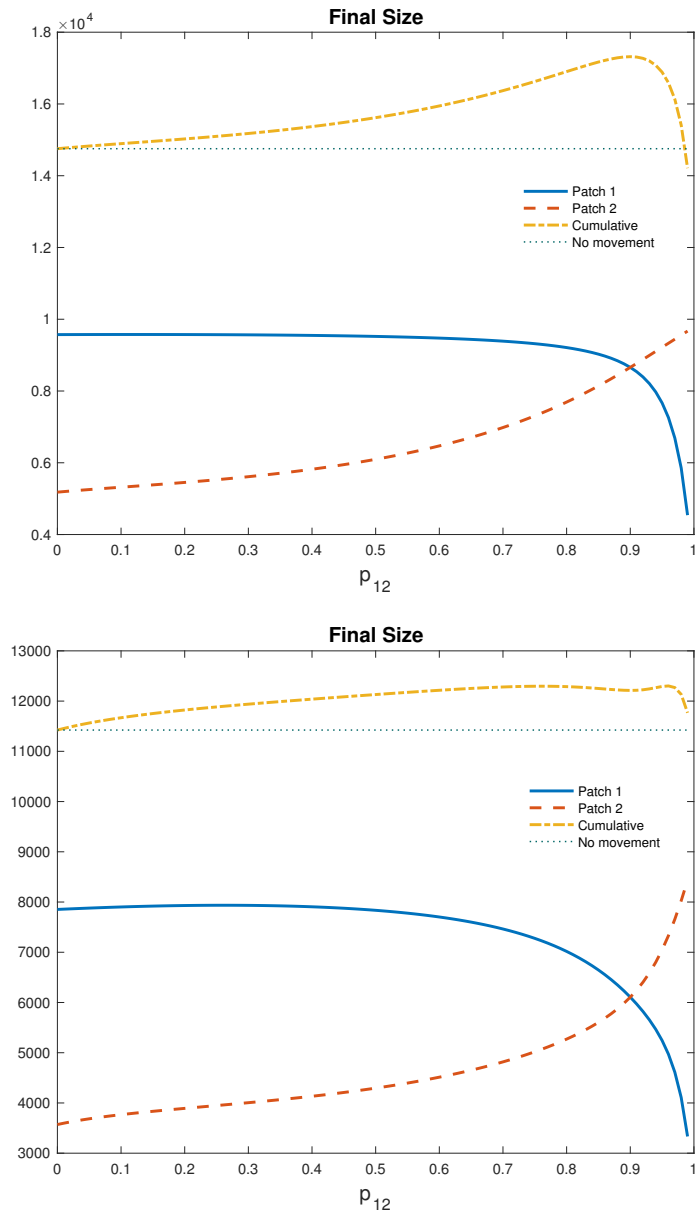

Figure 4.7: Scenario One: Final Sizes for Worst Case (Top) and Best Case (Bottom).

The results of simulations collected in Figures 4.5 and Figure 4.6 show similar final size epidemic curves for both cases. However, it is important to mention that while Patch 1 experiences some benefits from most mobility patterns, the increments on the total final epidemic size in Patch 2 are greater. Thus while mobility may provide benefits within Patch 1 (under the above assumptions) the fact remains that

it does it at a cost to Patch 2. In short, it is also observed that the final epidemic size per patch does not respond linearly to changes in mobility even when only p_{12} is increased (see Figure 4.7).

The Role of Risk Heterogeneity in the Dynamics of Zika Virus Transmission

Moreover, the results presented thus far only provide partial information of the total impact that short term mobility might have on the transmission dynamics of ZIKV. The impact of risk heterogeneity on ZIKV dynamics within the overall two-patch system requires the numerical estimation of the global reproduction number as a function of the mobility matrix $\mathbb{P}$. By fixing the mobility from Patch 2 to Patch 1, the simulations focused only on the impact of changes in mobility from Patch 1 to Patch 2.

Using the previously defined scenarios ($\mathcal{R}_{01} = 1.52, 2$), simulations are carried out, again assuming equal population sizes ($N_1 = N_2$). However, when looking at the impact of changes in risk on Patch 2 ($\mathcal{R}_{02} = 0.9, 0.8, 0.7, 0.6,$ and 0.5), simulations identify a growing final epidemic size as risk in Patch 2 increases for all residence times in the "worst case" and for the most realistic residency times in the "best case." Specifically, Figure 4.8 captures the overall reductions on the global reproductive number (risk) for all residence times, while identifying the existence of a residence time interval for which mobility is beneficial (in some cases), decreasing the total size of the outbreak in the two patch system, when compared to the baseline case ($p_{12} = 0$). An expected outcome as a result of the myriad of assumptions that have been incorporated, namely, the restrictions placed on population density; the population in Patch 1 is the same as that in Patch 2.

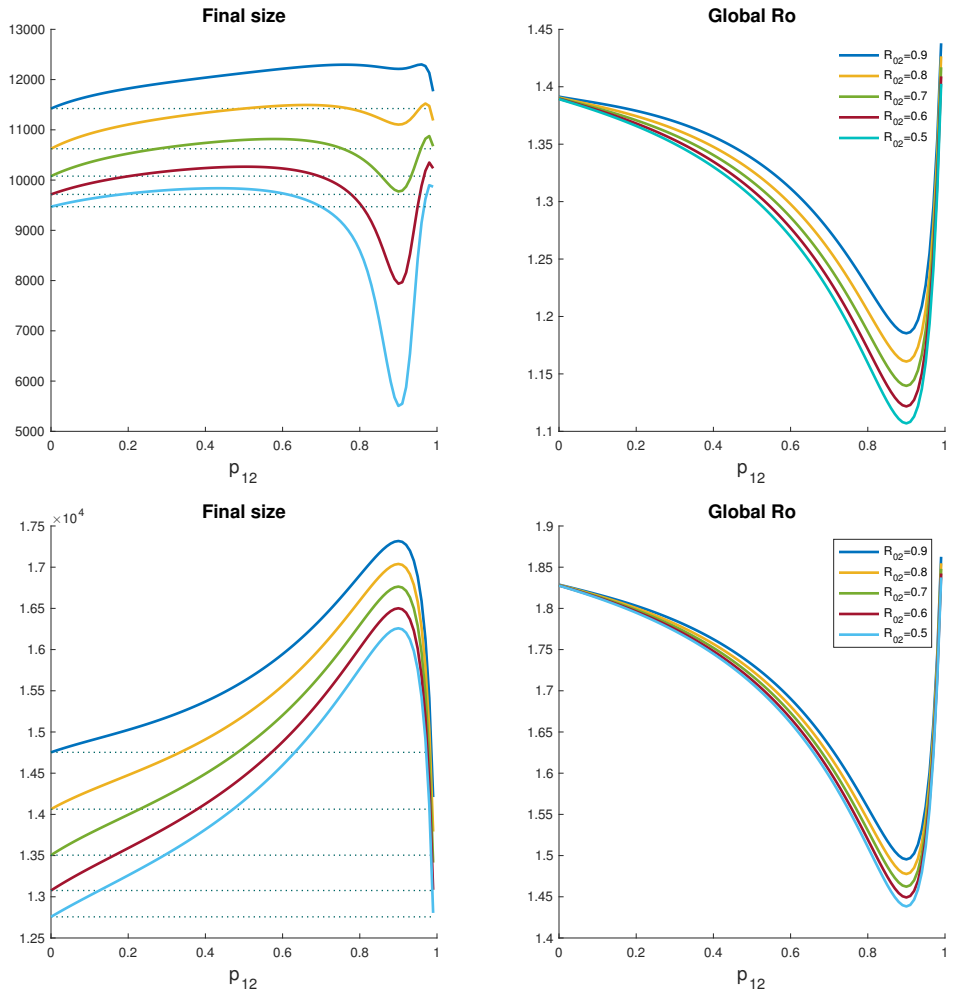

Figure 4.8: Scenario One: Total Final Size and Global Basic Reproductive Number Through Mobility Values When $p_{21} = 0.10$, $\mathcal{R}_{02}$ Varies and $\mathcal{R}_{01} = 1.52$ (Top); 2 (Bottom).

The Role of Population Size Heterogeneity in the Dynamics of Zika Virus Transmission.

The role of population density on the total final epidemic size and global basic reproductive number are now explored using the two scenarios previously defined, but now under the assumption that patch densities (population sizes) are different. More specifically, when $N_1 = N_2$, $5N_2$, $10N_2$ and when $N_2 = 5N_1$, $10N_1$. Figure 4.9 shows that difference in population sizes do matter. Specifically, it is observed that (under

the densities selected) great density differences translate into higher final epidemic sizes when the high risk patch is denser.

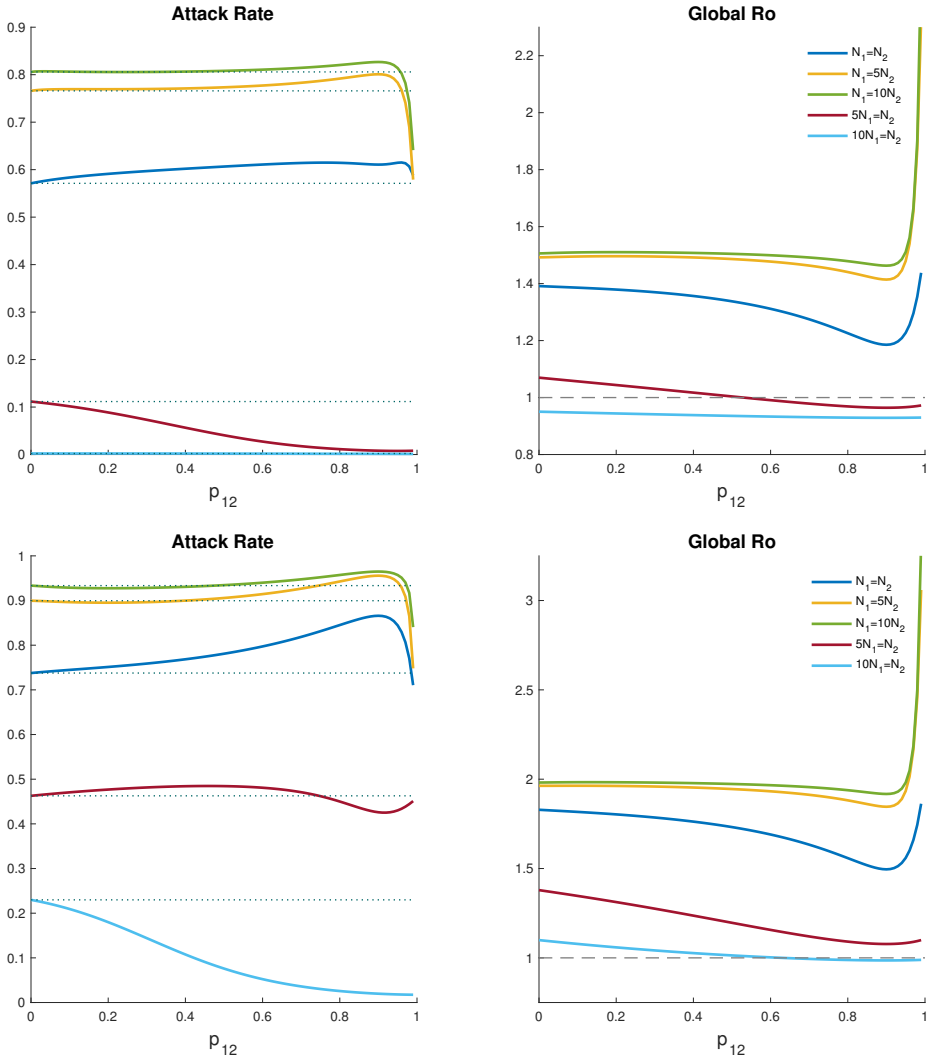

Figure 4.9: Scenario One: Total Final Size and Global Basic Reproductive Number Through Mobility Values When $p_{21} = 0.10$ Population Size Varies, $\mathcal{R}_{02} = 0.9$, and $\mathcal{R}_{01} = 1.52$ (Top); 2 (Bottom).

In the "worst case" scenario, infecting over 90% of the population is possible for some population densities. In addition, it is also observed that despite increases in the total final epidemic size, as mobility changes, the global $\mathcal{R}_0$ decrease monotonically, for most residence times, but only falls below unity when the safe population is much

greater. A sensible degree of magnification on the spread of the disease is observed as residence times change, whenever the differences between N_1 and N_2 are not too extreme. In fact, it is possible for mobility to be beneficial in the control of ZIKV under the above simplistic extreme scenarios. Nonetheless, simulations continue to show that under the prescribed conditions and assumptions, model generated ZIKV outbreaks remain unrealistically high.

For the two epidemiological scenarios $\mathcal{R}_{01} = 2$ and $\mathcal{R}_{01} = 1.52$, Tables 4.5 and 4.6 provide a summary of the average proportion of infected for low ($p_{12} = 0.01 - 0.33$), intermediate ($p_{12} = 0.34 - 0.66$) and high mobility ($p_{12} = 0.67 - 0.99$) when $p_{21} = 0.10$. The role of population scaling ($N_1 = N_2/10$, $N_2/5$, N_2, $5N_2$ and $10N_2$ when the largest population is 10000) is once again explored.

Table 4.5: Scenario One: Final Size (Patch 1, Patch 2), $\mathcal{R}_{01} = 2$, $\mathcal{R}_{02} = 0.9$ and $p_{21} = 0.10$.

N_2	Low Mobility	Intermediate Mobility	High Mobility	Min $\mathcal{R}_0$
$N_1 = N_2/10$	(0.3799, 0.1669)	(0.1383, 0.0736)	(0.0309, 0.0248)	0.9857
$N_1 = N_2/5$	(0.8125, 0.4068)	(0.7341, 0.4324)	(0.5011, 0.4362)	1.0775
$N_1 = N_2$	(0.9572, 0.5419)	(0.9513, 0.6141)	(0.8651, 0.8064)	1.4954
$N_1 = 5N_2$	(0.9713, 0.5215)	(0.9706, 0.5886)	(0.9461, 0.8626)	1.8457
$N_1 = 10N_2$	(0.9726, 0.4905)	(0.9722, 0.5659)	(0.9598, 0.8654)	1.9173

Table 4.6: Scenario One: Final Size (Patch 1, Patch 2), $\mathcal{R}_{01} = 1.52$, $\mathcal{R}_{02} = 0.9$ and $p_{21} = 0.10$.

N_2	Low Mobility	Intermediate Mobility	High Mobility	Min $\mathcal{R}_0$
$N_1 = N_2/10$	(0.0045, 0.0020)	(0.0036, 0.0018)	(0.0026, 0.0014)	0.9289
$N_1 = N_2/5$	(0.1766, 0.0746)	(0.0687, 0.0364)	(0.0139, 0.0023)	0.9643
$N_1 = N_2$	(0.7913, 0.3846)	(0.7806, 0.4321)	(0.6465, 0.5783)	1.1853
$N_1 = 5N_2$	(0.8472, 0.3796)	(0.8470, 0.4093)	(0.7965, 0.6948)	1.4141
$N_1 = 10N_2$	(0.8518, 0.3493)	(0.8513, 0.3809)	(0.8214, 0.7028)	1.4630

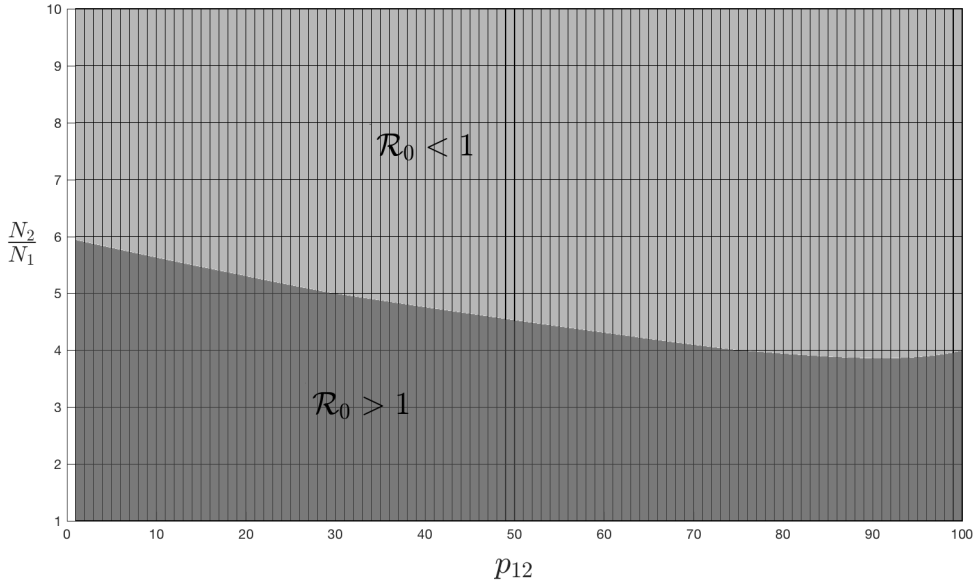

Figure 4.10: Scenario One: Effect of Mobility and Population Size Proportions on the Global Basic Reproductive Number $\mathcal{R}_0$ When $\mathcal{R}_{02} = 0.9$, and $\mathcal{R}_{01} = 1.52$.

However, potential changes in mobility patterns that host populations may cause or experience in response to ZIKV dynamics are being completely ignored when a mobility matrix $\mathbb{P}$ with constant entries p_{ij} is used. Nonetheless, the qualitative response of the final epidemic size within Patch 1 is qualitatively similar in both, the

worst and best case scenarios: increasing at first (for low mobility values), decreasing after a certain threshold and then eventually crossing down the baseline case, under some mobility regimes. Moreover, while the qualitative behavior of the final epidemic size in Patch 2 grows monotonically as mobility increases, reductions in risk and density yield significant benefits in terms of the total ZIKV burden even under such restrictive conditions and assumptions (see Figure 4.10).

4.5.2 Risk Defined by Poor Vector Control.

Similarly, the "best case" scenario presented in Figure 4.11 shows that while some mobility values can increase the final Patch 1 epidemic size, simulations suggest the existence of a mobility threshold from which the final epidemic size in Patch 1 benefits.

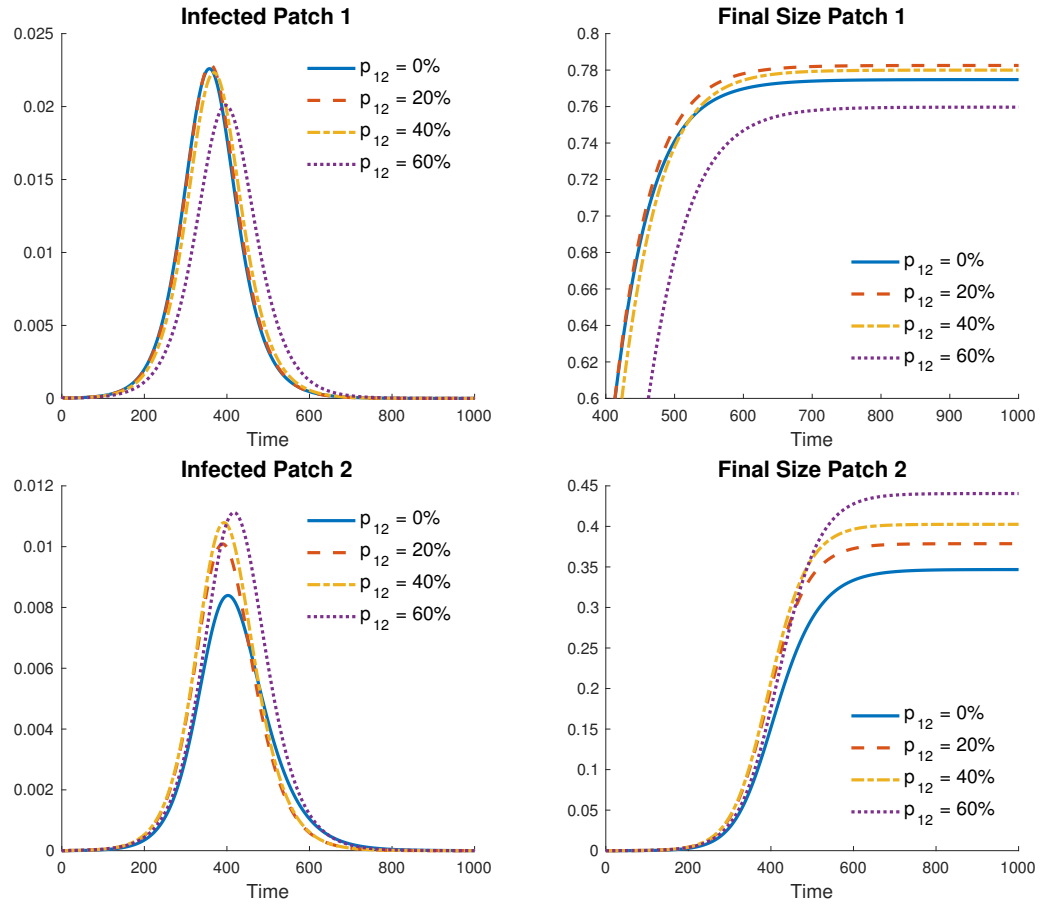

Figure 4.11: Scenario Two: Patch Incidence and Final Size Proportions for $p_{21} = 0.10$, $p_{12} = 0, 0.2, 0.4$ and 0.6 for Best Case.

Moreover, the "worst case" presented in Figure 4.12 shows that while mobility benefits the overall burden in Patch 1, increases in the total number of infections is the norm in Patch 2. The results suggest that the overall burden increases since, the negative impact in Patch 2 is greater than the benefits from Patch 1 (populations are assumed to be the same size).

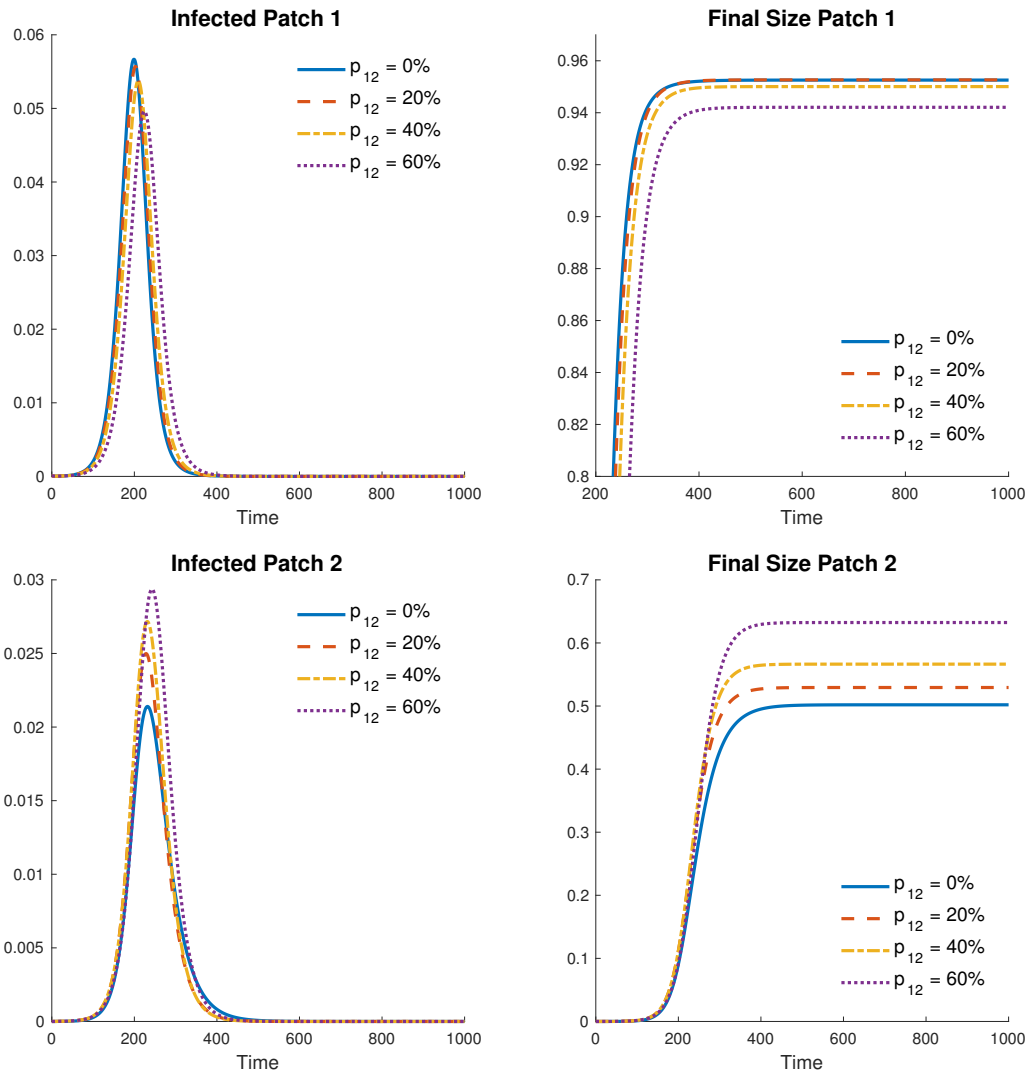

Figure 4.12: Scenario Two: Patch Incidence and Final Size Proportions for $p_{21} = 0.10$, $p_{12} = 0, 0.2, 0.4$ and 0.6 for Worst Case.

The results depicted in Figure 4.13 suggest that for most p_{12} mobility levels, the cumulative final ZIKV epidemic size supports monotonic growth in the total number of infected individuals.

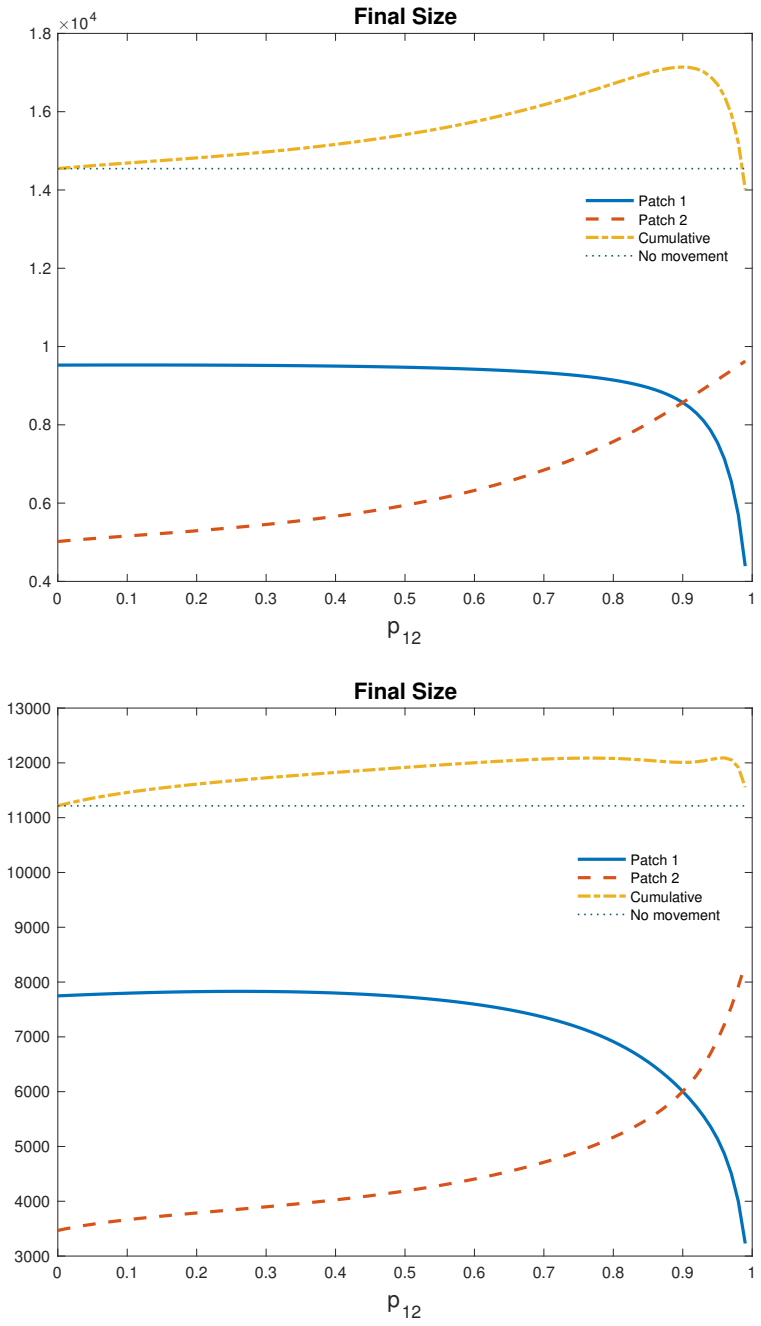

Figure 4.13: Scenario Two Final Sizes for Worst (Top) and Best (Bottom) Cases.

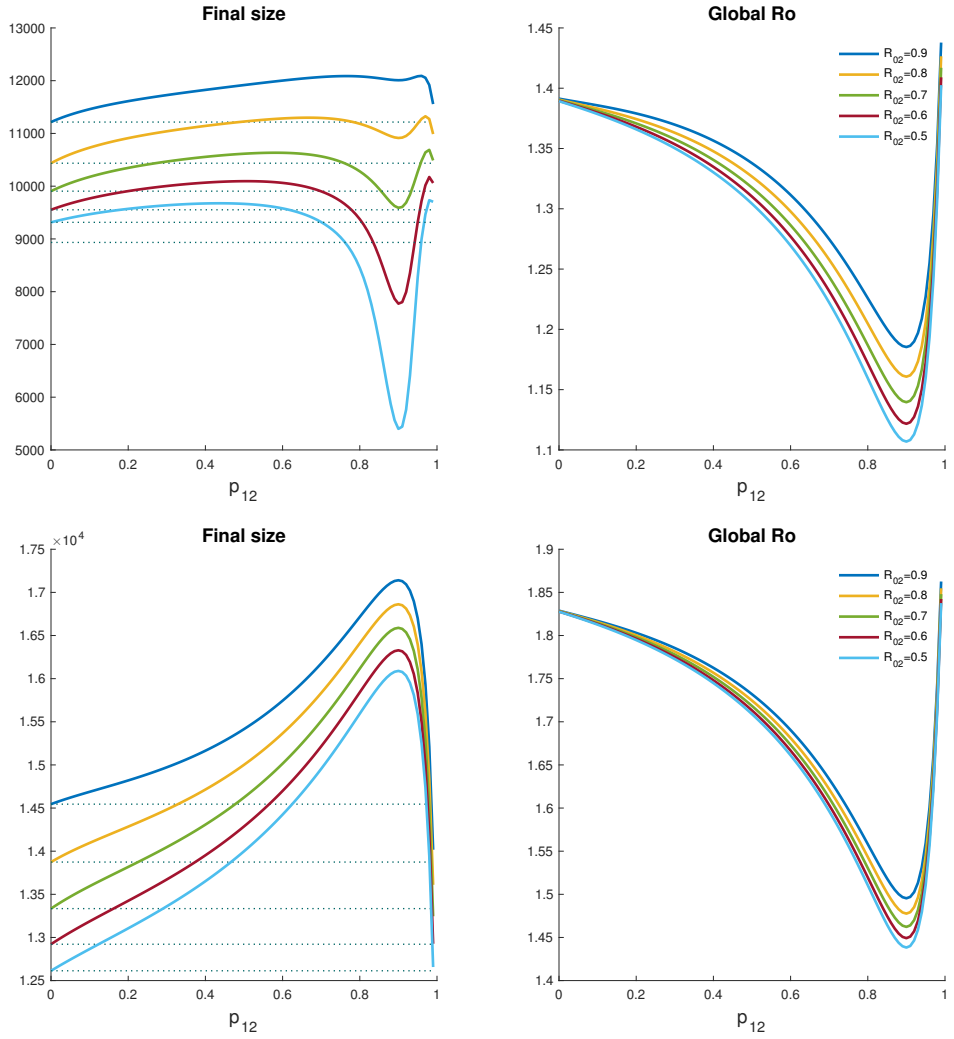

Figure 4.14: Scenario Two: Total Final Size and Global Basic Reproductive Number Through Mobility Values When $p_{21} = 0.10$, $\mathcal{R}_{02}$ Varies and $\mathcal{R}_{01} = 1.52$ (Top); 2 (Bottom).

Once again, when looking at the impact of changes in risk on Patch 2 ($\mathcal{R}_{02} = 0.9, 0.8, 0.7, 0.6,$ and 0.5), simulations identify a growing final epidemic size as risk increases, for all residence times in the "worst case" and most realistic residency times in the "best case." However, if the conditions in the safe patch (Patch 2) are

improved then short term mobility has a positive impact on the final size for certain mobility patterns. An expected outcome, but the impact is not enough to control the ZIKV outbreak when both patches have the same population size (see Figure 4.14).

The Role of Population Size Heterogeneity in the Dynamics of Zika Virus Transmission.

Now, the role of population density on the total final epidemic size and global basic reproductive number are explored. Using the two scenarios previously defined, and the following population sizes: $N_1 = N_2$, $5N_2$, $10N_2$ and $N_2 = 5N_1$, $10N_1$. Figure 4.15 shows that difference in population sizes do matter. Specifically, it is observed that (under the densities selected) great density differences translate into higher final epidemic sizes when the high risk patch is denser.

Once again, infecting over 90% of the population is possible for some population densities under the "worst case" scenario. Similarly, despite increases in the total final epidemic size, the global $\mathcal{R}_0$ decrease monotonically for most residence times, but only falls below unity when the safe population is much greater. Nonetheless, simulations continue to show that under the prescribed conditions and assumptions, model generated ZIKV outbreaks remain unrealistically high.

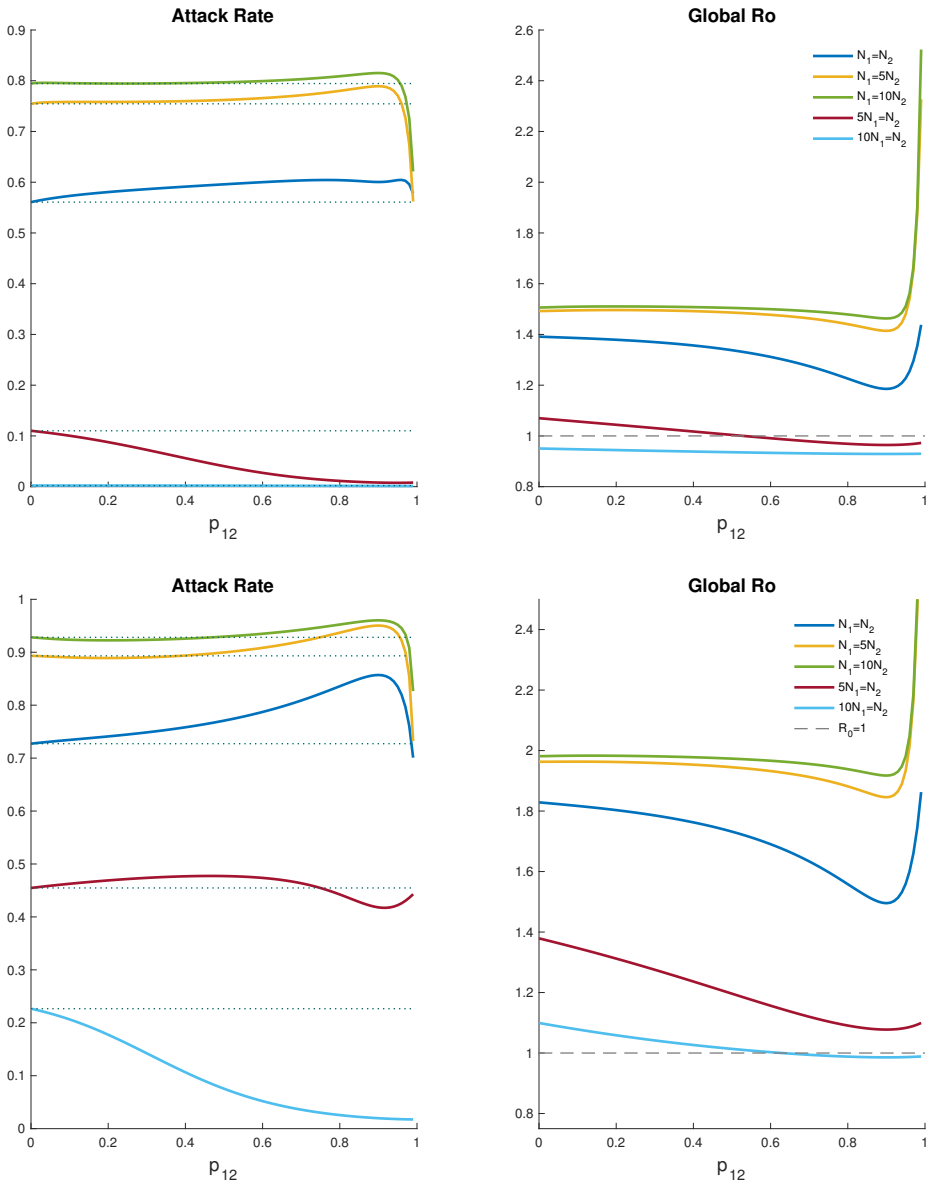

Figure 4.15: Scenario Two: Total Final Size and Global Basic Reproductive Number Through Mobility Values When $p_{21} = 0.10$, Population Size Varies, $\mathcal{R}_{02} = 0.9$, and $\mathcal{R}_{01} = 1.52$ (Top); 2 (Bottom).

Similarly, for the two epidemiological scenarios $\mathcal{R}_{01} = 2$ and $\mathcal{R}_{01} = 1.52$, Tables 4.7 and 4.8 provide a summary of the average proportion of infected for low ($p_{12} = 0.01 - 0.33$), intermediate ($p_{12} = 0.34 - 0.66$) and high mobility ($p_{12} = 0.67 - 0.99$) when $p_{21} = 0.10$. The role of population scaling ($N_1 = N_2/10$, $N_2/5$, N_2, $5N_2$ and

$10N_2$ when the largest population is 10000) is also explored.

Table 4.7: Scenario Two: Final Size (Patch 1, Patch 2), $\mathcal{R}_{01} = 2$, $\mathcal{R}_{02} = 0.9$ and $p_{21} = 0.10$.

N_2	Low Mobility	Intermediate Mobility	High Mobility	Min $\mathcal{R}_0$
$N_1 = N_2/10$	(0.3759, 0.1645)	(0.1372, 0.0730)	(0.0308, 0.0247)	0.9857
$N_1 = N_2/5$	(0.8062, 0.3986)	(0.7272, 0.4250)	(0.4934, 0.4286)	1.0775
$N_1 = N_2$	(0.9525, 0.5260)	(0.9461, 0.5990)	(0.8568, 0.7959)	1.4954
$N_1 = 5N_2$	(0.9673, 0.5048)	(0.9666, 0.5729)	(0.9403, 0.8538)	1.8457
$N_1 = 10N_2$	(0.9687, 0.4744)	(0.9682, 0.5509)	(0.9549, 0.8569)	1.9173

Table 4.8: Scenario Two: Final Size (Patch 1, Patch 2), $\mathcal{R}_{01} = 1.52$, $\mathcal{R}_{02} = 0.9$ and $p_{21} = 0.10$.

N_2	Low Mobility	Intermediate Mobility	High Mobility	Min $\mathcal{R}_0$
$N_1 = N_2/10$	(0.0045, 0.0020)	(0.0036, 0.0018)	(0.0026, 0.0014)	0.9289
$N_1 = N_2/5$	(0.1748, 0.0737)	(0.0683, 0.0362)	(0.0139, 0.0109)	0.9643
$N_1 = N_2$	(0.7808, 0.3740)	(0.7701, 0.4213)	(0.6361, 0.5679)	1.1853
$N_1 = 5N_2$	(0.8362, 0.3675)	(0.8359, 0.3969)	(0.7844, 0.6834)	1.4141
$N_1 = 10N_2$	(0.8407, 0.3378)	(0.8401, 0.3691)	(0.8093, 0.6915)	1.4630

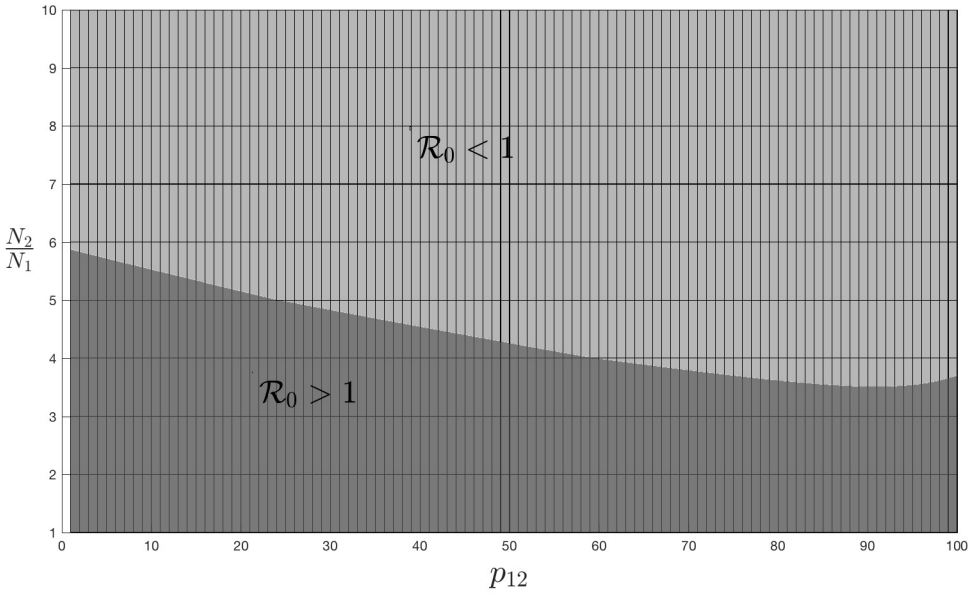

Figure 4.16: Scenario Two: Effect of Mobility and Population Size Proportions on the Global Basic Reproductive Number $\mathcal{R}_0$ When $\mathcal{R}_{02} = 0.9$, and $\mathcal{R}_{01} = 1.52$.

Consequently, the qualitative response of the final epidemic size within Patch 1 is qualitatively similar in both, the worst and best case scenarios. Moreover, reductions in risk and density do yield significant benefits in terms of the total ZIKV burden even under such restrictive conditions and assumptions (see Figure 4.16).

4.5.3 Risk Defined by Poor Bite Prevention and Poor Vector Control.

Figure 4.17 (top), shows the incidence and final ZIKV epidemic size when Patch 1 is under the "worst case scenario," defined by elevated risk and a basic reproduction number of $\mathcal{R}_{01} = 2$. Figure 4.17 shows that around $p_{12} = 0.2$, the final number of infected residents in Patch 1 starts to decrease from the number of infections caused by the baseline scenario when$p_{12} = 0$.

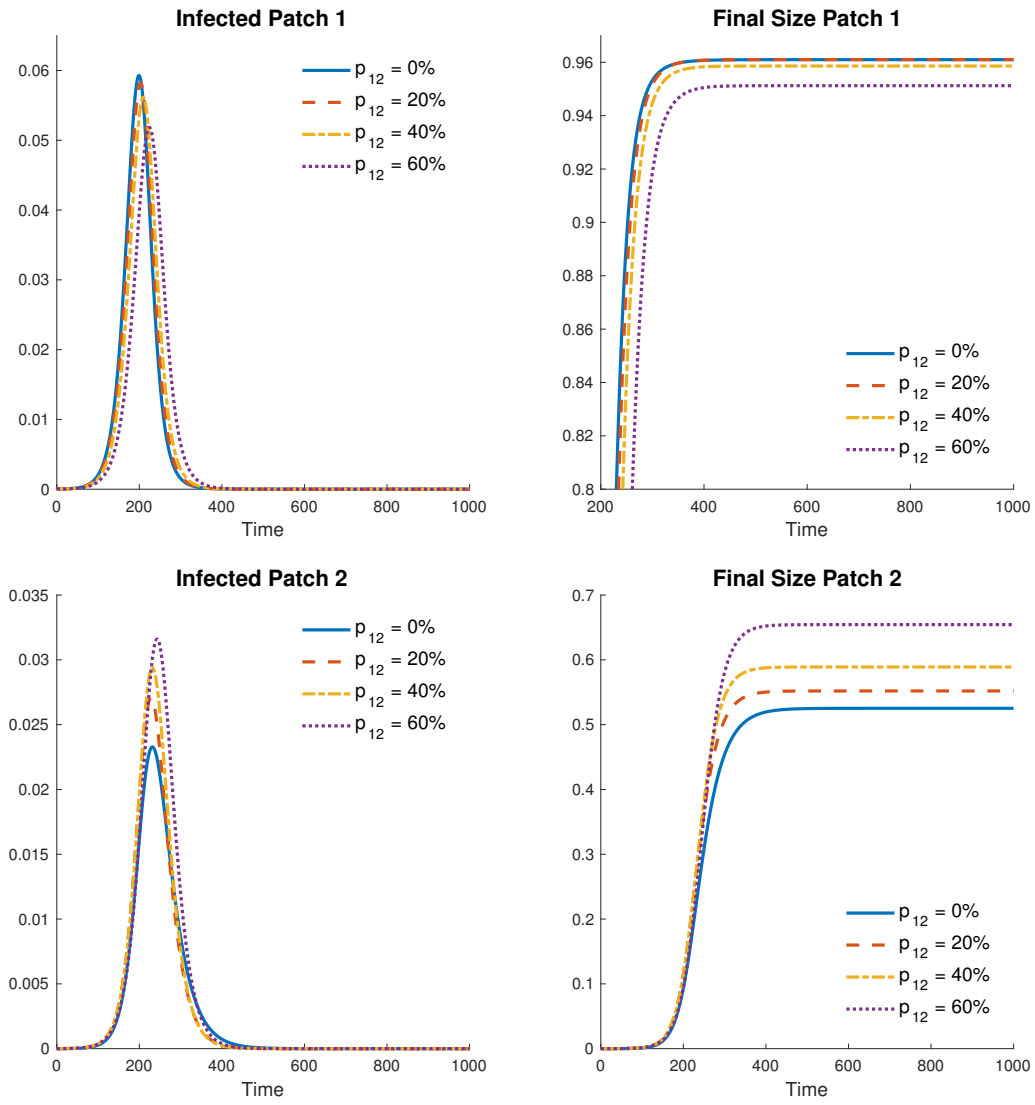

Figure 4.17: Scenario Three: Patch Incidence and Final Size Proportions for $p_{21} = 0.10$, $p_{12} = 0, 0.2, 0.4$ and 0.6 for Worst Case.

This worst case scenario for Patch 1 takes place when only Patch 2 residents are mobile, driving ZIKV infections in almost 96% of the population in Patch 1, an unrealistic value. Nonetheless, simulated p_{12} values greater than 0.2 show a beneficial reduction in the final Patch 1 epidemic size, reaching infection levels below the baseline case; a clear benefit of mobility.

Figure 4.17 highlights the case when the final Patch 2 epidemic size grows as mo-

bility from Patch 1 increases, when compared with the baseline case (no mobility from Patch 1). In addition, reductions in the final Patch 1 epidemic size for some mobility values accompanied by increments in the final Patch 2 epidemic size are observed. Again, when compared to the baseline case (no mobility from Patch 1). However, while mobility may provide benefits within Patch 1 (under the above assumptions) the fact remains that it does it at a cost to Patch 2. In short, it is also observed that the final epidemic size per patch does not respond linearly to changes in mobility even when only the mobility p_{12} is increased (see Figures 4.17 and 4.18).

Consider now the "best case" scenario, when the basic reproductive number is $\mathcal{R}_{01} = 1.52$ and once again under the assumption that the population in Patch 1 is the same as that in Patch 2. The results of simulations collected in Figure 4.18 show similar final size epidemic curves to those generated in the previous case (the "worst case" scenario for Patch 1). While some mobility values can increase the final Patch 1 epidemic size, the maximum epidemic size only reaches around 80% of the population when mobility is close to $p_{12} = 0.20$. Again, an unrealistic level, even when it was lower than in the "worst' case scenario as expected. Finally, once again observations from the simulations suggest the existence of a mobility threshold from which the final epidemic sizes in Patch 1 benefits.

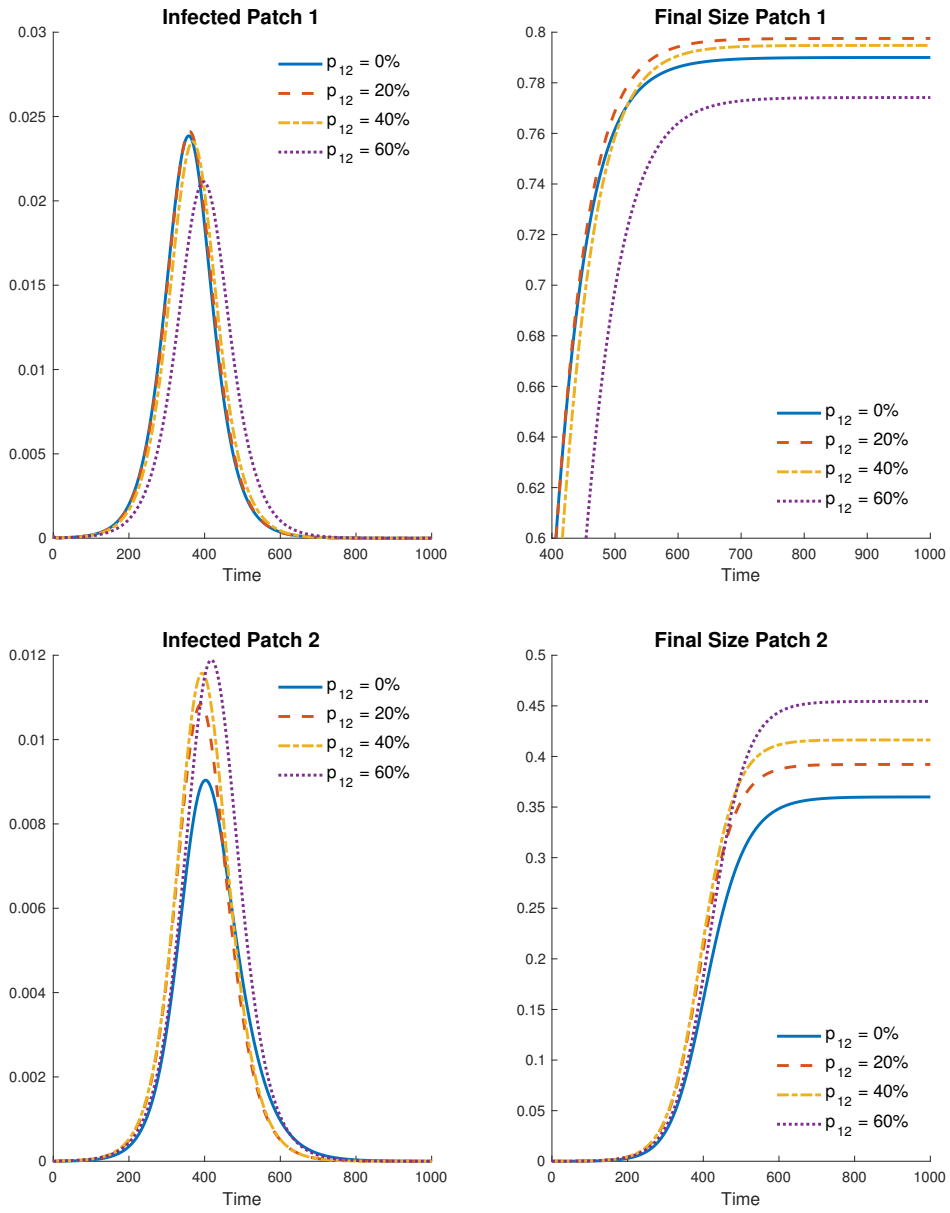

Figure 4.18: Scenario Three: Patch Incidence and Final Size Proportions for $p_{21} = 0.10$, $p_{12} = 0, 0.2, 0.4$ and 0.6 for Best Case.

The results depicted in Figure 4.18 suggest that under all p_{12} mobility levels, Patch 2 final ZIKV epidemic size supports monotonic growth in the total number of infected individuals. Moreover, the results presented thus far only provide partial information of the total impact that short term mobility might have on the transmission dynamics

of ZIKV. An expected outcome as a result of the myriad of assumptions that have been incorporated, namely, the restrictions placed on population density; the population in Patch 1 is the same as that in Patch 2. By fixing the mobility from Patch 2 to that of Patch 1, the simulations focused only on the impact of changes in mobility from Patch 1 to Patch 2. Further, potential changes in mobility patterns that host populations may cause or experience in response to ZIKV dynamics are being completely ignored when a mobility matrix $\mathbb{P}$ with constant entries p_{ij} is used. However, even under such specific restrictions and assumptions, the qualitative response of the final epidemic size within Patch 1 is qualitatively similar in both, the worst and best case scenarios: increasing at first (for low mobility values), decreasing after a certain threshold and then eventually crossing down the baseline case, under some mobility regimes. Furthermore, the qualitative behavior of the final epidemic size in Patch 2 grows monotonically as mobility increases (see Figure 4.19).

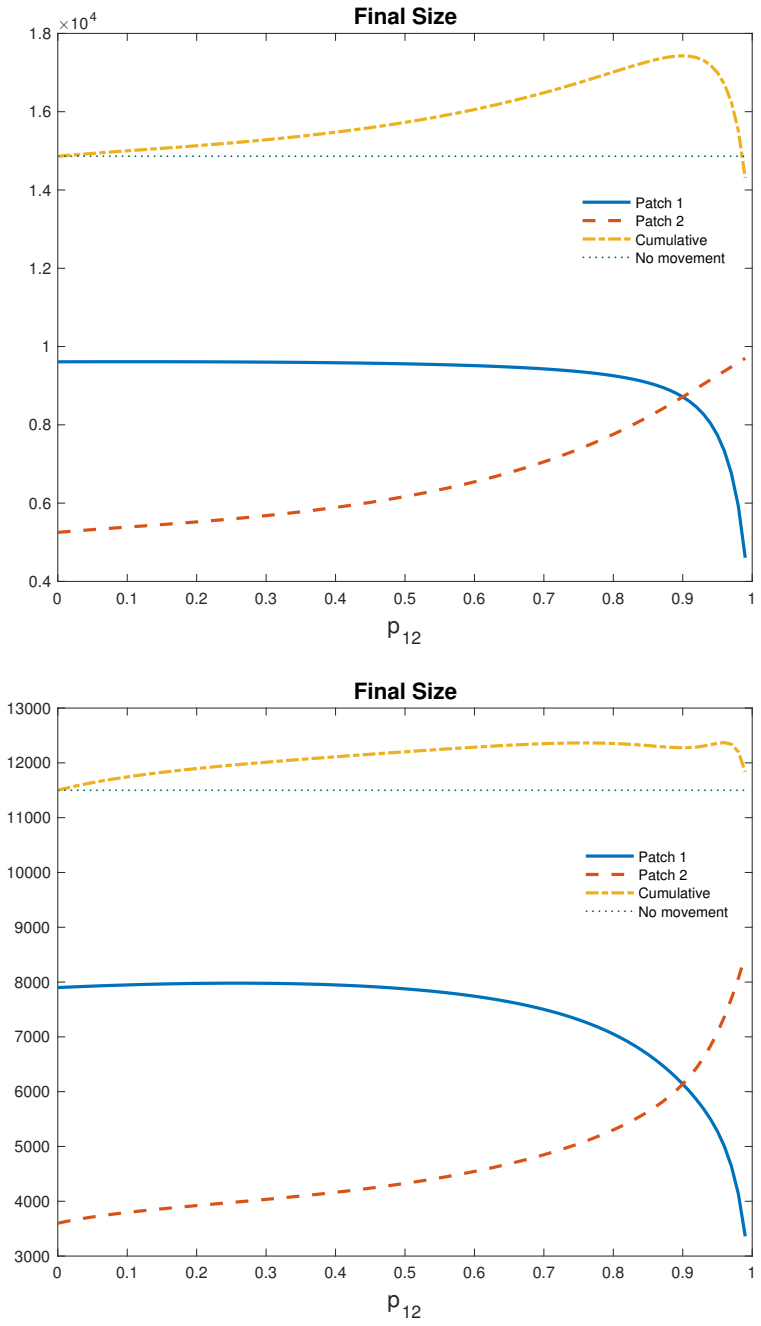

Figure 4.19: Scenario Three Final Sizes for Worst (Top) and Best (Bottom) Cases.

The Role of Risk Heterogeneity in the Dynamics of Zika Virus Transmission.

The impact of risk heterogeneity on ZIKV dynamics within the overall two-patch system is explored, an analysis that requires the numerical estimation of the global reproduction number as a function of the mobility matrix $\mathbb{P}$. Using the previously defined scenarios ($\mathcal{R}_{01} = 1.52, 2$), simulations are carried out, again assuming equal population sizes ($N_1 = N_2$). However, when looking at the impact of changes in risk on Patch 2 ($\mathcal{R}_{02} = 0.5, 0.6, 0.7, 0.8, 0.9$), simulations identify a growing epidemic in Patch 2 as risk increases with the overall community experiencing nonlinear changes in risk as residency times change from the baseline scenario given by $p_{12} = 0$. Specifically, Figure 4.20 captures the overall reductions on the global reproductive number (risk) for all residence times, while identifying the existence of a residence time interval for which mobility is beneficial, decreasing the total size of the outbreak in the two patch system, when compared to the baseline case ($p_{12} = 0$).

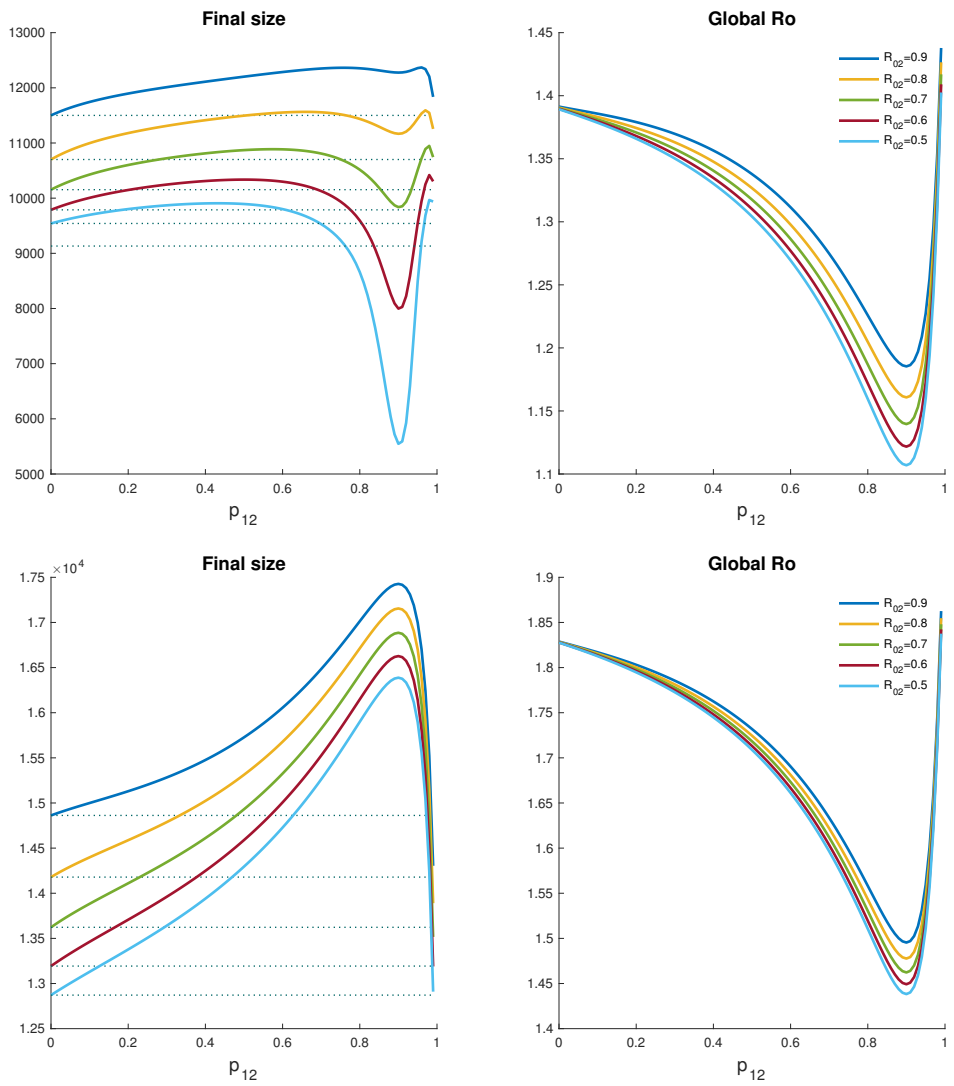

Figure 4.20: Scenario Three: Total Final Size and Global Basic Reproductive Number Through Mobility Values When $p_{21} = 0.10$, $\mathcal{R}_{02}$ Varies and $\mathcal{R}_{01} = 1.52$ (Top); 2 (Bottom).

In the case when mobility from Patch 1 is halted ($p_{12} = 0$), the final epidemic size increases as $\mathcal{R}_{0i}$ (risk) increases. While simulations suggest that mobility can slow down the speed of the outbreak (smaller global $\mathcal{R}_0$), simulation also re-affirm the obvious; the existence of a high risk, mobile and well connected patch, can serve as a disease source or an outbreak magnifier; a situation that has been explored within an n-patch system under various connective schemes (Bichara *et al.*, 2015; Castillo-

Chavez *et al.*, 2016). Moreover, it is observed that the global reproductive number $\mathcal{R}_0$ experiences reductions for almost all mobility values. Nonetheless, $\mathcal{R}_0$ never drops below unity for the two-patch scenarios selected in this study. Hence, under such assumptions and scenarios, it is seen that the use of fixed mobility patterns make the eliminating ZIKV extremely difficult, if not impossible, under the two scenarios. Figure 4.20 provides an example that highlights the relationship between the global reproductive number and the corresponding final epidemic size.

The Role of Population Size Heterogeneity in the Dynamics of Zika Virus Transmission.

The role of population density on the total final epidemic size and global basic reproductive number are now explored using the two scenarios previously defined, but now under the assumption that patch densities (population sizes) are different. More specifically, when $N_1 = N_2$, $5N_2$, $10N_2$ and $N_2 = 5N_1$, $10N_1$.

It is observed that difference in population sizes do matter. Specifically, it is observed that (under the densities selected) great density differences translate into higher final epidemic sizes. In the "worst case" scenario, infecting 90% of the population is possible for some global reproductive numbers exhibiting certain mobility patterns (see Figure 4.21). It is observed that despite increases in the total final epidemic size, as mobility changes, the global $\mathcal{R}_0$ decrease monotonically, for most residence times, but never falling below unity. A sensible degree of magnification on the spread of the disease is observed as residence times change, whenever the differences between N_1 and N_2 are not too extreme. In fact, it is possible for mobility to be beneficial in the control of ZIKV under the above simplistic extreme scenarios. Nonetheless, simulations continue to show that under the prescribed conditions and assumptions, model generated ZIKV outbreaks remain unrealistically high.

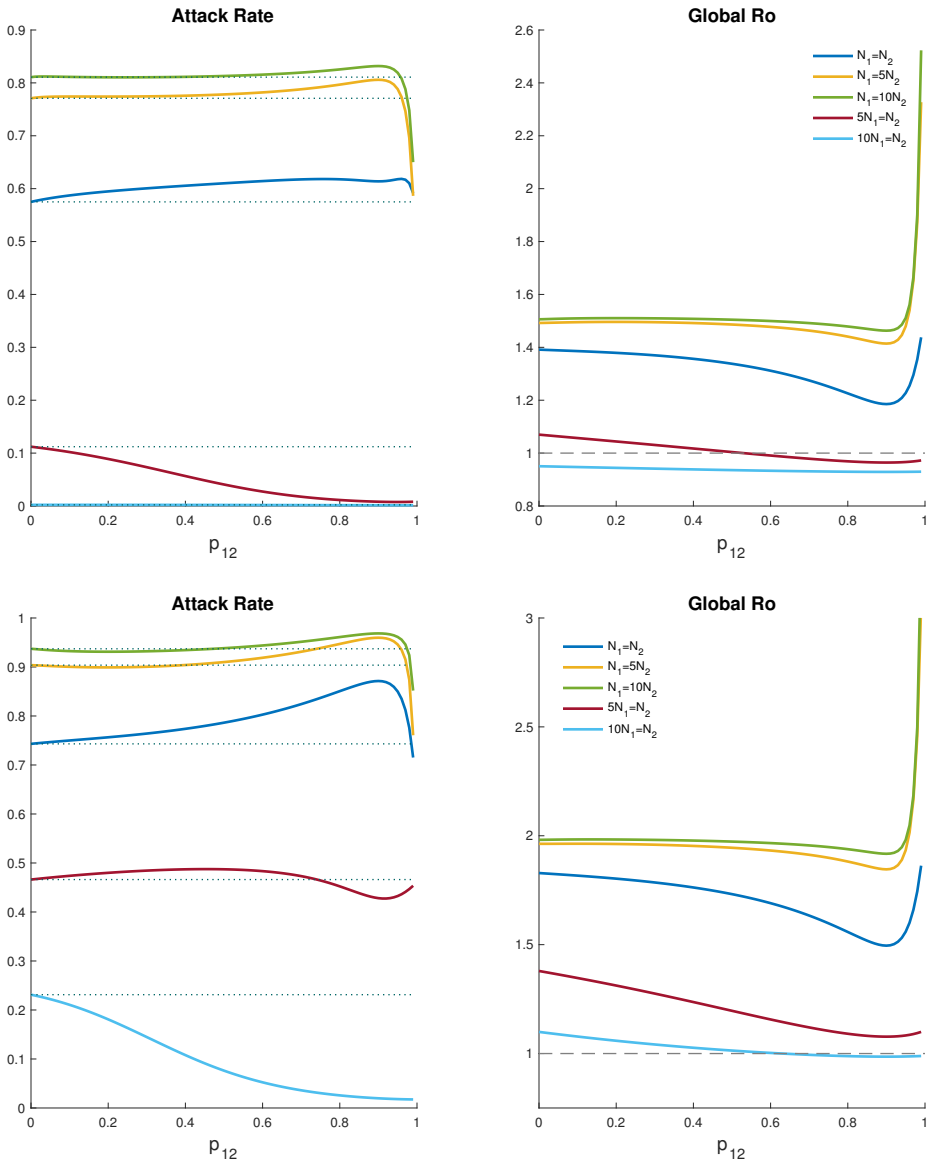

Figure 4.21: Scenario Three: Total Final Size and Global Basic Reproductive Number Through Mobility Values When $p_{21} = 0.10$, Population Size Varies, $\mathcal{R}_{02} = 0.9$, and $\mathcal{R}_{01} = 1.52$ (Top); 2 (Bottom).

Furthermore, the simulations show a minimum global reproductive number when $p_{12} \approx 0.90$. Figure 4.21 also shows that larger high risk population ($N_1 >> N_2$) exhibit a greater total final epidemic size when individuals from Patch 1 spend more than half of their time in Patch 2 (see also Figure 4.22).

For the two epidemiological scenarios $\mathcal{R}_{01} = 2$ and $\mathcal{R}_{01} = 1.52$, Tables 4.9 and 4.10

provide a summary of the average proportion of infected for low ($p_{12} = 0.01 - 0.33$), intermediate ($p_{12} = 0.34 - 0.66$) and high mobility ($p_{12} = 0.67 - 0.99$) when $p_{21} = 0.10$. The role of population scaling ($N_1 = N_2/10$, $N_2/5$, N_2, $5N_2$ and $10N_2$ when the largest population is 10000) is also explored.

Table 4.9: Scenario Three: Final Size (Patch 1, Patch 2), $\mathcal{R}_{01} = 2$, $\mathcal{R}_{02} = 0.9$ and $p_{21} = 0.10$.

N_2	Low Mobility	Intermediate Mobility	High Mobility	Min $\mathcal{R}_0$
$N_1 = N_2/10$	(0.3819, 0.1678)	(0.1387, 0.0738)	(0.0309, 0.0248)	0.9857
$N_1 = N_2/5$	(0.8167, 0.4097)	(0.7376, 0.4349)	(0.5036, 0.4385)	1.0775
$N_1 = N_2$	(0.9609, 0.5487)	(0.9550, 0.6213)	(0.8701, 0.8124)	1.4954
$N_1 = 5N_2$	(0.9746, 0.5296)	(0.9739, 0.5985)	(0.9506, 0.8692)	1.8457
$N_1 = 10N_2$	(0.9757, 0.4989)	(0.9753, 0.5766)	(0.9638, 0.8722)	1.9173

Table 4.10: Scenario Three: Final Size (Patch 1, Patch 2), $\mathcal{R}_{01} = 1.52$, $\mathcal{R}_{02} = 0.9$ and $p_{21} = 0.10$.

N_2	Low Mobility	Intermediate Mobility	High Mobility	Min $\mathcal{R}_0$
$N_1 = N_2/10$	(0.0045, 0.0020)	(0.0036, 0.0018)	(0.0026, 0.0014)	0.9289
$N_1 = N_2/5$	(0.1773, 0.0748)	(0.0688, 0.0364)	(0.0139, 0.0109)	0.9643
$N_1 = N_2$	(0.7959, 0.3875)	(0.7847, 0.4352)	(0.6499, 0.5816)	1.1853
$N_1 = 5N_2$	(0.8522, 0.3832)	(0.8519, 0.4137)	(0.8017, 0.6996)	1.4141
$N_1 = 10N_2$	(0.8568, 0.3529)	(0.8563, 0.3855)	(0.8267, 0.7077)	1.4630

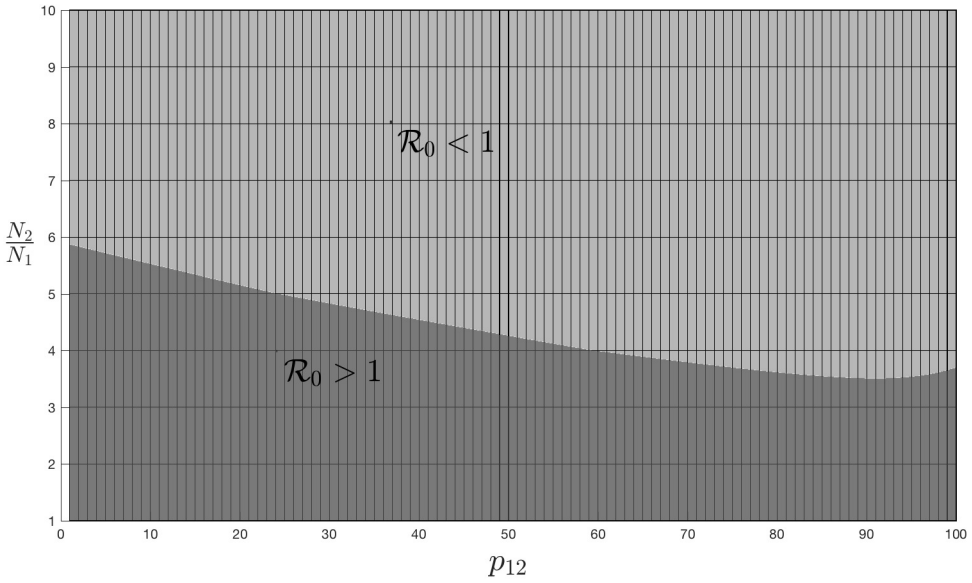

Figure 4.22: Scenario Three: Effect of Mobility and Population Size Proportions on the Global Basic Reproductive Number $\mathcal{R}_0$ When $\mathcal{R}_{02} = 0.9$, and $\mathcal{R}_{01} = 1.52$.

The results collected suggest that short-term mobility plays an important role in ZIKV dynamics, under a system involving two highly heterogeneous patches. Simulations also suggest that, even though mobility can reduce the global basic reproductive number, in most cases it is not enough to eliminate an outbreak or make a significant difference under the scenarios explored.

4.6 Conclusions and Discussion.

This study focuses on the dynamics of a single outbreak, albeit the modeling framework can be used to study long-term dynamics when the mobility patterns can be captured effectively by $\mathbb{P}$. A two-patch model where host-mobility is modeled using a Lagrangian approach is used to help understand the role of host-movement on the transmission dynamics of ZIKV. The patches were defined to be as distinct as they could be, hoping that simulations, in this simplified system, could capture some insight on the transmission dynamics of ZIKV in the presence of extreme health

disparities within neighboring communities or within urban centers. This framework can be used to study the dynamics of vector born diseases within a collection of neighboring communities or neighborhoods experiencing multiple levels of health disparities and diverse connectivity mobility structures (Bichara and Castillo-Chavez, 2016). The study of the role of mobility at larger scales can be best captured using question-specific related models that account for the possibility of long-term mobility (see for example (Herrera-Valdez *et al.*, 2011; Chowell *et al.*, 2003b; Baroyan *et al.*, 1971; Rvachev and Longini Jr, 1985; Elveback *et al.*, 1976; Banks and Castillo-Chavez, 2003; Khan *et al.*, 2009)).

Although the goal is not to fit specific outbreaks or specific situations, recently published parameter ranges were used since framing the system within the range of ZIKV accepted parameters helps highlight the impact that mobility may have within two highly distinct (bi-modal) communities in a more realistic way. The incorporation of a Lagrangian modeling approach to study epidemic outbreaks makes it possible to use measurable parameters like risk ($\hat{\beta}$), which affect individuals differently depending on the patch-residency times their mobility patterns (residency times).

As a result, the impact of ZIKV can be assessed locally (at the patch level) or globally (regional level, in this case two patch system). System risk assessment was carried out via the computation of the system $\mathcal{R}_0$, which must be carried out via the numerical solution of a system of nonlinear equations. Specifically, changes on the system $\mathcal{R}_0$ were computed (with respect to residency times) and compared to the local $\mathcal{R}_{0i}$ in the absence of mobility. Further, the mobility-dependent system final epidemic sizes were computed via simulations. These final sizes helped asses the impact of mobility (and risk) locally and globally, within the two selected scenarios, ($\mathcal{R}_{01} = 1.52$ and $\mathcal{R}_{01} = 2$). As expected, the impact of mobility on the final epidemic size depends on the local risk of infection and population size. Moreover, it was

also determined that there are certain cases in which mobility could be detrimental, highlighting the necessity to reduce health disparities in vulnerable communities. In fact, mobility from high to low risk patches can reduce or increase the total final epidemic size; mobility could be used as a strategy to ameliorate the impact of ZIKV outbreaks.

The challenges posed by policies that may be beneficial to the system but detrimental are also explored within this two-patch system. Situations where the total final epidemic size increased as R_{02} increased and situations where the total final epidemic size decreased under low mobility values when $R_{02} \sim 1$ were documented. Population density does make a difference and examples when $R_{02} < 1$ with mobility incapable of reducing the total final epidemic size under no differences in patch density (here measured by total population size in each patch, both assumed to have roughly the same area) were also identified. Differences in population density were also shown to be capable of generating reductions on the total final epidemic size within some mobility regimes.

The highly simplified two-patch model used seem to have shed some light on the role of mobility on the spread of ZIKV in areas where huge differences in the availability of public health programs and services,–the result of endemic crime, generalized violence and neglect– exist. Model simulations also seemed to have shed some light on the potential relevance of the factors not accounted for. The value of the use of single patch-specific risk parameters ($\hat{\beta}$) has strengths and limitations. It is important to notice that the model used did not account explicitly for changes in the levels of infection within the vector population nor does it account for impact of substantial differences in patch vector population sizes. The simplified model fails to account for the responses to outbreaks by patch residents as individuals may alter mobility patterns, use more protective clothing, and respond individually and independently

of official control programs in response to dramatic increases on vector population or a surge in cases. Clearly, the use of two patches and assumptions do limit the outcomes that such a system can support. Communities can't, in general, be modeled under a highly differentiated two-tier system and in the case of ZIKV, the possibility of vertical transmission in humans and vectors as well as sexually-transmitted ZIV can't be completely neglected (Brauer *et al.*, 2016). The introduction of changes in behavior in response to individuals' assessment of the levels of risk infection over time needs to be addressed (Castillo-Chavez *et al.*, 2016); a challenge that has yet to be met to the satisfaction of the scientific community involved in the study of epidemiological processes as complex adaptive systems (see for example (Perrings *et al.*, 2014; Fenichel *et al.*, 2011; Morin *et al.*, 2013)).

The limitations of the role of technology in the absence of the public health infrastructure –there is no silver bullet– has been recently addressed in the context of Ebola (Chowell *et al.*, 2015; Yong *et al.*, 2016) with applications of the Lagrangian approach as presented here in the context of communicable and vector born diseases, including dengue, tuberculosis and Ebola, in settings where health disparities are pervasive (Espinoza *et al.*, 2016; Moreno *et al.*, 2017a; Bichara *et al.*, 2016). Further, the use of simplified models, quite often tends to over-estimate the impact of an outbreak [see (Nishiura *et al.*, 2009, 2011)] and the model and scenarios used highlight the limitations on the use of simplified settings when the goal is to capture or mimic the dynamics of specific systems–not the goal of this study.

Certainly, the use of dramatic measures to limit the spread of diseases like SARS, Influenza or Ebola ((Chowell *et al.*, 2003a; Herrera-Valdez *et al.*, 2011; Chowell *et al.*, 2015)), as well as the rise of vector born diseases like Dengue and Zika are not uncommon, and the dramatic implications that some measures have had on local and global economies. The question remains, what can we do to mitigate or limit the

spread of disease, particularly emergent diseases without disrupting central components? Discussions on these issues are recurrent (Fenichel *et al.*, 2011; Morin *et al.*, 2013), most intensely in the context of SARS, Influenza, Ebola and Zika, in the last decade or so. The vulnerability of world societies is directly linked to the lack of action in addressing the challenges faced by the weakest links in the system must be accepted and acted on by the world community. We need global investments in communities and nations where health disparities and lack of resources are the norm. We must invest in research and surveillance within clearly identified world hot spots, where the emergence of new disease are most likely to emerge, and we must do so with the involvement, at all levels, of the affected communities (Perrings *et al.*, 2014; Castillo-Chavez *et al.*, 2015).

Chapter 5

THE ROLE OF MOBILITY AND HEALTH DISPARITIES ON THE TRANSMISSION DYNAMICS OF TUBERCULOSIS.

Background The transmission dynamics of Tuberculosis (TB) not only involves multiple transmission methods but also requires of the incorporation of complex epidemiological and socio-economical interactions between individuals living in highly distinct regional conditions. The different levels of the methods of transmission (exogenous reinfection and first time infection) within high-incidence settings may influence the impact of control programs on TB prevalence.

Methods The goal of this study is to improve the basic understanding of TB dynamics via scenarios, within simplified, two patch, risk-defined interconnected environments in the presence of short term mobility and variations in reinfection and infection rates. Using a modeling framework that captures the average proportion of time spent in places of residency, work or business the role of individuals' 'daily' dynamics within and between TB-risk environments (patches) was estimated. As a direct result, the effective population size of Patch i at time t must account for both visitor and residents of Patch i, at time t.

Results The impact that the distribution of individuals' residence times has on the effective population size and ultimately on TB transmission and control in different patches are studied using selected scenarios where risk is defined by the estimated or perceived first time infection and/or exogenous re-infection rates.

Conclusions The results suggest that allowing infected individuals to move from high to low TB prevalence areas (where the sharing of treatment and isolation facilities is possible) may lead to a reduction in the total TB prevalence in the overall (two-patch)

population under certain conditions.

5.1 Background

Tuberculosis (TB), a communicable disease caused by the bacteria *Mycobacterium tuberculosis*, remains among one of the leading causes of death in the world. According to the 2014 World Health Organization's (WHO) TB report, 9.6 million people developed symptomatic TB infections and 1.5 million TB-associated deaths (World Health Organization, 2015). Despite advances in TB research and the existence of treatment and vaccine, it is estimated that one-third of the world population serves as TB reservoirs. The majority of these TB reservoirs (latently infected individuals) live in developing countries where exposure to multiple TB risk factors is common. More specifically, individuals living in rural areas (mainly in developing countries) and below the poverty line, disproportionately contribute to the documented TB burden (Legesse *et al.*, 2010; Ahn *et al.*, 2005); or are exposed to a higher risk of infection. Recent data analysis has suggested a strong association between poverty and TB in economically underprivileged countries (Bhatt *et al.*, 2010). Vulnerable groups are at greater risk of TB infection compared with the general population because of poor urbanization, overcrowding and substandard living. In addition, poor working conditions, poor nutrition, inter-current diseases, and migration from (or to) higher-risk patches are also associated with higher risk of acquiring TB (Ahn *et al.*, 2005). Furthermore, the overall worldwide TB-burden continues to rise as the world population continues to grow rapidly (Lawn and Zumla, 2011), even when the worldwide TB incidence rates seemed to have peaked in 2004. The study of (Gomes *et al.*, 2012) suggest that TB-reinfection rates (reinfection after successful treatment), are higher than TB infection rates (among those with no prior TB-experience). In their study, they propose two mechanisms to maintain high TB prevalence: (i) past infections

increase susceptibility to reinfection (ii) differences in susceptibility to infection contribute to increased re-infection rates among the treated; something that needs to be supported by data. Consequently, (Gomes *et al.*, 2012) noted that, the rates of reinfection are higher at the population level than at the individual level. Additionally, inappropriate treatment and the use of poor quality drugs in recent years have led to wild and antibiotic resistant strains contributing to the already high TB-active incidence and making TB a major global health threat.

Population level studies require the use of metapopulation models that account for population aggregation at a given patch. Metapopulation type transmission models offer a powerful set up for the study of TB dynamics and the effectiveness of population-level TB interventions like treatment, movement restrictions, and local control measures [see (Castillo Chávez *et al.*, 2000)]. Similarly, (Tanaka *et al.*, 2014) and (Allen *et al.*, 2009) present models aimed at exploring the impact of immigration in mobile populations within an n-patch system with risk heterogeneity. However, these models made use of an Eulerian approach where the concepts of residence times and effective population size were not incorporated; in short this approach does not allow for the identification (of the place of residency) of treated or quarantined individuals as well as the impact of the effective population size on the transmission dynamics. Prior TB-related studies have estimated incidence growth, explored the impact of TB interventions and the impact of exogenous reinfection, however, movement of individuals that keep track of place of residency have been in general ignored [see (Castillo Chávez *et al.*, 2000)]. Moreover, limited studies have considered models incorporating movement via mass transportation within a Lagrangian approach based on budgeting contacts as a function of residency times [see (Castillo Chávez *et al.*, 2000)], taking into account the impact of sudden blips of immigration (Tewa *et al.*, 2012; Liu *et al.*, 2012; Zhou *et al.*, 2008; Brauer and van den Driessche, 2001;

Shim, 2006), co-infections, specially with HIV (Kapitanov, 2015; Nthiiri *et al.*, 2015; Bhunu *et al.*, 2009; Bowong and Kurths, 2010; Hohmann and Voss-Böhme, 2013; Roeger *et al.*, 2009), relapse (Gomes *et al.*, 2012; Millet *et al.*, 2013; Marx *et al.*, 2014; Luzze *et al.*, 2013; Tiemersma *et al.*, 2011), antibiotic, drug, and ultra-drug resistance (Okuonghae, 2013; Ozcaglar *et al.*, 2012; Bhunu, 2011; Lipsitch and Levin, 1998; Agusto and Adekunle, 2014; Cohen *et al.*, 2009) or TB re-activation and progression (Feng *et al.*, 2000; Cohen *et al.*, 2007; Zheng *et al.*, 2014a), which may be central to TB re-emergence. In addition, models assuming negligible immigration might not capture the real TB dynamics in certain populations where high levels of diversity are caused by immigration (Ozcaglar *et al.*, 2012).

Since research aimed at increasing the understanding of TB transmission dynamics explicitly incorporating heterogeneous TB-risk environments is limited, the goal of this study is to increase the basic understanding of the impact residence times and population sizes, across distinct risk environments have on the transmission dynamics of TB; when risk is defined in terms of new infections and/or exogenous re-infection rates. Here, residence time is defined as the average proportion of time an individual spends daily in a given environment. In particular, the following questions were addressed:

- How does mobility changes TB prevalence via the trade-off between exogenous and direct first time infection rates?,
- How differences in TB prevalence and population sizes can influence the impact of mobility on the total number of infections? and
- Which transmission method, direct first time infection or exogenous re-infection, is capable of sustaining higher TB prevalence?

5.2 Methods: TB Dynamic Modeling Framework

A model for the transmission dynamics of TB in two interacting populations identified by their place of residence was considered. First, a single patch model was introduced and then a Lagrangian approach via the explicit use of residence time in order to capture the interacting dynamics of a two patch system was incorporated. The two-patch residence time model is used to address the role of movement (implicit) and patch-risk on TB dynamics. Relevant definitions and case studies scenarios explored in this study are collected in Table 5.1.

Table 5.1: Definitions and Scenarios for TB

Nomenclature	
Risk	Interpreted based on levels of infection rate, prevalence, or average contacts (via population size)
High-risk patch	Defined either by high direct first time infection rate (i.e., high β which leads to high corresponding $\mathcal{R}_0$) or by high exogenous re-infection rate (i.e., high δ)
Enhanced socio-economic conditions (reducing health disparity)	Defined by better healthcare infrastructure which is incorporated by high prevalence of a disease (i.e., high $I(0)/N$) in a large population (i.e., large N)
Mobility	Captured by average residence times of an individual in different patches (i.e., by using $\mathbb{P}$ matrix)
Scenarios (assume high-risk and diminished socio-economic conditions in Patch 1 as compared to Patch 2)	
Scenario 1	$\underbrace{\beta_1 > \beta_2,\ \delta_1 = \delta_2;}_{\text{high risk}}$ $\underbrace{\frac{I_1(0)}{N_1} > \frac{I_2(0)}{N_2},\ N_1 > N_2;}_{\text{socio-economic conditions}}$ $\underbrace{\text{vary } p_{12} \text{ when } p_{21} \approx 0}_{\text{mobility}}$
Scenario 2	$\underbrace{\beta_1 = \beta_2,\ \delta_1 > \delta_2;}_{\text{high risk}}$ $\underbrace{\frac{I_1(0)}{N_1} > \frac{I_2(0)}{N_2},\ N_1 > N_2;}_{\text{socio-economic conditions}}$ $\underbrace{\text{vary } p_{12} \text{ when } p_{21} \approx 0}_{\text{mobility}}$

5.2.1 A Simple Single Patch TB Model with Homogenous Mixing

The transmission dynamics of TB in homogeneously mixed population is represented by a system of three differential equations describing the TB contagion pro-

cess. The population is divided into three sub-populations each corresponding to an epidemiological state of the TB contagion process: susceptible individuals (S), noninfectious infected or latent individuals (L), and actively infectious individuals (I).

The model considers three contagion pathways: direct progression (fast dynamics), endogenous reactivation (slow progression, often years after infection) and exogenous reinfection. A susceptible individual (S) may get infected through contacts with actively infectious individuals (I), proceeding to either the noninfectious latent class (L) with probability q or to the actively infectious (I) state with probability $(1-q)$ where $q \in [0,1]$. Meaning that the fraction $(1-q)$ denotes the proportion of recently infected individuals experiencing fast progression and move directly into the infectious stage (I). On the other hand, reactivation from a longstanding latent infections is modeled by the transition of individuals from the noninfectious to the infectious state via endogenous reactivation at the per capita rate γ, or via exogenous reinfection at the per capita rate δ. Finally, infectious individuals are treated at the per capita rate ρ moving to the non-infectious infected category L as total *mycobacterium* elimination in the human body is assumed to be not possible.

The model assumes the following conditions: (1) the population is constant; (2) TB-induced deaths are negligible and hence ignored; (3) only a fraction of individuals are infectious; (4) individuals may recover from an active infection without treatment moving back to the latent class; (5) latent individuals may relapse and develop active TB or remain in this class until death due to natural causes (not TB). The flow diagram associated with the transmission dynamics of the TB model used can be found in Figure 5.1.

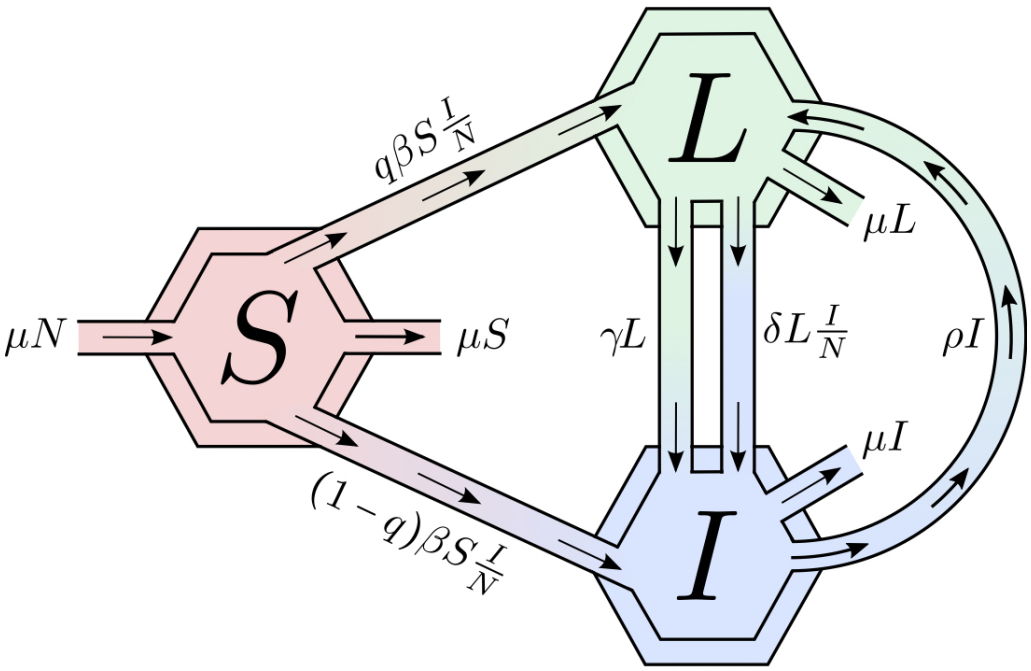

Figure 5.1: Flow Diagram for the Single Patch Three Compartment TB Model: Susceptible (S), Infected Latent (L) and Infectious (I).

This model follows the structure used in (Feng *et al.*, 2000; Mccluskey, 2006; Zheng *et al.*, 2014b) where all three contagion pathways are considered: exogenous reinfection, fast and slow progression. Similarly, the basic reproduction number as well as the conditions for the existence and stability equilibria (disease free and endemic steady states) are highlighted in (Feng *et al.*, 2000; Mccluskey, 2006; Zheng *et al.*, 2014b). The basic reproduction number for the model represented in Figure 5.1 is given by the algebraic expression

$$\mathcal{R}_0 = \frac{\beta(\gamma + (1-q)\mu)}{\mu(\mu + \rho + \gamma)} \qquad (\star)$$

The basic reproduction number ($\mathcal{R}_0$) gives the average number of secondary infections generated by a typically infected individual in a population of susceptible individuals. In $\star$, it was noticed that in a completely susceptible population there are only two pathways; slow and fast progression. In addition, in the case were exogenous reinfection is a pathway to TB contagion and excluding fast progression

(meaning that $q = 1$ and $\delta > 0$), it is known that the model can support two stable equilibria simultaneously (backward bifurcation) (Feng *et al.*, 2000). In consequence, the role of TB could be closely linked not only to the basic reproductive number ($\mathcal{R}_0$), but also to the initial conditions.

5.2.2 A Two-patch TB Model with Heterogeneity in Population Through Residence Times

Using the transmission dynamics outlined above and depicted in Figure 5.1, a two-patch model is now build, under a residency-time matrix $\mathbb{P}$.

Let N_1, N_2 be the host population of Patch 1 and 2, respectively and p_{ij} be the proportion of time an individual from Patch i spends on average in Patch j. Consequently, individuals from Patch 1 spend on average, the proportion p_{11} of their time in Patch 1 and the proportion p_{12} of their time in Patch 2 ($p_{11} + p_{12} = 1$). Similarly, residents of Patch 2 spend p_{22} of their time in Patch 2 and $p_{21} = 1 - p_{22}$ in Patch 1. Hence, without a loss of generality, at any given time t in Patch 1, the effective population in Patch 1 is $p_{11}N_1 + p_{21}N_2$, while the effective population of Patch 2 at time t is $p_{12}N_1 + p_{22}N_2$. Again, susceptible individuals from Patch 1 (S_1) may become infected in Patch 1 ($p_{11}S_1$) or in Patch 2 ($p_{12}S_2$). Similarly, using this Lagrangian approach that provides an implicit way to capture the movement of individuals, the effective proportion of infectious individuals in Patch 1 at time t is

$$\frac{p_{11}I_1 + p_{21}I_2}{p_{11}N_1 + p_{21}N_2}.$$

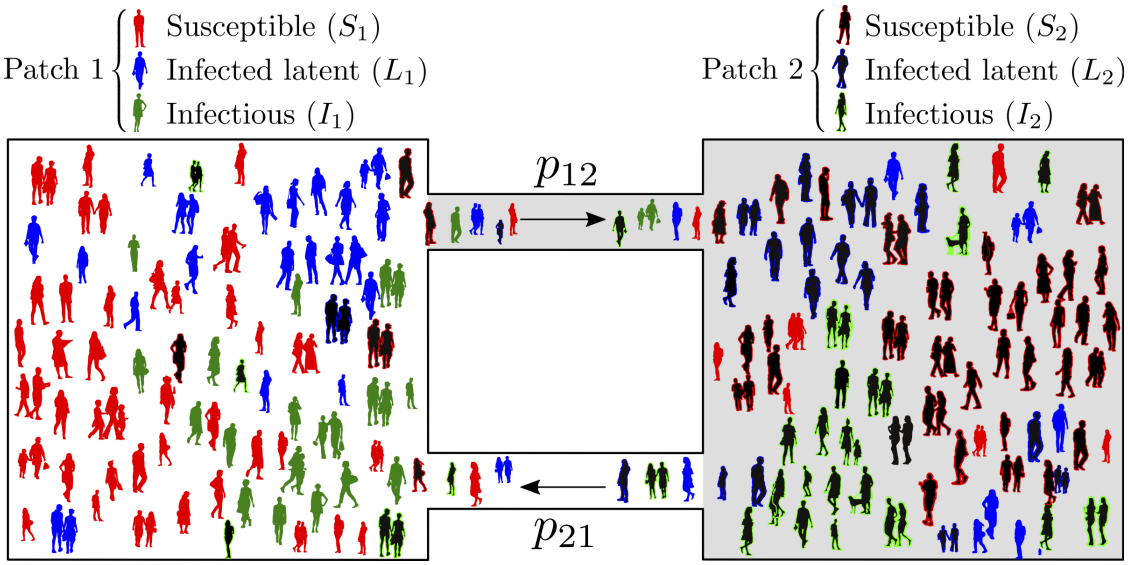

Figure 5.2: Schematic Description of the Lagrangian Approach Between Two Patches.

Hence, the transmission dynamics between infectious and susceptible residents from Patch 1 are given by

$$\dot{S}_1 = \mu_1 N_1 - \beta_1 p_{11} S_1 \frac{p_{11}I_1 + p_{21}I_2}{p_{11}N_1 + p_{21}N_2} - \beta_2 p_{12} S_1 \frac{p_{12}I_1 + p_{22}I_2}{p_{12}N_1 + p_{22}N_2} - \mu_1 S_1. \tag{5.1}$$

Subsequently, the latency dynamics among residents from Patch 1 are,

$$\begin{aligned}\dot{L}_1 = {} & q\beta_1 p_{11} S_1 \frac{p_{11}I_1 + p_{21}I_2}{p_{11}N_1 + p_{21}N_2} + q\beta_2 p_{12} S_1 \frac{p_{12}I_1 + p_{22}I_2}{p_{12}N_1 + p_{22}N_2} \\ & - \delta_1 p_{11} L_1 \frac{p_{11}I_1 + p_{21}I_2}{p_{11}N_1 + p_{21}N_2} - \delta_2 p_{12} L_1 \frac{p_{12}I_1 + p_{22}I_2}{p_{12}N_1 + p_{22}N_2} - (\gamma_1 + \mu_1)L_1 + \rho_1 I_1. \end{aligned} \tag{5.2}$$

Finally, the dynamics in which residents from Patch 1 reach the infectious state are

$$\begin{aligned}\dot{I}_1 = {} & (1-q)\beta_1 p_{11} S_1 \frac{p_{11}I_1 + p_{21}I_2}{p_{11}N_1 + p_{21}N_2} + (1-q)\beta_2 p_{12} S_1 \frac{p_{12}I_1 + p_{22}I_2}{p_{12}N_1 + p_{22}N_2} \\ & + \delta_1 p_{11} L_1 \frac{p_{11}I_1 + p_{21}I_2}{p_{11}N_1 + p_{21}N_2} + \delta_2 p_{12} L_1 \frac{p_{12}I_1 + p_{22}I_2}{p_{12}N_1 + p_{22}N_2} + \gamma_1 L_1 - (\mu_1 + \rho_1)I_1. \end{aligned} \tag{5.3}$$

Using (5.1), (5.2),(5.3), that describe TB dynamics in one patch, the transmission dynamics for a two patch system are given by the following System ($i = 1, 2$):

$$\begin{cases} \dot{S}_i = \mu_i N_i - \sum_{j=1}^{2} \beta_j p_{ij} S_i \frac{\sum_{k=1}^{2} p_{kj} I_k}{\sum_{k=1}^{2} p_{kj} N_k} - \mu_i S_i, \\ \dot{L}_i = q \sum_{j=1}^{2} \beta_j p_{ij} S_i \frac{\sum_{k=1}^{2} p_{kj} I_k}{\sum_{k=1}^{2} p_{kj} N_k} - \sum_{j=1}^{2} \delta_j p_{ij} L_i \frac{\sum_{k=1}^{2} p_{kj} I_k}{\sum_{k=1}^{2} p_{kj} N_k} - (\gamma_i + \mu_i) L_i + \rho_i I_i, \\ \dot{I}_i = (1-q) \sum_{j=1}^{2} \beta_j p_{ij} S_i \frac{\sum_{k=1}^{2} p_{kj} I_k}{\sum_{k=1}^{2} p_{kj} N_k} + \sum_{j=1}^{2} \delta_j p_{ij} L_i \frac{\sum_{k=1}^{2} p_{kj} I_k}{\sum_{k=1}^{2} p_{kj} N_k} + \gamma_i L_i - (\mu_i + \rho_i) I_i. \end{cases} \tag{5.4}$$

Notice that the total population of Patch i, $i = 1, 2$ could be also represented by $N_i = S_i + L_i + I_i$. Moreover, System (5.4) has the same qualitative dynamics as the following reduced system, since the total population is constant:

$$\begin{cases} \dot{L}_i = q \sum_{j=1}^{2} \beta_j p_{ij} (N_i - L_i - I_i) \frac{\sum_{k=1}^{2} p_{kj} I_k}{\sum_{k=1}^{2} p_{kj} N_k} - \sum_{j=1}^{2} \delta_j p_{ij} L_i \frac{\sum_{k=1}^{2} p_{kj} I_k}{\sum_{k=1}^{2} p_{kj} N_k} - (\gamma_i + \mu_i) L_i + \rho_i I_i, \\ \dot{I}_i = \sum_{j=1}^{2} p_{ij} \left((1-q) \beta_j (N_i - L_i - I_i) + \delta_j L_i \right) \frac{\sum_{k=1}^{2} p_{kj} I_k}{\sum_{k=1}^{2} p_{kj} N_k} + \gamma_i L_i - (\mu_i + \rho_i) I_i. \end{cases} \tag{5.5}$$

A schematic description of the two-patch dynamical model is provided in Figure 5.2 and the description of the parameters used as well as estimates from previous studies can be found in Table 5.2.

Table 5.2: Description of the Parameters Used in System (5.5)

Parameters	Description	Ranges(units)
β_i	Susceptibility to TB invasion in Patch i	0.01 - 0.0192 (y^{-1})
δ_i	Susceptibility to exogenous TB progression in Patch i	0.0026 - 0.0053 (y^{-1})
μ_i	Natural birth and death (per capita)	0.0104 - 0.0143 (y^{-1})
ρ	Relapse (per capita)	0.0010 - 0.0083(y^{-1})
γ_i	Activation from latency in Patch i (per capita)	0.0017 - 0.0036 (y^{-1})
q	Proportion of individuals that develop latent TB	0.9 (dimensionless)
p_{ij}	Proportion of time that residents of Patch i spend in Patch j	Varies (dimensionless)

For parameter ranges, see (Cohen *et al.*, 2007; Blower *et al.*, 1995; Gomes *et al.*, 2004; Okuonghae, 2013; Dowdy *et al.*, 2012; Langley *et al.*, 2014) .

5.3 Results

5.3.1 Model Analysis

The disease-free equilibrium of System (5.5) is located at the origin of the positive orthant $\mathbb{R}^4_+$, that is $E_0 = 0_{\mathbb{R}^4_+}$. The basic reproduction number ($\mathcal{R}_0$) of System (5.5) is computed following the next generation method described in (Van den Driessche and Watmough, 2002; Diekmann *et al.*, 1990). System (5.5) was then decomposed into two vectors: the "new infection" vector, denoted by $\mathcal{F}$, and the "transition" vector, denoted by $\mathcal{V}$. Hence,

$$
\begin{bmatrix} \dot{L}_1 \\ \dot{L}_2 \\ \dot{E}_1 \\ \dot{E}_2 \end{bmatrix} = \mathcal{F} + \mathcal{V}
$$

$$
= \begin{bmatrix} q\sum_{j=1}^{2}\beta_j p_{1j}(N_1 - L_1 - I_1)\frac{\sum_{k=1}^{2} p_{kj} I_k}{\sum_{k=1}^{2} p_{kj} N_k} \\ q\sum_{j=1}^{2}\beta_j p_{2j}(N_2 - L_2 - I_2)\frac{\sum_{k=1}^{2} p_{kj} I_k}{\sum_{k=1}^{2} p_{kj} N_k} \\ (1-q)\sum_{j=1}^{2}\beta_j p_{1j}(N_1 - L_1 - I_1)\frac{\sum_{k=1}^{2} p_{kj} I_k}{\sum_{k=1}^{2} p_{kj} N_k} \\ (1-q)\sum_{j=1}^{2}\beta_j p_{2j}(N_2 - L_2 - I_2)\frac{\sum_{k=1}^{2} p_{kj} I_k}{\sum_{k=1}^{2} p_{kj} N_k} \end{bmatrix} +
$$

$$
+ \begin{bmatrix} -\sum_{j=1}^{2}\delta_j p_{1j} L_1 \frac{\sum_{k=1}^{2} p_{kj} I_k}{\sum_{k=1}^{2} p_{kj} N_k} - (\gamma_1 + \mu_1)L_1 + \rho_1 I_1 \\ -\sum_{j=1}^{2}\delta_j p_{2j} L_2 \frac{\sum_{k=1}^{2} p_{kj} I_k}{\sum_{k=1}^{2} p_{kj} N_k} - (\gamma_2 + \mu_2)L_2 + \rho_2 I_2 \\ \sum_{j=1}^{2} p_{1j}\delta_j L_1 \frac{\sum_{k=1}^{2} p_{kj} I_k}{\sum_{k=1}^{2} p_{kj} N_k} + \gamma L_1 - (\mu_1 + \rho_1)I_1 \\ \sum_{j=1}^{2} p_{2j}\delta_j L_2 \frac{\sum_{k=1}^{2} p_{kj} I_k}{\sum_{k=1}^{2} p_{kj} N_k} + \gamma L_2 - (\mu_2 + \rho_2)I_2 \end{bmatrix}
$$

The rationale behind the presence of nonlinear terms, which represent the infectiousness progression of latent by the interaction with infectious individuals, in the "transition" vector ($\mathcal{V}$) is that these terms do not, technically, represent "new infections". Letting F and V be the Jacobian matrices of $\mathcal{F}$ and $\mathcal{V}$ respectively, evaluated

at the disease free equilibrium E_0, then the basic reproduction number is the spectral radius of the next generation matrix $-FV^{-1}$ (Van den Driessche and Watmough, 2002; Diekmann *et al.*, 1990). Hence, $\mathcal{R}_0 = \rho(-FV^{-1})$ where

$$-FV^{-1} = \begin{bmatrix} q\gamma_1 k_{11} & q\gamma_2 k_{12} & q(\mu_1+\gamma_1)k_{11} & q(\mu_2+\gamma_2)k_{21} \\ q\gamma_1 k_{21} & q\gamma_2 k_{22} & q(\mu_1+\gamma_1)k_{21} & q(\mu_2+\gamma_2)k_{22} \\ (1-q)\gamma_1 k_{11} & (1-q)\gamma_2 k_{12} & (1-q)(\mu_1+\gamma_1)k_{11} & (1-q)(\mu_2+\gamma_2)k_{12} \\ (1-q)\gamma_1 k_{21} & (1-q)\gamma_2 k_{22} & (1-q)(\mu_1+\gamma_1)k_{21} & (1-q)(\mu_2+\gamma_2)k_{22} \end{bmatrix}$$

where

$$\begin{aligned} k_{11} &= \left(\frac{\beta_1 p_{11}^2 N_1}{p_{11}N_1 + p_{21}N_2} + \frac{\beta_2 p_{12}^2 N_1}{p_{12}N_1 + p_{22}N_2}\right)\frac{1}{\mu_1(\gamma_1+\mu_1+\rho_1)} \\ &= \left(\frac{\beta_1 p_{11}^2 N_1}{p_{11}N_1 + p_{21}N_2} + \frac{\beta_2 p_{12}^2 N_1}{p_{12}N_1 + p_{22}N_2}\right)\frac{\mathcal{R}_{01}}{\beta_1(\gamma_1+(1-q)\mu_1)}, \end{aligned}$$

$$\begin{aligned} k_{12} &= \left(\frac{\beta_1 p_{11}p_{21} N_1}{p_{11}N_1 + p_{21}N_2} + \frac{\beta_2 p_{12}p_{22} N_1}{p_{12}N_1 + p_{22}N_2}\right)\frac{1}{\mu_2(\gamma_2+\mu_2+\rho_2)} \\ &= \left(\frac{\beta_1 p_{11}p_{21} N_1}{p_{11}N_1 + p_{21}N_2} + \frac{\beta_2 p_{12}p_{22} N_1}{p_{12}N_1 + p_{22}N_2}\right)\frac{\mathcal{R}_{02}}{\beta_2(\gamma_2+(1-q)\mu_2)}, \end{aligned}$$

$$\begin{aligned} k_{21} &= \left(\frac{\beta_1 p_{11}p_{21} N_2}{p_{11}N_1 + p_{21}N_2} + \frac{\beta_2 p_{12}p_{22} N_2}{p_{12}N_1 + p_{22}N_2}\right)\frac{1}{\mu_1(\gamma_1+\mu_1+\rho_1)} \\ &= \left(\frac{\beta_1 p_{11}p_{21} N_2}{p_{11}N_1 + p_{21}N_2} + \frac{\beta_2 p_{12}p_{22} N_2}{p_{12}N_1 + p_{22}N_2}\right)\frac{\mathcal{R}_{01}}{\beta_1(\gamma_1+(1-q)\mu_1)}, \end{aligned}$$

and

$$\begin{aligned} k_{22} &= \left(\frac{\beta_1 p_{21}^2 N_2}{p_{11}N_1 + p_{21}N_2} + \frac{\beta_2 p_{22}^2 N_2}{p_{12}N_1 + p_{22}N_2}\right)\frac{1}{\mu_2(\gamma_2+\mu_2+\rho_2)} \\ &= \left(\frac{\beta_1 p_{21}^2 N_2}{p_{11}N_1 + p_{21}N_2} + \frac{\beta_2 p_{22}^2 N_2}{p_{12}N_1 + p_{22}N_2}\right)\frac{\mathcal{R}_{02}}{\beta_2(\gamma_2+(1-q)\mu_2)}. \end{aligned}$$

Note that $\mathcal{R}_0 = f(\mathbb{P}, \mathcal{R}_{01}, \mathcal{R}_{02})$ where $\mathcal{R}_{01}$ and $\mathcal{R}_{02}$ are the basic reproductive numbers of patch 1 and 2, respectively, when there is no movement ($p_{11} = 1 =$

p_{22}). Recall that $\mathbb{P} = (p_{ij})_{1\leq i,j\leq 2}$ is the residence times matrix of the model and corresponding expressions for $\mathcal{R}_{01}$ and $\mathcal{R}_{02}$ are given by the algebraic expression ($\star$).

The analysis from Model (5.5) suggests a sharp threshold (that is, the disease dies out from both patches if $\mathcal{R}_0 \leq 1$ or persists in both patches otherwise), when $q = 1$ and $\delta = 0$ (i.e., in the absence of fast progression and exogenous infections) since the corresponding residence times matrix is irreducible. (See (Bichara *et al.*, 2015; Bichara and Castillo-Chavez, 2016; Bichara *et al.*, 2016) for the mathematical proofs). By assuming $q = 1$ through out this study and $\delta > 0$, numerical simulations suggest complex dynamics (i.e., multiple non-trivial equilibria) for the system.

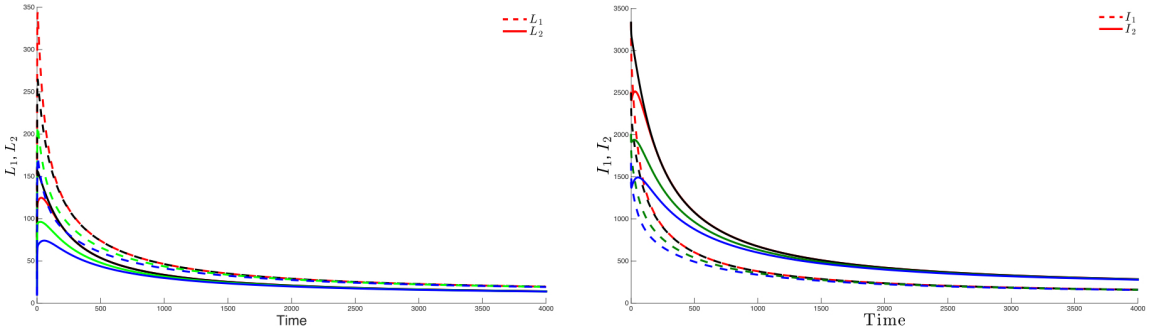

Figure 5.3: Dynamics of Infectious and Latent When the Two Patches Are Strongly Connected and $\mathcal{R}_0 > 1$.

Figure 5.3 highlights this robustness. Using four different sets of initial conditions, the trajectories of latently infected individuals (Figure 5.3 left) and actively-infected individuals (Figure 5.3 right) converge towards the endemic state as time progresses. On the other hand, the case when $\mathcal{R}_0 \leq 1$, leads to the eventual elimination of the disease from both patches regardless of the initial conditions as shown in Figure 5.4.

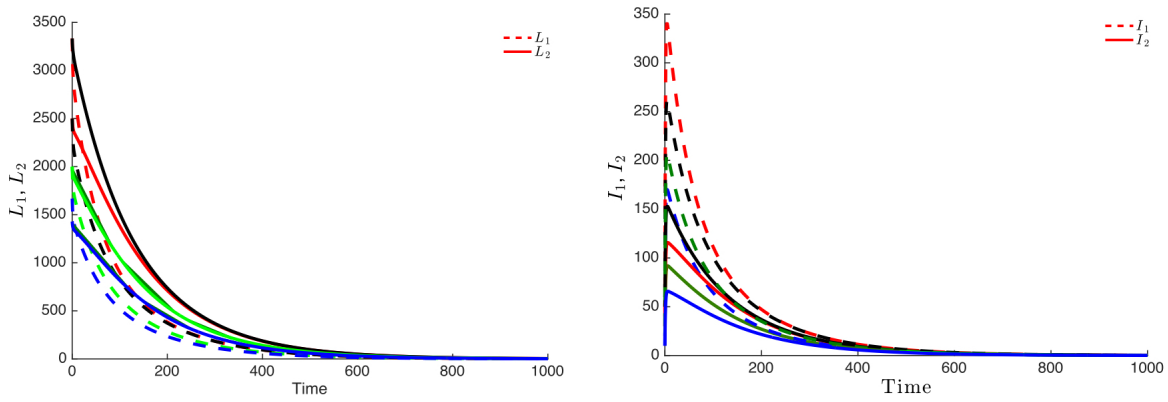

Figure 5.4: The Infectious and Latent Populations in the Two Patches Converge to Zero for Four Different Initial Conditions When $\mathcal{R}_0 \leq 1$.

Assuming Patch 1 is high risk ($\mathcal{R}_0 > 1$) and the connectivity between the two patches is not strong ($p_{21} \approx 0$ and $p_{12} \approx 0$), then the disease will persist in both patches, even though the number of latently-infected and actively-infectious individuals in Patch 2 is small (See Figure 5.5).

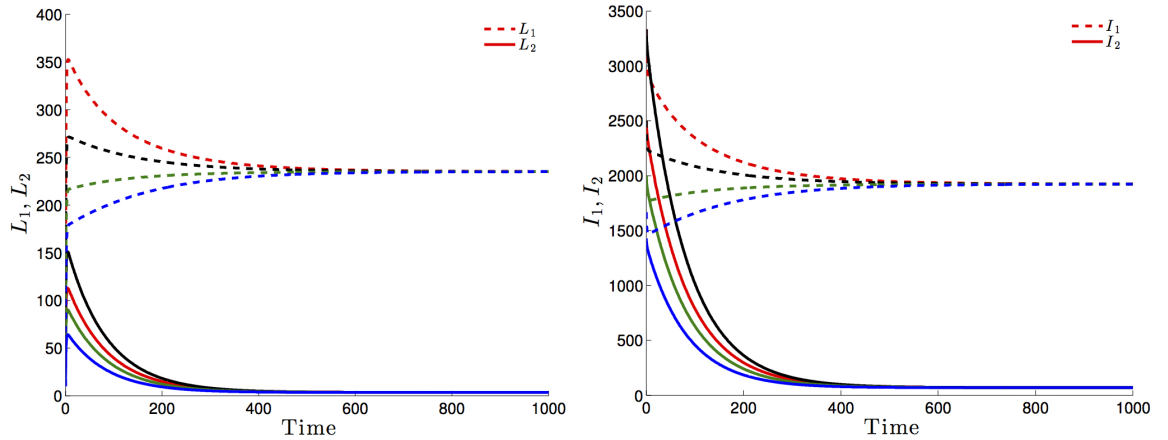

Figure 5.5: Dynamics of Two Weakly Connected Patches When $\mathcal{R}_0 > 1$ Reach an Endemic Level but Patch 2 Approaches a Lower Level of Endemicity ($\mathcal{R}_{01} = 1.4150$ and $\mathcal{R}_{02} = 0.1417$) If Completely Isolated.

The effects of the residence times matrix $\mathbb{P} = (p_{ij})_{1 \leq i,j \leq 2}$ on the basic reproduction number $\mathcal{R}_0(\mathbb{P})$ and, consequently on the disease dynamics, are highlighted in Figure 5.6 and Figure 5.7. Notice that the basic reproduction number is a decreasing function of the residence time of high risk residents (Patch 1) in the low risk environment

(Patch 2), in this case p_{12}. This reduction is capable to ultimately drive the basic reproduction number to a value less than one and consequently drive the latent and infected populations, under such mobility schedules, to zero in both patches (See Figure 5.6 and Figure 5.7).

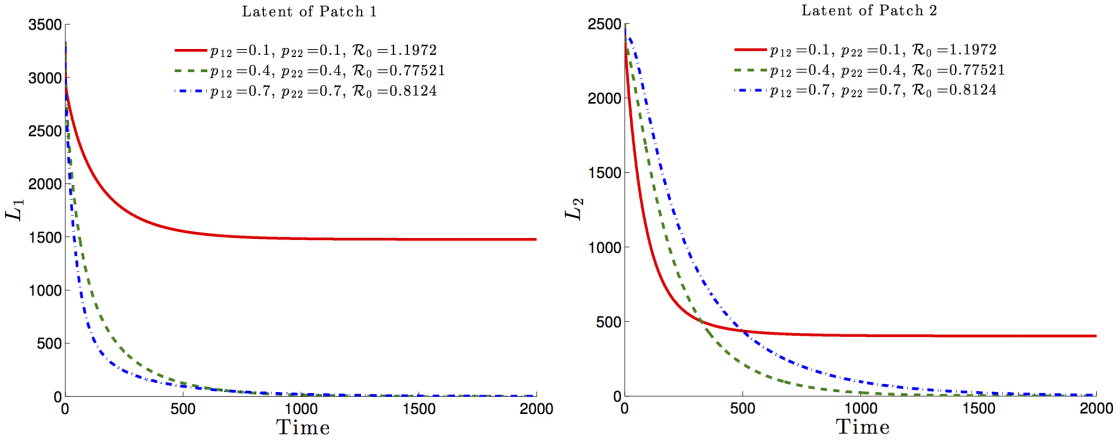

Figure 5.6: Effects of the Residence Time Matrix on the Basic Reproduction Number and the Disease Dynamics of the Latent Class.

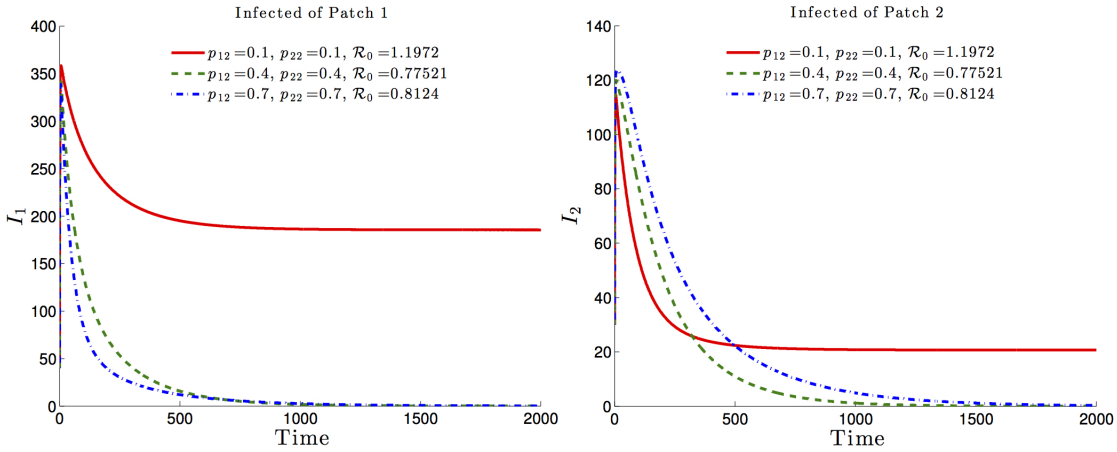

Figure 5.7: Effects of the Residence Time Matrix on the Basic Reproduction Number and the Disease Dynamics of the Infected Class.

Now, the role of mobility, risk and health disparities on TB prevalence levels in a two patch setting need to be addressed. In the next section, the role of the parameters representing mobility, risk and health disparities, on the dynamics of TB are explored.

5.3.2 The Role of Risk and Mobility on TB Prevalence.

Now, the dynamics of tuberculosis within a two-patch setting, described in Model (5.5), under various residence times schemes, are highlighted via numerical experiments. These numerical experiments were carried out using the two-patch Lagrangian modeling framework on pre-constructed scenarios. In particular, it is assumed that one of the two regions (say, Patch 1) has high TB prevalence and consequently has a higher risk of infection. While the scenarios simulated might be representative of certain regions, this study does not model specific cities or regions. See Table 5.1 for nomenclature and scenarios explored in this section.

The interconnection of individuals between the two idealized highly heterogeneous patches demands that individuals from Patch 1 travel to the "safer" Patch 2 driven by social factors like work, school or for other social activities. Likewise, it is assumed that the same socio-economic factors prevents individuals from the safer patch to travel and hence, the proportion of time that Patch 2-residents spend in Patch 1 is negligible.

In this study "high risk" is defined based on the probability of developing active TB (risk of infection) using two drivers. In section 5.3.2, the high risk patch is defined by having an elevated direct first time transmission rate ($\beta_1 > \beta_2$ and $\delta_1 = \delta_2$). Subsequently, in section 5.3.2 , the high risk patch is characterized by a higher exogenous reinfection rate ($\delta_1 > \delta_2$ and $\beta_1 = \beta_2$). In addition, in an attempt to gain a better understanding about the role of mobility, different scenarios with population size heterogeneity among the two patches are explored. These scenarios are build up by varying the population ratio (N_1/N_2). Particularly, it is assumed that Patch 1 is the denser patch, as a result of social factors, while Patch 2 is assumed to be less dense, more specifically, $\frac{1}{2}N_1$ and $\frac{1}{4}N_1$. In consequence, rates associated with the risk

of infection are higher in Patch 1 when compared to the corresponding rates in Patch 2.

The role of risk as defined by direct first time transmission rates

In this subsection, the impact of heterogeneity on direct first time transmission rates between patches are explored. Assuming Patch 1 has a higher risk of infection ($\beta_1 > \beta_2$ so that $\mathcal{R}_{01} > 1$), while Patch 2, in the absence of visitors would be unable to sustain an epidemic ($\mathcal{R}_{02} < 1$). Furthermore, the effect of different population ratios (N_1/N_2) is also included and explored.

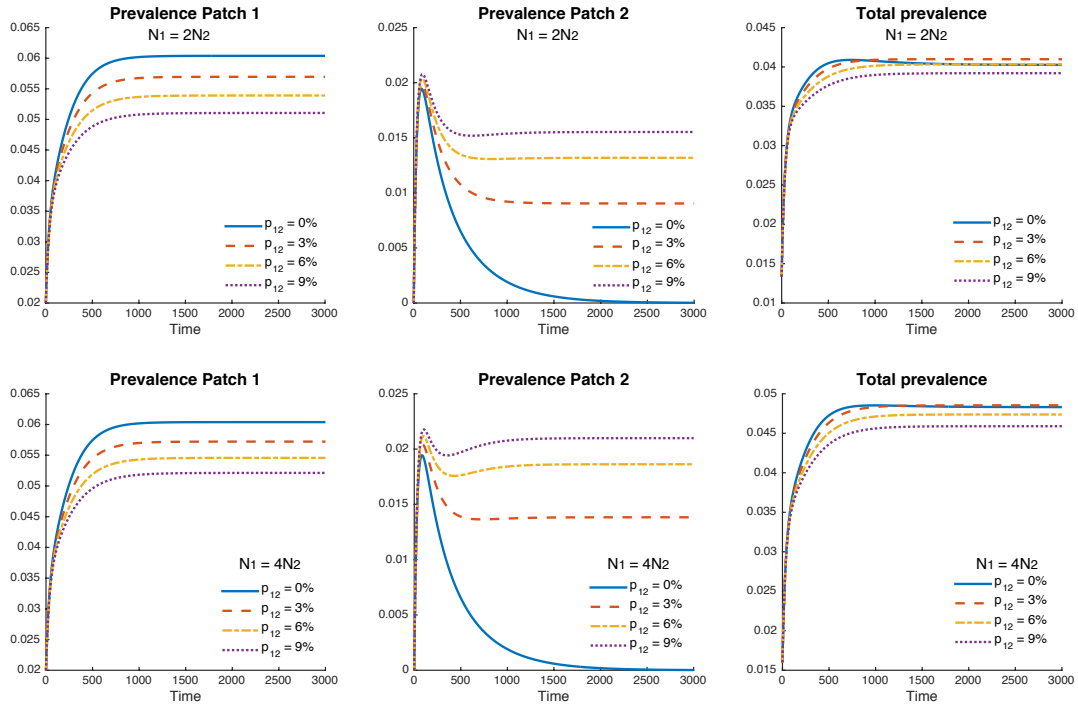

Figure 5.8: Effect of Mobility for $p_{12} = 0\%$, 3%, 6% and 9%, When Risk is Defined by Direct First Time Transmission Rates $0.13 = \beta_1 > \beta_2 = 0.07$ ($\mathcal{R}_{01} = 1.5$, $\mathcal{R}_{02} = 0.8$) and $\delta_1 = \delta_2 = 0.0026$.

Figure 5.8 shows similar but contrasting effects on patch prevalence when different residency times (mobility schemes) are explored (0% 3%, 6% and 9%). While Figure 5.8 shows the existence of mobility values (p_{12}), capable of reducing the overall

prevalence of the two patch system, it is important to notice the existence of mobility patterns that would have a detrimental impact on the overall prevalence of the system. Furthermore, it is observed that population densities just like residence times have a noticeable effect on disease prevalence.

Interestingly, these results suggest that if individuals from Patch 1 increase their residence time in Patch 2 (p_{12}), this behavior would reduce TB prevalence in Patch 1, whiled increasing it in Patch 2. However, the number of total infected individuals from both patches experiences a global beneficial effect for certain mobility patterns.

Figure 5.9, provides a better representation of mobility values (p_{12}) and their impact on TB prevalence at both the patch and at the system level. At the individual patch level, similar trends as in Figure 5.8 are observed, but in this case the existence of a threshold value can be observed for prevalence in terms of p_{12} (see red and yellow curves in Figure 5.9), for which mobility is always beneficial. As a result, this suggests that completely cordoning off infected regions may not be an effective control measure for TB. On the other hand, as long as mobility between high risk and low-risk regions is maintained above the critical value, mobility might become an important factor in the control of TB.

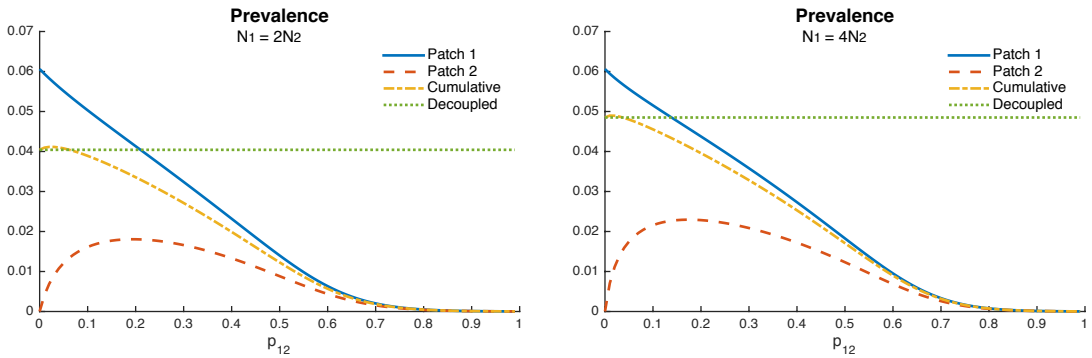

Figure 5.9: Effect of Mobility When Risk Is Defined by Direct First Time Transmission Rates $0.13 = \beta_1 > \beta_2 = 0.07$ ($\mathcal{R}_{01} = 1.5$, $\mathcal{R}_{02} = 0.8$) and $\delta_1 = \delta_2 = 0.0026$.

Furthermore, it is suggested that when the riskier patch has the bigger population size, the impact of mobility may turn out to be beneficial; results suggest that the higher the ratio between population sizes, the higher the range of beneficial "traveling" times (p_{12}).

The impact of risk as defined by exogenous reinfection rates

Similarly, focusing on the impact exogenous reinfection has on the transmission dynamics of TB it is assumed that direct first time transmission rates are the same in both patches ($\beta_1 = \beta_2$). In addition, it is assumed the disease has reached an endemic state in both patches ($\mathcal{R}_{01} > 1$ and $\mathcal{R}_{02} > 1$). However, once again, Patch 1 remains the riskier and consequently the exogenous reinfection rate in Patch 1 is higher than that of Patch 2 ($\delta_1 > \delta_2$).

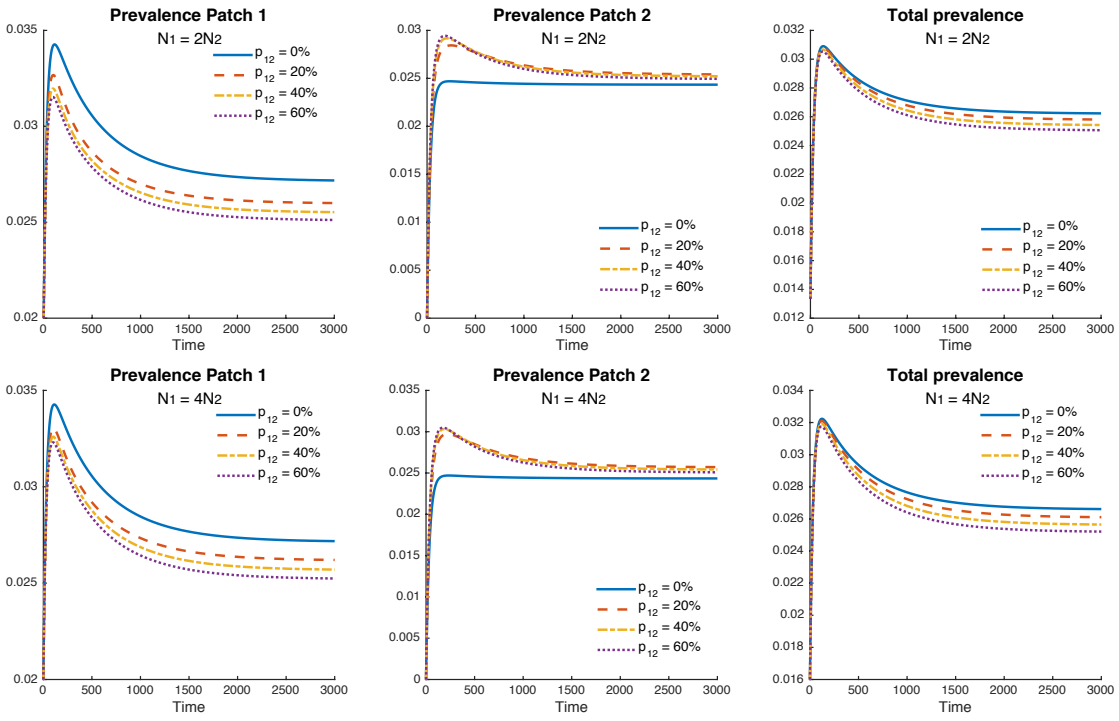

Figure 5.10: Effect of Mobility for $p_{12} = 0\%$, 20%, 40% and 60%, When Risk Is Defined by the Exogenous Reinfection Rates $0.0053 = \delta_1 > \delta_2 = 0.0026$ and $\beta_1 = \beta_2 = 0.1$ ($\mathcal{R}_{01} = \mathcal{R}_{02} = 1.155$).

As in the previous case, prevalence levels in Patch 1 are reduced by mobility (p_{12}), while prevalence in Patch 2 increase. Nevertheless, this prevalence reduction in Patch 1 is noticeable greater than the prevalence increment in Patch 2 for most mobility values p_{12}. Once again, Figure 5.10 suggests the existence of a threshold for which mobility has a beneficial impact on the entire system. Furthermore, the effect of population density once again could have a favorable impact on the total prevalence.

Figure 5.11 shows the mobility threshold and how it is impacted by population density suggesting that mobility between two patches undergoing TB outbreaks with high density heterogeneity (in which the riskier patch is denser) would result in lower TB prevalence levels for the overall system.

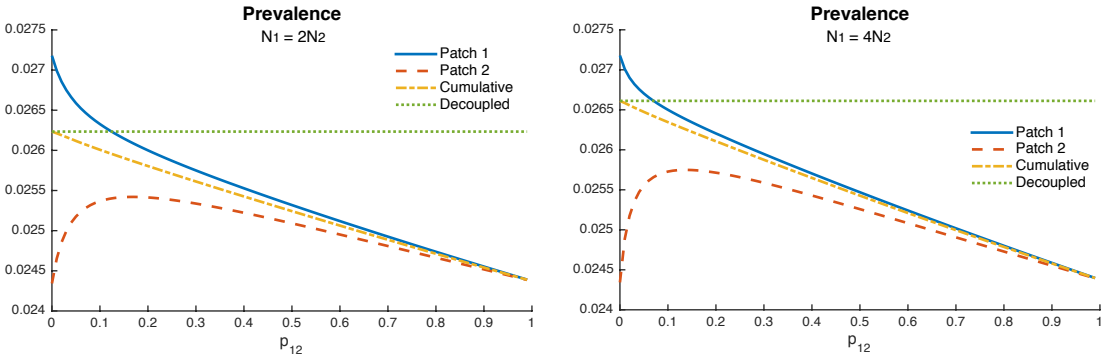

Figure 5.11: Effect of Mobility When Risk Is Defined by the Exogenous Reinfection Rates $0.0053 = \delta_1 > \delta_2 = 0.0026$ and $\beta_1 = \beta_2 = 0.1$ ($\mathcal{R}_{01} = \mathcal{R}_{02} = 1.155$).

Within this framework, parameters and scenarios, the simulations presented in this section suggest that direct first time transmission plays a central role on TB dynamics when mobility is considered. Although exogenous reinfection also reduces the overall prevalence when mobility is incorporate, its not as important as the impact generated by direct first time transmission.

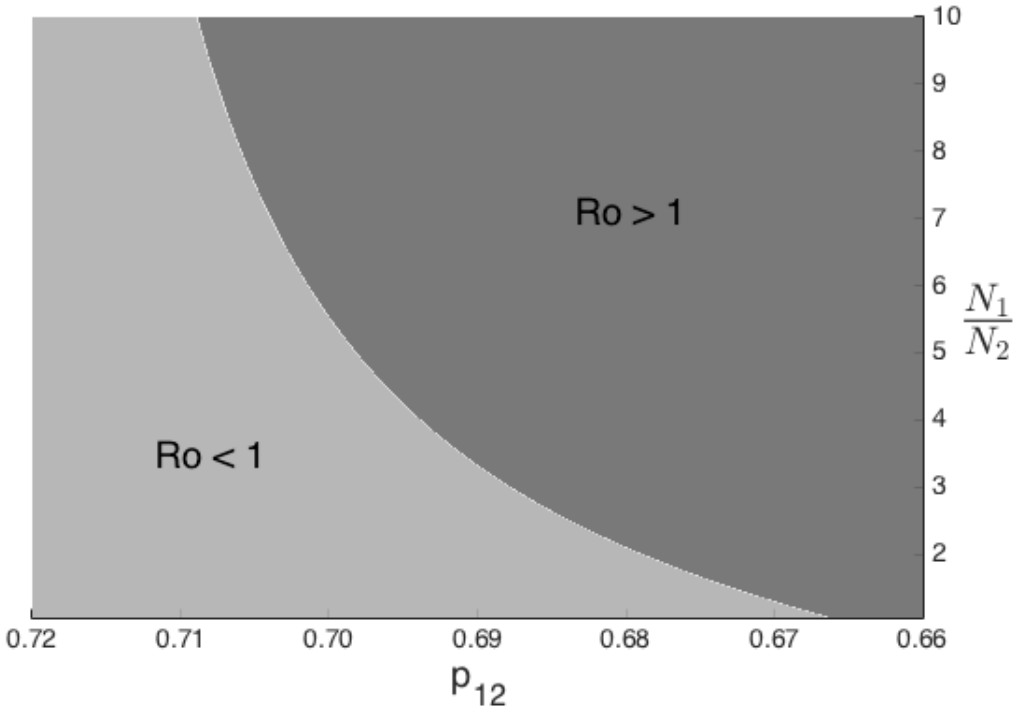

Figure 5.12: Effect of Mobility and Population Size Proportions on the Global Basic Reproductive Number $\mathcal{R}_0$ When $0.13 = \beta_1 > \beta_2 = 0.07$ and $\delta_1 = \delta_2 = 0.0026$.

Finally, Figure 5.12 depicts the relationship between population densities and mobility (p_{12}) with respect to the basic reproductive number $\mathcal{R}_0$. Notice that only the first case was explored (direct first time transmission heterogeneity) suggesting that mobility could indeed be an effective control measure capable of eliminating an regional (active) TB outbreak.

5.4 Discussion

According to the World Health Organization (WHO) (World Health Organization, 2015), in 2014, 80% of reported TB cases occurred in 22 countries (all developing countries). Efforts to control TB have been successful in many regions of the globe and yet, 1.5 million people die annually. In consequence, TB, faithful to its history, still poses one of the greatest challenges to global health (Daniel, 2006) and a threat

to humanity. Recent reports suggest that established TB control measures have not been adequately implemented, particularly in sub-Saharan countries (Andrews *et al.*, 2013; Chatterjee and Pramanik, 2015), one of the few regions heavily burdened by TB. Even though rates have decreased in Brazil, relapse has become more important than reinfection (de Oliveira *et al.*, 2013; Luzze *et al.*, 2013). Similarly, in Cape Town, South Africa, a study (Verver *et al.*, 2005) showed that in high incidence areas, individuals who have received successful TB treatment and are no longer infectious are at the highest risk of developing TB instead of being the most protected, suggesting the existence of ignored mechanisms that might be driving the TB contagion (possibly socio-economic factors).

The main focus of this study was on the role of 'daily' mobility within high and low-risk areas, as well as, the potential impact of short-term mobility on TB dynamics and control. A situation that is common in regions experiencing extreme levels of social, economic and health disparities. Using a simplified framework, a two-patch system, that captures, in a rather 'dramatic' way the dynamics between two close and yet, distinct worlds (the world of the haves and the have nots) suggests the existence of possible mechanisms, driven by social and economical factors, impacting disease spread. Moreover, it is important to mention that since the main objective of this study was to stress the impact of disparities, as a consequence, the highlighted results (via the simulation) come from simplified extreme scenarios.

As expected, the model analysis suggests that the dynamics of TB depend on the basic reproduction number ($\mathcal{R}_0$), which in turn is the function of model parameters that includes the direct first transmission rate for a single patch system and residence times for a two patch system. The simulations of specific extreme scenarios suggest that short term mobility between heterogeneous patches does not always contributes to overall increases in TB prevalence, to the contrary, in some cases it could be a

solution. The results show that when risk is considered only in terms of exogenous reinfection, the global TB prevalence remains almost unchanged, compared to the effect of direct first transmission. In the case of a high risk direct first time transmission, it is observed that mobile populations may pose detrimental effects on the prevalence levels in both environments (patches) under certain mobility patterns. Simulations show that when individuals from the risky population spend on average less than 25% of their time in the safer patch the overall prevalence reaches its maximum. However, if they spend more ($p_{12} > 25\%$), the overall prevalence decreases. Further, in the absence of exogenous reinfections, the model is robust and exhibits a sharp threshold; the disease dies out or persists based on whether or not the basic $\mathcal{R}_0$ is below or above unity, respectively. Although, the role of exogenous reinfection seems not that relevant on overall prevalence when mobility is included, the fact remains that such mode of transmission increases the risk that come from large displacement of individuals, due to catastrophes or conflict, to TB-free areas.

Hence, policies that do not account for population heterogeneity and regional- and community-specific factors are unlikely to be effective. It is clear that without a basic understanding of the attributes of the communities in question, it is almost impossible to successfully implement intervention programs capable of lowering reinfection rates for multiple pathways while at the same time maintain a low number of drug resistant cases. It is paramount for intervention programs to educate the affected populations and their government officials on the benefits, factors, and cost associated with population-based TB prevention and control programs in order to make them sustainable in the long run. At the same time, intervention must account for the risks inherent with high levels of migration as well as with local and regional mobility patterns between areas defined by high heterogeneity in TB risk and prevalence.

The ability to interpret information regarding the local origin of mobile individuals

accurately, would facilitate prompt responses in the face of initiation of an epidemic or ideally help in the creation of a disease resilient community. In addition, during the development and implementation of training and educational programs the necessity to avoid stigmatizing and further marginalization of groups that may have already experienced some kind of discrimination is essential, since it prevents integration, reduces compliance and promotes isolation (Gushulak and MacPherson, 2000b). A situation that cannot be ignored in today's world where millions of refugees have been dislocated and generated new migration patterns, as a result of armed conflicts. Failure to adequately incorporate and address these challenges may result in considerable delays and consequently promotes the emergence of new diseases and the reemergence of disease thought to be under control. As noted in (Feng *et al.*, 2000), ignoring factors like exogenous reinfections, that is, establishing policies that focus exclusively on the reproductive number $\mathcal{R}_0$, would amount to ignoring the role of dramatic changes in initial conditions, now more common than before, due to the displacement of large groups of individuals, the result of catastrophes and conflict.

5.5 Conclusions

This modeling study highlights critical social behaviors mechanisms that can facilitate or eliminate Tuberculosis infection in vulnerable populations. In particular, it highlights the importance that factors like mobility, density and dominant modes of transmission play an important role in the contagion process of Tuberculosis. The results suggest that allowing infected individuals to move from high to low TB prevalence areas (where the sharing of treatment and isolation facilities is possible) may lead to a reduction in the total TB prevalence in the overall (two-patch) population under certain conditions. More specifically, an increase in mobility between the two distinct risks regions produces a reduction on TB prevalence in the high risk patch

(and a slightly increase in the low risk patch), while decreasing the total number of infected individuals in both patches. Furthermore, when population size heterogeneity between patch 1 and patch 2 is large ($N_1 >> N_2$), mobility to the low risk patch might provide global benefits in terms of low overall prevalence. Moreover, the higher the ratio in population sizes between distinct risk patches, the larger the benefit (under the same "traveling" pattern).

Finally, direct first time transmission seems to play a central role on TB dynamics when mobility is incorporated. Nonetheless, mobility also reduces the overall prevalence, when exogenous reinfection is the dominant transmission pathway, however, its impact on the prevalence is relatively small compared to the impact of direct first time transmission.

Chapter 6

DISCUSSION

Disease outbreaks, ranking from locally restricted to global pandemics, have been reshaping the course of human society, even before humans became the dominant species in this planet (Moodie, 1918). Due to their unquantifiable impact on both economic and human capital, events such the black plague, the 1918 Spanish Flu pandemic, and the recent Ebola outbreak are a few of the most devastating events in history; based on their elevated numbers of disease induced deaths. Nonetheless, there are many other events that without a doubt have been affecting specific communities for decades and even centuries. Everything would point that seasonal epidemics in a way are more impactful; due to the constant shock that they provide to already burdened communities. Recent research points to the possible creation of poverty traps as a result of these disease shocks. (Bonds *et al.*, 2010) used a deterministic approach in which they are able to analyze the impact of these outbreaks in the economy of the region. Their results suggest that once a community fells into a poverty tramp, the constant shocks of disease outbreaks make it almost impossible to escape. Making disease burden one of the most complex and thus intractable problems today.

As stated by (Perrings, 1991),

> Many of the most intractable environmental problems are those in which the use of environmental resources in novel ways has effects that are highly uncertain in both their spread and duration. The greater the uncertainty of the effects of technologically innovative use of the environmental re-

> sources, the greater is the difficulty in evaluating associated environmental damage or the marginal social cost. The wider and more durable the environmental effects of economic activities are, the less is the scope of a market solution involving the allocation of property rights. Problems of uncertain environmental effects that may be global in spread or may endure for generations require responses that go beyond existing evaluation techniques.

It seems as if whenever a new solution is developed, the precautionary principle is not taken into account. In essence, sequential decision making under uncertainty, usually takes a cautious approach at first but then it may be relaxed as data sets are enriched by experience; even when the probability of distant but potentially catastrophic damage is admitted, but thought to be very low.

Similarly, Simon Levin in his address as the 2004 recipient of the Heineken award, mentions social norms as a possible source of uncertainty not only in the use of resources but in the way groups behave,

> "A great challenge before us is thus to understand the dynamics of social norms, how they arise, how they spread, how they are sustained and how they change. Models of these dynamics have many of the same features as models of epidemic spread, no great surprise, since many aspects of culture have the characteristics of being social diseases. 1998 Heineken award winner Paul Ehrlich and I have been directing our collective energies to this problem, convinced that it is as important to understand the dynamics of the social systems in which we live as it is to understand the ecological systems themselves. Understanding the links between individual behavior and societal consequences, and characterizing the networks

> of interaction and influence, create the potential to change the reward structures so that the social costs of individual actions are brought down to the level of individual payoffs. It is a daunting task, both because of the amount we still must learn, and because of the ethical dilemmas that are implicit in any form of social engineering. But it is a task from which we cannot shrink, lest we squander the last of our diminishing resources."

Consequently, any planning for enhancing community disease response, regardless of the context, depends greatly in a highly heterogeneous process determined by the involvement of individuals of such communities at all levels. It is clear that their response to epidemic events do change the impact it has on the community and public health infrastructure, as well as, its resources aimed at controlling such epidemic events. Therefore, the development of disease resilience communities requires a collaborative and transparent process in which the tools for achieving disease resilience are easily available for the individuals at the lower and most affected levels. In this way, policies aimed at improving disease resilience can be customized to include interventions that could impact the underlying vulnerability drivers specific to a region or community.

In the case of many infectious diseases, the global aim at urbanization has in part collaborated with the explosion of outbreaks across the globe. In consequence, the need to have responsible urbanization, improved infrastructure, and appropriate planning is essential in these urban areas. In addition, efficient policies that can take into account a prompt response to disease shocks and incorporate the corresponding health care infrastructure are desperately needed. Furthermore, the attributes of the community associated with factors that could improve sanitation are likely to be influential in reducing disease vulnerability dynamics of the community. Keep in mind that these factors could include hard, soft infrastructure and environmental

management.

Stages or components of disease vulnerability in a given community or the risk of infection inherent to its inhabitants needs to be determined in the nearby future. Some of the community components believed to be important are:

- Livelihood: inherent risk associated with existing abiotic and biotic factors. In the case of vector borne diseases, this could be the impact caused by location and the ability of the vectors and disease to efficiently complete their live cycle.
- Well-being: baseline statistics like nutrition, physical and mental health levels. In the case of TB, nutrition seems to be an important once since this could cause a negative impact in the immune response and thus facilitates progression from latent to active TB.
- Self-protection: community self organization to prevent infections. This could be measured as locally organized cleaning campaigns targeting nesting sites, as well as the use of repellents and bed nets in the case of many vector borne diseases.
- Social Protection: corresponding violence levels and local perception of safety in each community.
- Governance: implementation and efficacy of control measures and the maintenance of hard public health infrastructure.

While these are some factors that might have a direct impact on the risk of infection, there are others that need to be investigated and then incorporated to the Lagrangian modeling framework and estimate a more realistic impact of factors like short-term mobility, the existing of contrasting risk communities, immunity or more specific cross immunity from past outbreaks, and population size on past and recent

epidemic outbreaks. At the same time, we are left puzzled by the methodology needed in order to quantify the impact of these mechanisms or factors. How do we assess the risk of infection in a given community? What kind of data do we need? What would be some setbacks from this methods? Most importantly, what will be the impact of these results? Would they be used as a reactionary policy or a preventive one?

In conclusion, as it was mentioned in (Moreno *et al.*, 2017b), surveillance measures must be improved...

> Certainly, the use of dramatic measures to limit the spread of diseases like SARS, Influenza or Ebola [(Chowell *et al.*, 2003a; Herrera-Valdez *et al.*, 2011; Chowell *et al.*, 2015)], as well as the rise of vector born diseases like Dengue and Zika are not uncommon, and the dramatic implications that some measures have had on local and global economies. The question remains, what can we do to mitigate or limit the spread of disease, particularly emergent diseases without disrupting central components? Discussions on these issues are recurrent (Fenichel *et al.*, 2011; Morin *et al.*, 2013), most intensely in the context of SARS, Influenza, Ebola and Zika, in the last decade or so. The vulnerability of world societies is directly linked to the lack of action in addressing the challenges faced by the weakest links in the system must be accepted and acted on by the world community. We need global investments in communities and nations where health disparities and lack of resources are the norm. We must invest in research and surveillance within clearly identified world hot spots, where the emergence of new disease are most likely to emerge, and we must do so with the involvement, at all levels, of the affected communities (Perrings *et al.*, 2014; Castillo-Chavez *et al.*, 2015).

Chapter 7

CONCLUSION

While this study focuses on the dynamics of a single outbreak, the modeling framework can be used to study long-term dynamics when the mobility patterns can be captured effectively by $\mathbb{P}$. A two-patch model where host-mobility is modeled using a Lagrangian approach is used to help understand the role of host-movement on the transmission dynamics of ZIKV and TB. The patches were defined to be as distinct as they could be, hoping that simulations, in this simplified system, could capture some insight on the transmission dynamics of ZIKV and TB in the presence of extreme health disparities within neighboring communities or within urban centers. This framework can be used to study the dynamics of vector born diseases within a collection of neighboring communities or neighborhoods experiencing multiple levels of health disparities and diverse connectivity mobility structures (Bichara and Castillo-Chavez, 2016). The study of the role of mobility at larger scales can be best captured using question-specific related models that account for the possibility of long-term mobility (see for example (Herrera-Valdez *et al.*, 2011; Chowell *et al.*, 2003b; Baroyan *et al.*, 1971; Rvachev and Longini Jr, 1985; Elveback *et al.*, 1976; Banks and Castillo-Chavez, 2003; Khan *et al.*, 2009)).

The incorporation of a Lagrangian modeling approach to study epidemic outbreaks makes it possible to use measurable parameters like risk of infection ($\hat{\beta}$), which affect individuals differently depending on patch-residency and mobility patterns (residency times). As expected, the impact of mobility on the final epidemic size depends on the local risk of infection and population size. Moreover, it was also determined

that there are certain cases in which mobility could be detrimental, highlighting the necessity to reduce health disparities in vulnerable communities. On the other hand, mobility from high to low risk patches can reduce or increase the total final epidemic size; under such conditions, mobility could be used as a strategy to ameliorate the impact of disease outbreaks. Furthermore, population size matters; differences in population density (size) were also shown to be capable of generating reductions on the total final epidemic size within some mobility regimes. Nonetheless, examples when $R_{0i} < 1$ with mobility incapable of reducing the total final epidemic size under no differences in patch density (here measured by total population size in each patch, both assumed to have roughly the same area) were also identified.

In this dissertation, the role of heterogeneity as captured in a Lagrangian setting was explored. While this modeling perspective simplifies the modeling of communicable and vector born diseases, it is not sufficient to divide a population in just two groups (high and low risk), in order to capture the levels of heterogeneity observed in real societies. There is indeed a gradient of risks that must be considered, but the question then becomes: how many levels will be enough? A question that has no simple answers albeit the right level of aggregation to capture the dynamics of realistic systems must be addressed when the goal is to implement policies generated by these models in realistic settings.

Agusto, F. B. and A. I. Adekunle, "Optimal control of a two-strain tuberculosis-hiv/aids co-infection model", BioSystems **119**, 1, 20–44, URL http://dx.doi.org/10.1016/j.biosystems.2014.03.006 (2014).

Ahn, D. I., W. H. Organization and S. T. Partnership, "Addressing poverty in tb control : options for national tb control programmes", Tech. Rep. WHO/HTM/TB/2005.352, Geneva : World Health Organization, URL http://www.who.int/iris/handle/10665/43256#sthash.a0lwjVsl.dpuf (2005).

Allen, L. J., F. Brauer, P. Van den Driessche and J. Wu, *Mathematical epidemiology*, vol. 1945 (Springer, 2008).

Allen, L. J., Y. Lou and A. L. Nevai, "Spatial patterns in a discrete-time sis patch model", Journal of mathematical biology **58**, 3, 339–375 (2009).

Althaus, D. and D. Schiller, *CHRON: Mexico declares national emergency*, URL http://www.chron.com/news/health/article/Mexico-declares-national-emergency-1731456.php (April 25, 2009).

Andrews, J. R., C. Morrow and R. Wood, "Modeling the role of public transportation in sustaining tuberculosis transmission in south africa.", Am J Epidemiol **177**, 6, 556–561 (2013).

Arino, J., "Diseases in metapopulations", Modeling and dynamics of infectious diseases **11**, 65–123 (2009).

Arino, J., R. Jordan and P. Van den Driessche, "Quarantine in a multi-species epidemic model with spatial dynamics", Mathematical biosciences **206**, 1, 46–60 (2007).

Arino, J. and P. Van Den Driessche, "The basic reproduction number in a multi-city compartmental epidemic model", in "Positive Systems", pp. 135–142 (Springer, 2003).

Arino, J. and P. Van den Driessche, "A multi-city epidemic model", Mathematical Population Studies **10**, 3, 175–193 (2003).

Arino, J. and P. van den Driessche, "Metapopulation epidemic models. a survey", Fields Institute Communications **48**, 1–13 (2006).

Banks, H. T. and C. Castillo-Chavez, *Bioterrorism: mathematical modeling applications in homeland security* (SIAM, 2003).

Baroyan, O., L. Rvachev, U. Basilevsky, V. Ermakov, K. Frank, M. Rvachev and V. Shashkov, "Computer modelling of influenza epidemics for the whole country (ussr)", Advances in Applied Probability **3**, 2, 224–226 (1971).

Bauch, S. C., A. M. Birkenbach, S. K. Pattanayak and E. O. Sills, "Public health impacts of ecosystem change in the brazilian amazon", Proceedings of the National Academy of Sciences **112**, 24, 7414–7419 (2015).

Bettencourt, L., A. Cintron-Arias, D. I. Kaiser and C. Castillo-Chavez, "The power of a good idea: Quantitative modeling of the spread of ideas from epidemiological models", Physica A: Statistical Mechanics and its Applications **364**, 513–536 (2006).

Bhatt, C., A. Bhatt and B. Shrestha, "Nepalese people's knowledge about tuberculosis", SAARC Journal of Tuberculosis, Lung Diseases and HIV/AIDS **6**, 2, 31–37, URL `http://www.nepjol.info/index.php/SAARCTB/article/view/3055` (2010).

Bhunu, C. P., "Mathematical analysis of a three-strain tuberculosis transmission model", Applied Mathematical Modelling **35**, 9, 4647–4660, URL `http://www.sciencedirect.com/science/article/pii/S0307904X11001739` (2011).

Bhunu, C. P., W. Garira and Z. Mukandavire, "Modeling hiv/aids and tuberculosis coinfection", Bulletin of Mathematical Biology **71**, 7, 1745–1780, URL `http://dx.doi.org/10.1007/s11538-009-9423-9` (2009).

Bichara, D. and C. Castillo-Chavez, "Vector-borne diseases models with residence times–a lagrangian perspective", Mathematical biosciences **281**, 128–138 (2016).

Bichara, D., S. A. Holechek, J. Velázquez-Castro, A. L. Murillo and C. Castillo-Chavez, "On the dynamics of dengue virus type 2 with residence times and vertical transmission", Letters in Biomathematics **3**, 1, 140–160 (2016).

Bichara, D., Y. Kang, C. Castillo-Chavez, R. Horan and C. Perrings, "Sis and sir epidemic models under virtual dispersal", The Bulletin of Mathematical Biology, DOI: 10.1007/s11538-015-0113-5 (2015).

Black, F. L., F. d. P. Pinheiro, W. J. Hierholzer and R. V. Lee, "Epidemiology of infectious disease: the example of measles", Health and disease in tribal societies pp. 115–135 (1977).

Blinder, A., "New york times: In rural alabama, a longtime mistrust of medicine fuels a tuberculosis outbreak", Online, URL `https://www.nytimes.com` (January 17, 2016).

Blower, S. M., A. R. Mclean, T. C. Porco, P. M. Small, P. C. Hopewell, M. A. Sanchez and A. R. Moss, "The intrinsic transmission dynamics of tuberculosis epidemics", Nature Medicine **1**, 8, 815–821, URL `http://www.nature.com/doifinder/10.1038/nm0895-815` (1995).

Bonds, M. H., D. C. Keenan, P. Rohani and J. D. Sachs, "Poverty trap formed by the ecology of infectious diseases", Proceedings of the Royal Society of London B: Biological Sciences **277**, 1685, 1185–1192 (2010).

Bowong, S. and J. Kurths, "Modelling tuberculosis and hepatitis b co-infections", Mathematical Modelling of Natural Phenomena **5**, 6, 196–242, URL http://dx.doi.org/10.1051/mmnp/20105610 (2010).

Brauer, F., C. Castillo-Chavez, A. Mubayi and S. Towers, "Some models for epidemics of vector-transmitted diseases", Infectious Disease Modelling (2016).

Brauer, F. and P. van den Driessche, "Models for transmission of disease with immigration of infectives", Math. Biosci. **171** (2001).

Brauer, F. *et al.*, *Mathematical models for communicable diseases*, vol. 84 (SIAM, 2012).

California Department of Public Health, C., "California measles cases", Online, URL http://www.cdph.ca.gov/HealthInfo/discond/Pages/Measles.aspx (2014).

Cao-Lormeau, V.-M. and D. Musso, "Emerging arboviruses in the pacific", The Lancet **384**, 9954, 1571–1572 (2014).

Cao-Lormeau, V. M., C. Roche, A. Teissier, E. Robin, A.-L. Bery, H.-P. Mallet, A. A. Sall and D. Musso, "Zika virus, french polynesia, south pacific, 2013", (2014).

Castillo-Chavez, C., K. Barley, D. Bichara, D. Chowell, E. D. Herrera, B. Espinoza, V. Moreno, S. Towers and K. Yong, "Modeling ebola at the mathematical and theoretical biology institute (mtbi)", Notices of the AMS **63**, 4 (2016).

Castillo Chávez, C., A. Capurro, J. Velasco Hernández and M. Zellner, "El transporte público y la dinámica de la tuberculosis a nivel poblacional", Rev. argent. tórax **61**, 1/4, 21–35, URL http://bases.bireme.br/cgi-bin/wxislind.exe/iah/online/?IsisScript=iah/iah.xis&src=google&base=LILACS&lang=p&nextAction=lnk&exprSearch=328311&indexSearch=ID (2000).

Castillo-Chavez, C., R. Curtiss, P. Daszak, S. A. Levin, O. Patterson-Lomba, C. Perrings, G. Poste and S. Towers, "Beyond ebola: Lessons to mitigate future pandemics", The Lancet Global Health **3**, 7, e354–e355 (2015).

Centers for Disease Control and Prevention (b), C., "Zoonotic diseases", Online, URL http://www.cdc.gov/onehealth/zoonotic-diseases.html,[citedOctober8, 2016] (2016).

Centers for Disease Control and Prevention (f), C., "Cdc measles cases", Online, URL http://www.cdc.gov/measles/cases-outbreaks.html (2014).

Centers for Disease Control and Prevention (g), C., *Ten Great Public Health Achievements - United States, 2001-2010*, URL http://www.cdc.gov/mmwr/preview/mmwrhtml/mm6019a5.htm (May 20, 2011).

Centers for Disease Control and Prevention (i), C., "Zika virus", Online, URL http://www.cdc.gov/zika/index.html (2016).

Centers for Disease Control and Prevention (k), C., "CDC adds 2 destinations to interim travel guidance related to zika virus", Online, URL http://www.cdc.gov/media/releases/2016/s0203-zika-travel-guidance.html (2016).

Centers for Disease Control and Prevention (l), C., "Zika virus in South America", Online, URL http://wwwnc.cdc.gov/travel/notices/alert/zika-virus-south-america (2016).

Centers for Disease Control and Prevention (m), C., "Zika virus in Central America", Online, URL http://wwwnc.cdc.gov/travel/notices/alert/zika-virus-central-america (2016).

Centers for Disease Control and Prevention (n), C., "Zika virus", Online, URL http://www.cdc.gov/zika/geo/americas.html (2016).

Chatterjee, D. and A. K. Pramanik, "Tuberculosis in the african continent: A comprehensive review.", Pathophysiology **22**, 1, 73–83 (2015).

Chen, P., *NYT: Putting Us All at Risk for Measkes*, URL http://mobile.nytimes.com/blogs/well/2014/06/26/putting-us-all-at-risk-for-measles/ (June 26, 2014).

Chen, R. T. and F. DeStefano, "Vaccine adverse events: causal or coincidental?", The Lancet **351**, 9103, 611–612 (1998).

Chowell, D., C. Castillo-Chavez, S. Krishna, X. Qiu and K. S. Anderson, "Modelling the effect of early detection of ebola", The Lancet Infectious Diseases **15**, 2, 148–149 (2015).

Chowell, G., P. W. Fenimore, M. A. Castillo-Garsow and C. Castillo-Chavez, "Sars outbreaks in ontario, hong kong and singapore: the role of diagnosis and isolation as a control mechanism", Journal of theoretical biology **224**, 1, 1–8 (2003a).

Chowell, G., J. M. Hyman, S. Eubank and C. Castillo-Chavez, "Scaling laws for the movement of people between locations in a large city", Physical Review E **68**, 6, 066102 (2003b).

Ciota, A. T., S. M. Bialosuknia, D. J. Ehrbar and L. D. Kramer, "Vertical transmission of zika virus by aedes aegypti and ae. albopictus mosquitoes", Emerging infectious diseases **23**, 5, 880 (2017).

Cohen, T., C. Colijn, B. Finklea and M. Murray, "Exogenous re-infection and the dynamics of tuberculosis epidemics: local effects in a network model of transmission.", J R Soc Interface **4**, 14, 523–531 (2007).

Cohen, T., C. Dye, C. Colijn, B. Williams and M. Murray, "Mathematical models of the epidemiology and control of drug-resistant tb.", Expert Rev Respir Med **3**, 1, 67–79 (2009).

Daniel, T. M., "The history of tuberculosis", Respiratory Medicine **100**, 11, 1862–1870, URL http://linkinghub.elsevier.com/retrieve/pii/S095461110600401X (2006).

de Oliveira, G. P., A. W. Torrens, P. Bartholomay and D. Barreira, "Tuberculosis in Brazil: last ten years analysis – 2001–2010", The Brazilian Journal of Infectious Diseases **17**, 2, 218–233, URL http://linkinghub.elsevier.com/retrieve/pii/S1413867013000536 (2013).

Di Luca, M., F. Severini, L. Toma, D. Boccolini, R. Romi, M. E. Remoli, M. Sabbatucci, C. Rizzo, G. Venturi, G. Rezza *et al.*, "Experimental studies of susceptibility of italian aedes albopictus to zika virus", Eurosurveillance **21**, 18 (2016).

Dick, G., S. Kitchen and A. Haddow, "Zika virus (i). isolations and serological specificity", Transactions of the Royal Society of Tropical Medicine and Hygiene **46**, 5, 509–520 (1952).

Diekmann, O., J. Heesterbeek and J. A. Metz, "On the definition and the computation of the basic reproduction ratio r 0 in models for infectious diseases in heterogeneous populations", Journal of mathematical biology **28**, 4, 365–382 (1990).

Dowdy, D. W., J. E. Golub, R. E. Chaisson and V. Saraceni, "Heterogeneity in tuberculosis transmission and the role of geographic hotspots in propagating epidemics.", Proc Natl Acad Sci U S A **109**, 24, 9557–9562 (2012).

Duffy, M. R., T.-H. Chen, W. T. Hancock, A. M. Powers, J. L. Kool, R. S. Lanciotti, M. Pretrick, M. Marfel, S. Holzbauer, C. Dubray *et al.*, "Zika virus outbreak on yap island, federated states of micronesia", New England Journal of Medicine **360**, 24, 2536–2543 (2009).

Dupont-Rouzeyrol, M., O. O'Connor, E. Calvez, M. Daures, M. John, J.-P. Grangeon and A.-C. Gourinat, "Co-infection with zika and dengue viruses in 2 patients, new caledonia, 2014", Emerging infectious diseases **21**, 2, 381 (2015).

Elveback, L. R., J. P. Fox, E. Ackerman, A. Langworthy, M. Boyd and L. Gatewood, "An influenza simulation model for immunization studies", American journal of epidemiology **103**, 2, 152–165 (1976).

Engelthaler, D. M., T. Fink, C. Levy and M. Leslie, "The reemergence of aedes aegypti in arizona.", Emerging infectious diseases **3**, 2, 241 (1997).

Espinoza, B., V. Moreno, D. Bichara and C. Castillo-Chavez, "Assessing the efficiency of movement restriction as a control strategy of ebola", in "Mathematical and Statistical Modeling for Emerging and Re-emerging Infectious Diseases", pp. 123–145 (Springer, 2016).

Fauci, A. S. and D. M. Morens, "Zika virus in the americas—yet another arbovirus threat", New England Journal of Medicine (2016).

Faye, O., C. C. Freire, A. Iamarino, O. Faye, J. V. C. de Oliveira, M. Diallo, P. M. Zanotto *et al.*, "Molecular evolution of zika virus during its emergence in the 20 th century", PLoS Negl Trop Dis **8**, 1, e2636 (2014).

Feng, Z., C. Castillo-Chavez and A. F. Capurro, "A Model for Tuberculosis with Exogenous Reinfection", Theoretical Population Biology **57**, 3, 235–247, URL `http://linkinghub.elsevier.com/retrieve/pii/S0040580900914515` (2000).

Fenichel, E. P., C. Castillo-Chavez, M. Ceddia, G. Chowell, P. A. G. Parra, G. J. Hickling, G. Holloway, R. Horan, B. Morin, C. Perrings *et al.*, "Adaptive human behavior in epidemiological models", Proceedings of the National Academy of Sciences **108**, 15, 6306–6311 (2011).

Fox, S., "The engaged e-patient population", Washington, DC: Pew Internet & American Life Project (2008).

Fox, S. and L. Rainie, *The online health care revolution: How the Web helps Americans take better care of themselves* (Pew internet & American life project, 2000).

Gellin, B. G., E. W. Maibach, E. K. Marcuse *et al.*, "Do parents understand immunizations? a national telephone survey", Pediatrics **106**, 5, 1097–1102 (2000).

Gomes, M. G. M., R. Aguas, J. S. Lopes, M. C. Nunes, C. Rebelo, P. Rodrigues and C. J. Struchiner, "How host heterogeneity governs tuberculosis reinfection?", Proceedings of the Royal Society of London B: Biological Sciences **279**, 1737, 2473–2478, URL `http://rspb.royalsocietypublishing.org/content/279/1737/2473.abstract` (2012).

Gomes, M. G. M., A. O. Franco, M. C. Gomes and G. F. Medley, "The reinfection threshold promotes variability in tuberculosis epidemiology and vaccine efficacy", Proceedings of the Royal Society of London B: Biological Sciences **271**, 1539, 617–623 (2004).

Gubler, D. J., "The global emergence/resurgence of arboviral diseases as public health problems", Archives of medical research **33**, 4, 330–342 (2002).

Gushulak, B. D. and D. W. MacPherson, "Population mobility and infectious diseases: the diminishing impact of classical infectious diseases and new approaches for the 21st century", Clinical Infectious Diseases **31**, 3, 776–780 (2000a).

Gushulak, B. D. and D. W. MacPherson, "Population Mobility and Infectious Diseases: The Diminishing Impact of Classical Infectious Diseases and New Approaches for the 21st Century", Clinical Infectious Diseases **31**, 3, 776–780, URL `http://cid.oxfordjournals.org/lookup/doi/10.1086/313998` (2000b).

Haddow, A. D., A. J. Schuh, C. Y. Yasuda, M. R. Kasper, V. Heang, R. Huy, H. Guzman, R. B. Tesh and S. C. Weaver, "Genetic characterization of zika virus strains: geographic expansion of the asian lineage", PLoS Negl Trop Dis **6**, 2, e1477 (2012).

Hanski, I. and M. Gilpin, "Metapopulation dynamics: brief history and conceptual domain", Biological journal of the Linnean Society **42**, 1-2, 3–16 (1991).

Harvard Gazette, H. G., "Paper disc can quickly detect zika virus in the field", Online, URL http://news.harvard.edu/gazette/story/2016/05/paper-disc-can-quickly-detect-zika-virus-in-the-field/ (2016).

Hayes, E. B. *et al.*, "Zika virus outside africa", Emerg Infect Dis **15**, 9, 1347–1350 (2009).

Herrera-Valdez, M. A., M. Cruz-Aponte and C. Castillo-Chavez, "Multiple outbreaks for the same pandemic: Local transportation and social distancing explain the different" waves" of a-h1n1pdm cases observed in méxico during 2009", Mathematical Biosciences & Engineering **8**, 1, 21–48 (2011).

Hohmann, N. and A. Voss-Böhme, "The epidemiological consequences of leprosy-tuberculosis co-infection", Mathematical Biosciences **241**, 2, 225–237, URL http://www.sciencedirect.com/science/article/pii/S0025556412002283 (2013).

Iacono, G. L., A. A. Cunningham, E. Fichet-Calvet, R. F. Garry, D. S. Grant, M. Leach, L. M. Moses, G. Nichols, J. S. Schieffelin, J. G. Shaffer *et al.*, "A unified framework for the infection dynamics of zoonotic spillover and spread", PLoS Negl Trop Dis **10**, 9, e0004957 (2016).

Jacobson, R. M., P. V. Targonski and G. A. Poland, "A taxonomy of reasoning flaws in the anti-vaccine movement", Vaccine **25**, 16, 3146–3152 (2007).

Jaitman, L., *Los costos del crimen y la violencia en el bienestar en America Latina y el Caribe, Laura Jaitman Ed.* (Banco Interamericano del Desarrollo, 2015).

Jansen, C. C. and N. W. Beebe, "The dengue vector aedes aegypti: what comes next", Microbes and infection **12**, 4, 272–279 (2010).

Kapitanov, G., "A double age-structured model of the co-infection of tuberculosis and hiv", Mathematical Biosciences and Engineering **12**, 1, 23–40, URL http://dx.doi.org/10.3934/mbe.2015.12.23 (2015).

Kata, A., "A postmodern pandora's box: Anti-vaccination misinformation on the internet", Vaccine **28**, 7, 1709–1716 (2010).

Khan, K., J. Arino, W. Hu, P. Raposo, J. Sears, F. Calderon, C. Heidebrecht, M. Macdonald, J. Liauw, A. Chan *et al.*, "Spread of a novel influenza a (h1n1) virus via global airline transportation", New England journal of medicine **361**, 2, 212–214 (2009).

Kucharski, A. J., S. Funk, R. M. Eggo, H.-P. Mallet, J. Edmunds and E. J. Nilles, "Transmission dynamics of zika virus in island populations: a modelling analysis of the 2013-14 french polynesia outbreak", bioRxiv p. 038588 (2016).

Lafferty, K. D., "The ecology of climate change and infectious diseases", Ecology **90**, 4, 888–900 (2009).

Langley, I., H.-H. Lin, S. Egwaga, B. Doulla, C.-C. Ku, M. Murray, T. Cohen and S. B. Squire, "Assessment of the patient, health system, and population effects of xpert mtb/rif and alternative diagnostics for tuberculosis in tanzania: an integrated modelling approach", The Lancet Global Health **2**, 10, e581–e591, URL `http://www.sciencedirect.com/science/article/pii/S2214109X14702918` (2014).

Lawn, S. D. and A. I. Zumla, "Tuberculosis.", Lancet **378**, 9785, 57–72 (2011).

Lee, S. and C. Castillo-Chavez, "The role of residence times in two-patch dengue transmission dynamics and optimal strategies", Journal of theoretical biology **374**, 152–164 (2015).

Legesse, M., G. Ameni, G. Mamo, G. Medhin, D. Shawel, G. Bjune and F. Abebe, "Knowledge and perception of pulmonary tuberculosis in pastoral communities in the middle and lower awash valley of afar region, ethiopia.", BMC Public Health **10**, 187 (2010).

Liang, G., X. Gao and E. A. Gould, "Factors responsible for the emergence of arboviruses; strategies, challenges and limitations for their control", Emerging microbes & infections **4**, 3, e18 (2015).

Lipsitch, M. and B. R. Levin, "Population dynamics of tuberculosis treatment: mathematical models of the roles of non-compliance and bacterial heterogeneity in the evolution of drug resistance.", Int J Tuberc Lung Dis **2**, 3, 187–199 (1998).

Liu, L., J. Wu and X.-Q. Zhao, "The impact of migrant workers on the tuberculosis transmission: General models and a case study for china", Mathematical Biosciences and Engineering **9**, 4, 785–807, URL `http://aimsciences.org/journals/displayArticlesnew.jsp?paperID=7807` (2012).

Luzze, H., D. F. Johnson, K. Dickman, H. Mayanja-Kizza, A. Okwera, K. Eisenach, M. D. Cave, C. C. Whalen, J. L. Johnson, W. H. Boom, M. Joloba and Tuberculosis Research Unit, "Relapse more common than reinfection in recurrent tuberculosis 1–2 years post treatment in urban Uganda", International Journal of Tuberculosis and Lung Disease **17**, 3, 361–367, URL `http://dx.doi.org/10.5588/ijtld.11.0692` (2013).

Macnamara, F., "Zika virus: a report on three cases of human infection during an epidemic of jaundice in nigeria", Transactions of the Royal Society of Tropical Medicine and Hygiene **48**, 2, 139–145 (1954).

Marx, F. M., R. Dunbar, D. A. Enarson, B. G. Williams, R. M. Warren, G. D. van der Spuy, P. D. van Helden and N. Beyers, "The Temporal Dynamics of Relapse and Reinfection Tuberculosis After Successful Treatment: A Retrospective Cohort Study", Clinical Infectious Diseases **58**, 12, 1676–1683, URL `http://cid.oxfordjournals.org/content/58/12/1676.abstract` (2014).

Maxian, O., A. Neufeld, E. J. Talis, L. M. Childs and J. C. Blackwood, "Zika virus dynamics: When does sexual transmission matter?", Epidemics **21**, 48–55 (2017).

Mccluskey, C. C., "Lyapunov functions for tuberculosis models with fast and slow progression", Mathematical Biosciences and Engineering **3**, 4, 603–614, URL http://www.aimsciences.org/journals/displayArticles.jsp?paperID=1959 (2006).

McCullagh, P. *et al.*, "Nelder. ja (1989), generalized linear models", CRC Monographs on Statistics & Applied Probability, Springer Verlag, New York (1973).

Millet, J.-P., E. Shaw, À. Orcau, M. Casals, J. M. Miró, J. A. Caylà and The Barcelona Tuberculosis Recurrence Working Group, "Tuberculosis Recurrence after Completion Treatment in a European City: Reinfection or Relapse?", PLoS ONE **8**, 6, e64898, URL http://dx.plos.org/10.1371/journal.pone.0064898 (2013).

Moodie, R. L., *Studies in Paleopathology: General Consideration of the Evidences of Pathological Conditions Found Among Fossil Animals. I* (Paul B. Hoeber, 1918).

Moreno, V., B. Espinoza, K. Barley, M. Paredes, D. Bichara, A. Mubayi and C. Castillo-Chavez, "The role of mobility and health disparities on the transmission dynamics of tuberculosis", Theoretical Biology and Medical Modelling **14**, 1, 3 (2017a).

Moreno, V. M., B. Espinoza, D. Bichara, S. A. Holechek and C. Castillo-Chavez, "Role of short-term dispersal on the dynamics of zika virus in an extreme idealized environment", Infectious Disease Modelling **2**, 1, 21–34 (2017b).

Morin, B. R., E. P. Fenichel and C. CASTILLO-CHAVEZ, "Sir dynamics with economically driven contact rates", Natural resource modeling **26**, 4, 505–525 (2013).

Mossong, J., N. Hens, M. Jit, P. Beutels, K. Auranen, R. Mikolajczyk, M. Massari, S. Salmaso, G. S. Tomba, J. Wallinga *et al.*, "Social contacts and mixing patterns relevant to the spread of infectious diseases", PLoS medicine **5**, 3, e74 (2008).

Musso, D., V. M. Cao-Lormeau and D. J. Gubler, "Zika virus: following the path of dengue and chikungunya?", The Lancet **386**, 9990, 243–244 (2015).

Musso, D., E. Nilles and V.-M. Cao-Lormeau, "Rapid spread of emerging zika virus in the pacific area", Clinical Microbiology and Infection **20**, 10, O595–O596 (2014).

Nishiura, H., C. Castillo-Chavez, M. Safan and G. Chowell, "Transmission potential of the new influenza a (h1n1) virus and its age-specificity in japan", Eurosurveillance **14**, 22, 19227 (2009).

Nishiura, H., G. Chowell and C. Castillo-Chavez, "Did modeling overestimate the transmission potential of pandemic (h1n1-2009)? sample size estimation for post-epidemic seroepidemiological studies", Plos one **6**, 3, e17908 (2011).

Norton, A., *CBS: How one unvaccinated child sparked Minnesota measles outbreak*, URL http://www.cbsnews.com/news/how-one-unvaccinated-child-sparked-minnesota-measles-outbreak/ (June 9, 2014).

Nthiiri, J. K., G. O. Lawi and A. Manyonge, "Mathematical modelling of tuberculosis as an opportunistic respiratory co-infection in hiv/aids in the presence of protection", Applied Mathematical Sciences **9**, 105-108, 5215–5233, URL http://dx.doi.org/10.12988/ams.2015.54365 (2015).

Okuonghae, D., "A mathematical model of tuberculosis transmission with heterogeneity in disease susceptibility and progression under a treatment regime for infectious cases", Applied Mathematical Modelling **37**, 10–11, 6786–6808, URL http://www.sciencedirect.com/science/article/pii/S0307904X13000929 (2013).

Ozcaglar, C., A. Shabbeer, S. L. Vandenberg, B. Yener and K. P. Bennett, "Epidemiological models of mycobacterium tuberculosis complex infections", Mathematical Biosciences **236**, 2, 77–96, URL http://www.ncbi.nlm.nih.gov/pmc/articles/PMC3330831/ (2012).

Pan American Health Organization, P., "Regional zika epidemiological update (americas) august 25, 2017", Online, URL http://www.paho.org (2017).

Patterson-Lomba, O., E. Goldstein, A. Gómez-Liévano, C. Castillo-Chavez and S. Towers, "Per capita incidence of sexually transmitted infections increases systematically with urban population size: a cross-sectional study", Sex Transm Infect **91**, 8, 610–614 (2015).

Patterson-Lomba, O., M. Safan, S. Towers and J. Taylor, "Modeling the role of healthcare access inequalities in epidemic outcomes", MATHEMATICAL BIOSCIENCES AND ENGINEERING **13**, 5, 1011–1041 (2016).

Perrings, C., "Reserved rationality and the precautionary principle: Technological change, time and uncertainty in environmental decision making", Ecological Economics–The Science and Management of Sustainablity, New York pp. 153–166 (1991).

Perrings, C., C. Castillo-Chavez, G. Chowell, P. Daszak, E. P. Fenichel, D. Finnoff, R. D. Horan, A. M. Kilpatrick, A. P. Kinzig, N. V. Kuminoff *et al.*, "Merging economics and epidemiology to improve the prediction and management of infectious disease", EcoHealth **11**, 4, 464–475 (2014).

Petersen, E. E., "Interim guidelines for pregnant women during a zika virus outbreak—united states, 2016", MMWR. Morbidity and mortality weekly report **65** (2016).

Pluciński, M. M., C. N. Ngonghala and M. H. Bonds, "Health safety nets can break cycles of poverty and disease: a stochastic ecological model", Journal of The Royal Society Interface **8**, 65, 1796–1803 (2011).

Poland, G. A. and R. M. Jacobson, "Understanding those who do not understand: a brief review of the anti-vaccine movement", Vaccine **19**, 17, 2440–2445 (2001).

Roeger, L.-I. W., Z. Feng and C. Castillo-Chavez, "Modeling TB and HIV co-infections.", Mathematical Biosciences and Engineering (MBE) **6**, 4, 815–837, URL http://www.aimsciences.org/journals/displayArticles.jsp?paperID=4516 (2009).

Rvachev, L. A. and I. M. Longini Jr, "A mathematical model for the global spread of influenza", Mathematical biosciences **75**, 1, 3–22 (1985).

Sachs, J. and P. Malaney, "The economic and social burden of malaria", Nature **415**, 6872, 680–685 (2002).

Salmon, D. A., L. H. Moulton, S. B. Omer, M. Patricia deHart, S. Stokley and N. A. Halsey, "Factors associated with refusal of childhood vaccines among parents of school-aged children: a case-control study", Archives of pediatrics & adolescent medicine **159**, 5, 470–476 (2005).

Salvador, F. S. and D. M. Fujita, "Entry routes for zika virus in brazil after 2014 world cup: New possibilities", Travel medicine and infectious disease (2015).

Sattenspiel, L. and K. Dietz, "A structured epidemic model incorporating geographic mobility among regions", Mathematical biosciences **128**, 1, 71–91 (1995).

Scott, T. W. and W. Takken, "Feeding strategies of anthropophilic mosquitoes result in increased risk of pathogen transmission", Trends in parasitology **28**, 3, 114–121 (2012).

Shih, J., *CNN: Why worry about the measles outbreak?*, URL http://www.cnn.com/2014/08/07/opinion/shih-measles-vaccine/ (August 7, 2014).

Shim, E., "A note on epidemic models with infective immigrants and vaccination", Mathematical Biosciences and Engineering **3**, 3, 557 (2006).

Stroud, P., S. Del Valle, S. Sydoriak, J. Riese and S. Mniszewski, "Spatial dynamics of pandemic influenza in a massive artificial society", Journal of Artificial Societies and Social Simulation **10**, 4, 9 (2007).

Tanaka, G., C. Urabe and K. Aihara, "Random and targeted interventions for epidemic control in metapopulation models", Scientific reports **4**, 5522 (2014).

Tewa, J. J., S. Bowong and S. C. Oukouomi Noutchie, "Mathematical analysis of a two-patch model of tuberculosis disease with staged progression", Applied Mathematical Modelling **36**, 12, 5792–5807, URL http://www.sciencedirect.com/science/article/pii/S0307904X12000418 (2012).

The Biodesign Institute, T. B. I., "Green named health care hero finalist for zika virus detection device", Online, URL https://biodesign.asu.edu/news/green-named-health-care-hero-finalist-zika-virus-detection-device (2016).

Tiemersma, E. W., M. J. van der Werf, M. W. Borgdorff, B. G. Williams and N. J. D. Nagelkerke, "Natural History of Tuberculosis: Duration and Fatality of Untreated Pulmonary Tuberculosis in HIV Negative Patients: A Systematic Review", PLoS ONE **6**, 4, e17601, URL http://dx.plos.org/10.1371/journal.pone.0017601 (2011).

Towers, S., F. Brauer, C. Castillo-Chavez, A. K. Falconar, A. Mubayi and C. M. Romero-Vivas, "Estimate of the reproduction number of the 2015 zika virus outbreak in barranquilla, colombia, and estimation of the relative role of sexual transmission", Epidemics **17**, 50–55 (2016).

Towers, S. and Z. Feng, "Pandemic h1n1 influenza: Predicting the course of vaccination programme in the united states", Euro. Surveill **14** (2009).

Towers, S., O. Patterson-Lomba and C. Castillo-Chavez, "Temporal variations in the effective reproduction number of the 2014 west africa ebola outbreak", PLOS Currents Outbreaks (2014).

Van den Driessche, P. and J. Watmough, "Reproduction numbers and sub-threshold endemic equilibria for compartmental models of disease transmission", Mathematical biosciences **180**, 1, 29–48 (2002).

Verver, S., R. M. Warren, N. Beyers, M. Richardson, G. D. van der Spuy, M. W. Borgdorff, D. A. Enarson, M. A. Behr and P. D. van Helden, "Rate of Reinfection Tuberculosis after Successful Treatment Is Higher than Rate of New Tuberculosis", American journal of respiratory and critical care medicine **171**, 12, 1430–1435, URL http://www.atsjournals.org/doi/abs/10.1164/rccm.200409-1200OC (2005).

Wakefield, A. J., S. H. Murch, A. Anthony, J. Linnell, D. Casson, M. Malik, M. Berelowitz, A. P. Dhillon, M. A. Thomson, P. Harvey *et al.*, "Retracted: Ileal-lymphoid-nodular hyperplasia, non-specific colitis, and pervasive developmental disorder in children", The Lancet **351**, 9103, 637–641 (1998).

WHO (a), W. H. O., "Dengue and severe dengue", Online, URL http://www.who.int/mediacentre/factsheets/fs117/en/ (2017).

Wolfe, N. D., C. P. Dunavan and J. Diamond, "Origins of major human infectious diseases", Nature **447**, 7142, 279–283 (2007).

World Health Organization, W., "Tuberculosis, fact sheet no. 104", Online, URL http://www.who.int/mediacentre/factsheets/fs104/en/ (2015).

World Health Organization (b), W. H. O., "Zika virus, fact sheet", Online, URL http://www.who.int/mediacentre/factsheets/zika/en/ (2016).

Yong, K., E. D. Herrera and C. Castillo-Chavez, "From bee species aggregation to models of disease avoidance: The ben-hur effect", in "Mathematical and Statistical Modeling for Emerging and Re-emerging Infectious Diseases", pp. 169–185 (Springer, 2016).

Zanluca, C., V. C. A. d. Melo, A. L. P. Mosimann, G. I. V. d. Santos, C. N. D. d. Santos and K. Luz, "First report of autochthonous transmission of zika virus in brazil", Memórias do Instituto Oswaldo Cruz **110**, 4, 569–572 (2015).

Zhao, H., Z. Feng and C. Castillo-Chavez, "The dynamics of poverty and crime", Journal of Shanghai Normal University (Natural Sciences· Mathematics) pp. 225–235 (2014).

Zheng, N., C. C. Whalen and A. Handel, "Modeling the potential impact of host population survival on the evolution of m. tuberculosis latency", PLoS ONE (2014a).

Zheng, N., C. C. Whalen and A. Handel, "Modeling the Potential Impact of Host Population Survival on the Evolution of M. tuberculosis Latency", PLoS ONE **9**, 8, e105721, URL `http://dx.plos.org/10.1371/journal.pone.0105721` (2014b).

Zhou, Y., K. Khan, Z. Feng and J. Wu, "Projection of tuberculosis incidence with increasing immigration trends", Journal of Theoretical Biology **254**, 2, 215–228, URL `http://linkinghub.elsevier.com/retrieve/pii/S0022519308002713` (2008).